DECEMBER 2021 Ph.D. in Electrical and Electronic Engineering ALHASSAN OSMAN

REPUBLIC OF TURKEY
GAZİANTEP UNIVERSITY
GRADUATE SCHOOL OF NATURAL & APPLIED SCIENCES

EXPONENTIAL REACHING LAW BASED ADAPTIVE SLIDING MODE CONTROL OF MULTIVARIABLE LIQUID LEVEL PROCESSES: AN EXPERIMENT STUDY ON QUADRUPLE TANK PROCESS CONTROL

Ph. D. THESIS
IN
ELECTRICAL AND ELECTRONIC ENGINEERING

BY
ALHASSAN OSMAN
DECEMBER 2021

EXPONENTIAL REACHING LAW BASED ADAPTIVE SLIDING MODE CONTROL OF MULTIVARIABLE LIQUID LEVEL PROCESSES: AN EXPERIMENT STUDY ON QUADRUPLE TANK PROCESS CONTROL

Ph.D. Thesis

in

Electrical and Electronic Engineering

Gaziantep University

Supervisor

Assoc. Prof. Dr. Tolgay KARA

By

Alhassan OSMAN

December 2021

EXPONENTIAL REACHING LAW BASED ADAPTIVE SLIDING MODE CONTROL OF MULTIVARIABLE LEVEL PROCESSES: AN EXPERIMENT STUDY ON QUADRUPLE TANK PROCESS CONTROL

submitted by **Alhassan OSMAN** in partial fulfillment of the requirements for the degree of Doctor of Philosophy in **Electrical and Electronic Engineering, Gaziantep University** is approved by,

Prof. Dr. Mehmet İshak YÜCE
Director of the Graduate School of Natural and Applied Sciences ……….............

Prof. Dr. Ergun ERÇELEBİ
Head of the Department of Electrical and Electronics Engineering ……….............

Assoc. Prof. Dr. Tolgay KARA
Supervisor, Electrical and Electronics Engineering
Gaziantep University ……….............

Exam Date: 21 December 2021

Examining Committee Members:

Assoc. Prof. Dr. Tolgay KARA
Supervisor, Electrical and Electronics Engineering
Gaziantep University ……….............

Prof. Dr. Arif NACAROĞLU
Electrical and Electronics Engineering
Gaziantep University ……….............

Prof. Dr. Ergun ERÇELEBİ
Electrical and Electronics Engineering
Gaziantep University ……….............

Assoc. Prof. Dr. Alkan ALKAYA
Electrical and Electronics Engineering
Mersin University ……….............

Asst. Prof. Dr. Murat FURAT
Electrical Electronic Engineering
İskenderun Technical University ……….............

I hereby declare that all information in this document has been obtained and presented in accordance with academic rules and ethical conduct. I also declare that, as required by these rules and conduct, I have fully cited and referenced all material and results that are not original to this work.

Alhassan OSMAN

ABSTRACT

EXPONENTIAL REACHING LAW BASED ADAPTIVE SLIDING MODE CONTROL OF MULTIVARIABLE OF LIQUID LEVEL PROCESSES: AN EXPERIMENT STUDY ON QUADRUPLE TANK PROCESS CONTROL

OSMAN, Alhassan
Ph. D. in Electrical and Electronics Engineering
Supervisor: Assoc. Prof. Dr. Tolgay KARA
December 2021
90 Pages

Industrial processes are complex and have uncertainties. The dynamic behaviour of these processes are needed in order to analyse and effectively control the process outputs of the system. An example of such a system is a Quadruple Tank Process (QTP) with multiple inputs and multiple outputs and nonlinearity due to coupling of the tanks. Therefore, Exponential Reaching Law Based Adaptive Sliding Mode Control (ERL-ASMC) has been proposed to solve the problem of nonlinearity, disturbances and parameter uncertainties. It is able to adjust to the control gain of the discontinous switching function so as to reduce the reaching time. It is very useful in minimizing chattering due to high frequency gain. It has also been compared with Adaptive Sliding Mode Control (ASMC) and Adaptive Pole Placement Control (APPC) which also use Parameter Estimation method like the ERL to determine the parameters of the QTP. These controllers are then finally compared with a Proportional-Integral-Derivative (PID) in order to better evaluate their performances. The evaluations are carried out based on the transient response specifications and the performances indices. The controllers are first simulated and then implemented on the real QTP in the laboratory. The proposed ERL-ASMC has the best performance in simulation and satisfactory results in the experiment.

Key words: Quadruple Tank, Parameter Estimation, Adaptive Pole Placement control Sliding Mode Control, Exponential Reaching Law Based Adaptive Sliding Mode control

ÖZET

ÇOK DEĞİŞKENLİ SIVI SEVİYE SÜREÇLERİNİN ÜSTEL ERİŞİM KURALI TABANLI UYARLANIR KAYAN KİPLİ DENETİMİ: DÖRTLÜ TANK SÜRECİ DENETİMİ ÜZERİNE DENEYSEL BİR ÇALIŞMA

OSMAN, Alhassan

Doktora Tezi, Elektrik-Elektronik Mühendisliği

Danışman: Doç. Dr. Tolgay KARA

Aralık 2021

90 sayfa

Endüstriyel süreçlerin çoğu karmaşıktır ve birçok belirsizliğe sahiptir. Sistemin süreç çıktılarını analiz etmek ve etkin bir şekilde kontrol etmek için bu süreçlerin dinamik davranışının bilinmesi gerekir. Böyle bir sisteme örnek olarak, tankların etkileşiminden kaynaklı doğrusal olmayan ve çoklu giriş çoklu çıkış yapılı dörtlü tank süreci (QTP) gösterilebilir. Bu nedenle, doğrusal olmayan etkiler, bozucular ve parametre belirsizlikleri sorunlarını çözmek için üstel erişim kuralı (ERL) önerilmiştir. Bu yöntem, erişim süresini azaltmak için süreksiz anahtarlama işlevinin kontrol kazancına göre ayarlanabilmektedir. Yüksek frekans kazancı nedeniyle oluşan çatırtıyı en aza indirmede çok yararlıdır. Ayrıca, bu yöntem, QTP parametrelerini belirlemek için ERL gibi parametre kestirimi kullanılan uyarlanır kayan kipli denetim (ASMC) ve uyarlanır kutup atama denetimi (APPC) yöntemleriyle de karşılaştırılmıştır. Bu denetleyiciler daha sonra son olarak performanslarını daha iyi değerlendirmek için bir oransal-integral-türevsel (PID) denetleyici ile de karşılaştırılmışlardır. Bu değerlendirmeler, geçici yanıt özelliklerine ve başarım göstergelerine göre yürütülmüştür. Denetleyiciler önce benzetim yoluyla ve daha sonra laboratuvarda gerçek QTP üzerinde uygulanmıştır. Önerilen ERL benzetimde en iyi başarıma ulaşmış ve deneylerde tatmin edici sonuçlar vermiştir.

Anahtar Kelimeler: Dörtlü Tank, Parametre Kestirimi, Uyarlanır Kutup Atama Denetimi, Kayan Kipli Denetim, Üstel Erişim Kuralı.

Dedicated to my friends and entire family

ACKNOWLEDGEMENTS

I wish to express my deepest gratitude to my supervisor Dr. Tolgay KARA for his guidance, advice, encouragement, kindness, and insight throughout this report. I will also like to thank all the staff and professors at the department of electrical and electronics engineering in Gaziantep University. Finally, I equally acknowledge and thank the Turkish Government Scholarship office for their financial support.

TABLE OF CONTENT

Page

LIST OF TABLES

LIST OF FIGURES

LIST OF SYMBOLS

π	Pi
α	Coefficients of the desired poles
θ	The parameters of the system
β	Parameters of the Adaptive Pole Placement controller
ε	Estimation Error
γ	Adaptation gain
τ	time
ω	Frequency
φ	Regressor Vector

LIST OF ABBREVIATIONS

QTP	Quadruple Tank Processes
MLLP	Multivariable Liquid Level Processes
LLP	Liquid Level Processes
APPC	Adaptive Pole Placement Control
SMC	Sliding Mode Control
ASMC	Adaptive with Sliding Mode Control
ERL-ASMC	Exponential Reaching Law Based Adaptive Sliding Mode Control
ERL	Exponential Reaching Law
MSE	Mean Square Error
ISE	Integral Square Error
IAE	Integral Absolute Error
ITAE	Integral Time Weighted Absolute Error
VSS	Variable Structure Systems
PI	Proportional Integral
PID	Proportional Integral Derivative
MRAC	Model Reference Adaptive Control

CHAPTER I

INTRODUCTION

1.1 Motivation

Multivariable Liquid Level Processes (MLLP) are sequence of operations that require the use of measurement for effective performance. Liquid Level Processes (LLP) are important to the development of the economy in many countries in the world because they facilitate mass production and less cost with a short amount of time. The simple technology used by the LLP allow it to pump water into a tank through a valve which makes it useful in the food processing and chemical industries. In the case of a MLLP that involve multiple pumps and tanks. The chemical industry alone has created millions of jobs in the global economy. Many of these jobs are high paying jobs which enable a lot of people to have a much better life. Notwithstanding, the large amount of products ranging from plastics to fertilizers that are being produced from crude oil through distillation which are used almost by every human being on the planet earth. The LLP can also improve the quality of products tremendously. Especially, in the beverage industries where different concentrations of liquids are mixed together to guarantee a very taste or nutritious product. The LLP takes into consideration the temperature of the liquids in question to enhance easy solvability.

Additionally, water can be pumped into a reactor vessel through a reactor core which is being heated by fission in the case of nuclear energy by effectively monitoring of the water level in the vessel ensuring that there is always enough water to continue the process constantly. The heated water produces steam to help turn the turbines thereby generating electricity in the process. Nowadays, despite the difficulties in managing nuclear power stations to prevent leakages of the radiations into the atmosphere or contamination of water, soil or water bodies by the radioactive waste, nuclear energy is increasing seen as an alternative to fossil fuel based on power production due to the over alarming concerns of global warming.

Moreover, the model of the MLLP serves as a stepping stone in understanding and analyzing other multivariable systems. A great example of a multivariable system is a robotic manipulator. Robots are becoming widely used in the society. To accomplish a very reliable and robust systems, there is the need to introduce a controller to ensure that the desired signal is being achieve very accurately. However, because multivariable systems are sophisticated and complex and in many cases highly nonlinear, controllers are constantly being developed and researched so as to provide good control performances. Control design is an ongoing process and many control methods have been developed over the pass decades.

Finally, the knowledge gain from the study of LLP is useful in different fields of research.

1.2 Problem Statement

In the laboratory, Quadruple Tank Processes (QTP) is used to study and analyze MLLP. It has in four tanks and valves which regulate the inflow of water to the tanks. This allows for coupling and interactions between the tanks which create nonlinearities and uncertainties within the system. It is also subjected to parameter variation and disturbances. These problems are difficult to deal by a conventional controller. This has drawn the attention of many researchers to design more effective, robust and good performance controllers that can withstand the challenges that are occurring within the system. One important thing about the controller that is going to be designed is that it will have the potential to be applied not just only MLLP but also other multivariable system. Adaptive control and robust control strategies are going to be the focus of study due to their ability to handle disturbances, parameter variations and uncertainties effectively.

1.3 Literature Review

There are many multivariable systems that have been discussed and simulated over the past years since the introduction of automatic control in 1950 [1] in order to improve the performances of the systems. Multivariable systems are combinations of series of processes that are interacting with one another which can create a complex structure at the industrial level, thereby facilitating the need for much simpler process that is capable of not only representing the multiple inputs and multiple outputs process but can also describes the different shifting phases and makes it easy to integrate into a control system. The multivariable nature of the system makes it harder to control than Single Input Single Output (SISO) systems [2-4]. There has been some research into multivariable processes in order to solve these process problems [5-8]. So to accomplish this a simplified version of a sophisticated industrial process, the University of Lund, Sweden in 1996 developed a QTP in the laboratory.

Mathematical model of the QTP is very important in the control design process. The derived mathematical model can be found in [1], [14-15]. In [14], it is demonstrated that a multivariable zero can be shifted by changing the valves of the system. It also provides insight about experiment and theory in regarding MIMO systems [9-13]. The QTP as shown in [14] consisted of four interconnected tanks with two inputs voltage supplied valves. As the multivariable zero is being adjusted, the system moves from minimum phase to non-minimum phase which provides a clue about how a small change can move the system into nonlinearity. The mathematical model of the system had two operating points representing both phases of the process. Direct simulation of QTP produced slower settling time responses and the system became unstable in some cases. QTP is very useful in demonstrating the dynamic behavior of multivariable linear or nonlinear systems.

After modeling the QTP, Feedback control of the process is needed in order to be able to provide a very fast time response and also making sure that the QTP is very stable. These feedback controllers can be grouped as Conventional or Traditional Controllers and Advanced Controllers. The conventional controllers vary from Lead Controller to a Proportional-Integral-Derivative (PID) Controller. It is shown in [14] that in using two different Proportional-Integral (PI) controller in feedback loop to stabilize the process in the minimum phase, the system produced a slow time response. On the other hand, the simulated PI controller in the non- minimum phase system produced a 10 times slower time response compared to the former phase. A decoupled PID control of the linearized Four Tank Process in [15] had a faster settling for the first tank than the second tank. However, the time responses for both of tanks were still faster than the time responses of the corresponding tanks of the decoupled PI controller. The multivariable tuning methods discussed in [14-15] cannot handle the automatic controller design for minimum phase and non-minimum phase very well by enhancing better performances. The right half plane zero made it difficult to control due to oscillations. The oscillations occurred because the system had become nonlinear. The challenge was to develop a nonlinear controller that could deal with the non-minimum system very effectively. Over the years, they have been work done on variable control systems and sliding mode control [16]. The theory of sliding mode control (SMC) and variable structure systems (VSS) are well presented in [17-19]. There have also been studies done on the sliding mode method with other control techniques [20-27]. Lino et al. [19] presented a control oriented model and a SMC design for a common rail injection system. Iglesias et al. [28] described a new controller based on a combination of SMC and Fuzzy Logic. Chen and Peng [29] consider the robust control of non-linear uncertain chemical processes in the presence of input-delay and inverse response. Their scheme can be utilized for regulation control of a non-minimum phase process and they extended it for a system having dynamics of first order with dead time. Solutions to the problems of chattering are well documented in [30-40], [109-110]. Two promising reaching laws, power reaching law (PRL) and exponential reaching law (ERL) are being introduced in [110]. They largely function by adjusting the variation of the control gain of a conventional SMC. ERL has shown that it is capable of producing a smooth output response [110]. Pinak et al. proposed [41] a linearization feedback coupled with sliding algorithm for the control of the QTP. The SMC is capable of addressing many problems associated with the four tank system like estimation of bounds, parametric changes, disturbances and stability by making the system asymptotically stable to its desired values in presence of modeling uncertainty [41]. The SMC outperformed the PI controller method in both servo and regulation control [30]. However, sliding mode control algorithm could only control the quadruple tank process within a narrow zone of stability where the system has non-minimum phase behavior [41]. The settling time in [42-43] is slow as well.

While the feedback control has been successful in achieving stability for linear multivariable systems, adaptive control design methods are capable of enhancing better performances for uncertain dynamic systems. They have been numerous development in the area of multivariable adaptive control systems over the past decades [47-51], [53], [55-58], [75], [98-99]. Additional work in multivariable systems adaptive control are carried out on discrete multivariable systems [67-69], and nonlinear multivariable systems [70-72]. In order to deal with non-minimum phase systems effectively the adaptive controllers have made use of pole placement methods [70-71], while having difficulties in processing complex systems and worked only for some special class of multivariable systems. Additionally, Linear Multivariable Systems are also designed by using intelligent schemes and multiple adaptive models for transient improvement [101], [102] and reduction of error [103]. The concepts of intelligent control using switching, multiple and Tuning are detailed in [104]. This method is not a new ideal but it is based on the work of other authors [104], [105]. As parameters of many multiple inputs and many multiple outputs are being estimated, large systems require many estimated parameters and this increases the computational burden on the controller causing the deterioration of the system. There has been some work done on the reduction of the number of parameters [106-108]. In [108], one parameter is proposed. Other way of dealing with nonlinear systems is by using a model reference adaptive controller based on Lyaponuv's direct method, and the Meyer-Kalman-Yacubovich lemma [69]. More contributions were also made to discrete multivariable systems by Borrison [73] and Koivo [74]. Extension has been done on multivariable discrete systems to include time varying plants and systems with poles on the right half plane [74]. Before the interest in multivariable control, the focus had been given to single input single output systems [44]- [47], [54]. The adaptive single input single output linear systems detail in the latter literatures are based on state observer adaptation schemes. The state observer system can be built from the input to the system and the output of the system under consideration [52]. The observer adaptation law which is rooted in Lyapunov stability theory ensured that the system becomes asymptotically stable [44-47]. The estimation of the parameters of the state observe system are taken when the actually measurements of some of the state vectors are not available and this is often so in many practical operational systems. Though in this method, the error is guaranteed to vanish regardless of the size of the constant, it suffers from state vector constrains and cannot handle external disturbances [47]. The adaptive observer method has been also extended to certain class of many inputs and many outputs systems [47],

[53]. Prior to the design of an adaptive controller that could estimate both the variable states and the parameters of the unknown plant, the controllers were designed directly by using a reference model and the model of the plant while assuming the measurements of the state vectors are available [54]- [62]. Whitaker et al. [14] introduced the first model reference adaptive control based on the M.I.T rule of adaptation with some little improvement in [60]. Despite the fact that stability is not guaranteed for high adaptation gains and many inputs signals, it has gained popularity due to its simplicity in practical applications [62]. On the contrary, Lyapunov method developed by C. Sparks et al. besides guaranteeing stability for all kinds of inputs, it also allows high gains in the loops to be used [62]. Another way of trying to estimate the parameters of a known or unknown plant is to use a self-tuning controller by using a recursive algorithm in the adaptation process. Research on self-tuning control started roughly same period as other adaptive control strategies emerged in the 1950s and 60s. The earliest self-tuner was developed by Kalman [63]. After some couple of years, a self-tuning based on minimum variance and least square estimation was proposed by Astrom and Wittenmark [43]. Further work has been carried on the convergence and effects of noise inputs [65] as well as pole-zero placement for the system [66]. As research in adaptive control design evolves, there is still the problem of nonlinear system's stability and the ability of the system to disturbance rejection. Researchers started to combine adaptive schemes with variable structure systems to improve the asymptotic stability and tracking performances of the multivariable plants using Model Reference Adaptive Control (MRAC) [56-79]. Observers have also been employed with sliding mode systems to handle uncertain dynamic models and error [80-81]. Other similar works have also been done on SISO systems [82-85]. Prior to implementation of the above adaptive schemes, nonlinear systems are either linearized around equilibrium points [88], similar to Gain scheduling control technique that transformed the uncertain system into an equivalent linear canonical form [87-88] but these methods could not be applied to complex systems. Three different adaptive controllers and PID controller are applied to a three tank system in [89]. Indirect Model Reference Adaptive control with Recursive Least Square Estimation output performed all the other controllers, followed by Direct Model Reference Adaptive Controller. Another problem for MRAC design is system time delay which can be either unknown accurately or time varying [90]. There are other methods of achieving robust adaptive control for

unknown time varying systems in [91] and [92]. Decentralized control methods are used for large scale systems [93], [94].

It has been shown that Adaptive control design techniques are very powerful in handing very highly complex systems and therefore application of these methods to QTP is step in the right direction. Recently, Adaptive Pole Placement Methods have been applied on QTP [95-97]. Decentralized control has been extended to QTP in [59] to deal with the complex nature of the system. The design decentralized PI controller with MRAC techniques had a rapid response time in both two phases of the QTP [100].

A great amount of work has been done in an attempt to understand and find the problems associated with the existing control methods that are applied to MS especially with regard to QTP. The aim is now to find an innovative, creative and simple strategy to improve the tracking performance of the controllers. This can be done using Parameter Estimation method combined with SMC to provide better output responses and robustness to disturbances and uncertainties. The chattering in SMC can be minimized by using an adapting control gain. ERL which uses the variation gain technique has been proposed to deal to reduce chattering in the output signals

CHAPTER II

LIQUID LEVEL PROCESSES

LLP have been enormously used in many sectors like refinery industry, nuclear, water treatment, and many more. The control of Liquid Level Processes requires the modeling and analyzing of processes as a way of obtaining good performance and accurate tracking. A simple water level tank is a perfect example of a liquid level process.

The tanks can be arranged in series or parallel. A combination of both series and parallel can be used to form a QTP which is also a Multivariable Tank Process (MTP). MTP has nonlinearities and coupling which are difficult to control. This has spike a huge interest in recent years.

2.1 Water Tanks

Water level tanks processes consist of interconnected tanks and valves in order to maintain and regulate the level of the tanks as water is being pumped into the tanks from a reservoir. These are useful in the chemical and pharmaceutical industries for storage and mixing of chemicals. A simple tank is given below.

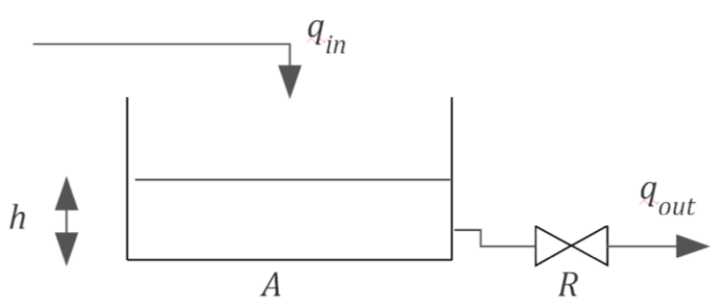

Figure 2.1 Water tank

Where,

h: height of water in the tank

q_{in}: Input signal

q_{out}: Output signal

A: Cross-sectional Area of tank

R: Valve fluid resistance

2.1.1 Water Tanks in Series

The interconnected tanks within the water level tank processes can be arranged in series to allow easy flow of water from one tank to the other. In chemical companies, the series connection is employed to enable materials to be transported and stored.

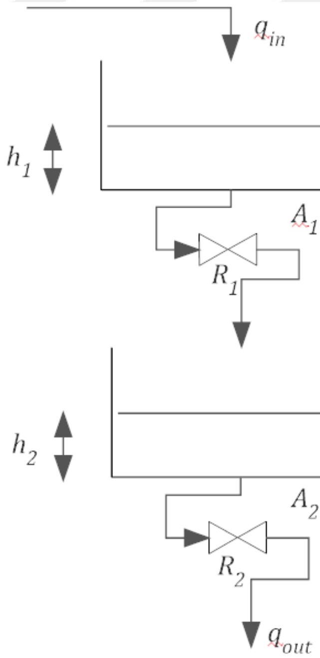

Figure 2.2 Two Tanks in series

Where

h_1 and h_2: Level of tank 1 and tank 2 respectively

q_{in}: Input flow rate

q_{out}: Output flow rate

R_1 and R_2: Valve fluid resistances

A_1 and A_2: Cross-sectional Area of tank 1 and tank 2 respectively.

2.1.2 Water Tanks in Parallel

Another way to combine the interconnected tanks of the water level tank processes are parallel connections. Theses arrangement allow different actions to be taken on each tank. For example, like heating or cooling. In the refinery industries, they are used to enable different tanks to be heated at different temperatures so as to obtain the oil products more efficiently.

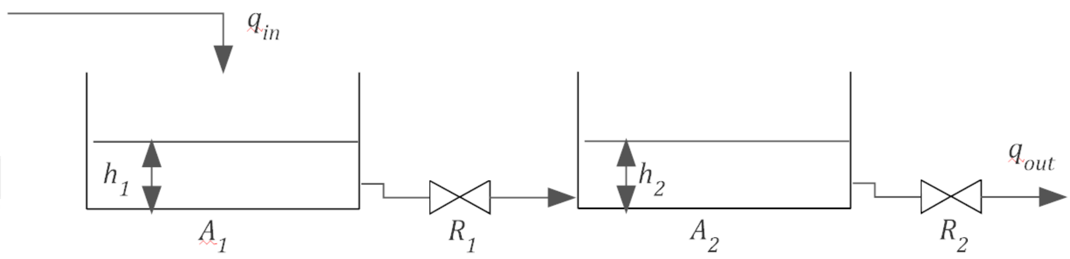

Figure 2.3 Two tanks interacting

Where

h_1 *and* h_2: Level of tank 1 and tank 2 respectively

q_{in}: Input signal

q_{out}: Output signal

R_1 *and* R_2: Valve fluid resistances

A_1 *and* A_2: Cross-sectional Area of tank 1 and tank 2 respectively.

2.2 Quadruple Tank Process

The QTP consists of four interconnected tanks and two pumps. Water is pumped from the reservoir to both the upper and the lower tanks. The input signals, v_1 and v_2 supply voltage to pump1 and pump2, respectively. Pump1 delivers water to Tank1 and Tank4, while pump2 delivers water to Tank2 and Tank3 [14]. The QTP structure used in this research is illustrated in Figure 1. The parameters of the QTP and the operational values are given in Tables 1 and 2, respectively [111].

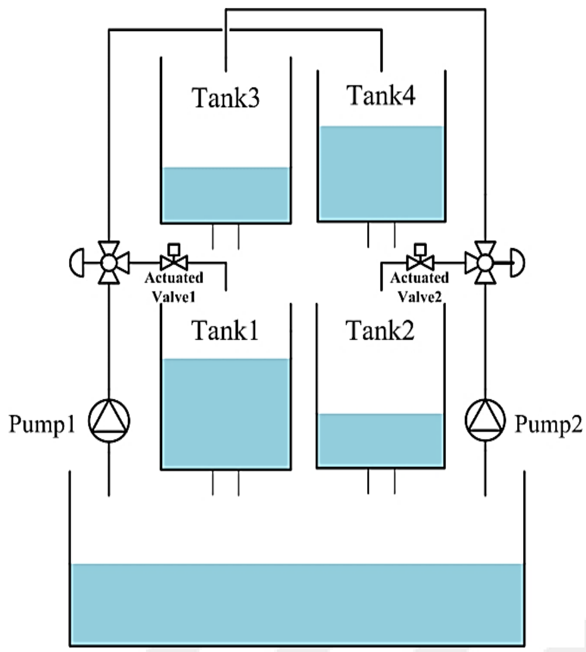

Figure 2.4 Schematic diagram of the quadruple tank process

Table 2.1 Parameter values for QTP

$A_1, A_3[cm^2]$	28
$A_2, A_4[cm^2]$	32
$a_1, a_3[cm^2]$	0.071
$a_2, a_4[cm^2]$	0.057
$K_c, [V/cm]$	0.5
$A_1, A_3[cm/s^2]$	981
$A_{max}[cm]$	20

Table 2.2 Operational values for minimum phase

$h_{01}, h_{02}[cm^2]$	12.4, 12.7
$h_{02}, h_{04}[cm^2]$	1.8, 1.4
$\mathrm{v}_1^0, \mathrm{v}_2^0[\mathrm{V}]$	3.00, 3.00
$k_1, k_2[cm^3/V]$	3.33, 3.35
γ_1, γ_2	0.7, 0.6

The aim is to control the level of water in the lower tanks, Tank1 and Tank2 by using two input signals which means that the lower tank levels are being chosen as the controlled variables of the QTP. The configuration of the valves gives the opportunity to introduce various couplings between the tanks. Tank1 and Tank2 levels are directly regulated by the two control valves in the level control process, and the upper tanks that are Tank3 and Tank4 are dynamically coupled with the lower tanks. This is because the lower tanks have water being delivered to them from both inputs (v_1 and v_2) through the upper tanks which made the system in coupled mode [112]. Control of lower tank levels by direct regulation of control valves is the preferred strategy for the solution of the level control problem. However, Tank3 and Tank4 each have water being pumped to them through single input signal (v_1 or $\boldsymbol{v_2}$) which creates two non-interacting simple tank processes. Using the mass balance and Bernoulli's law, the mathematical equations in (2.1) are obtained below:

$$\begin{cases} \frac{dh_1(t)}{dt} = -\frac{a_1}{A_1}\sqrt{2gh_1(t)} + \frac{a_3}{A_1}\sqrt{2gh_3(t)} + \frac{\gamma_1 k_1}{A_1} v_1 \\ \frac{dh_2(t)}{dt} = -\frac{a_2}{A_2}\sqrt{2gh_2(t)} + \frac{a_4}{A_2}\sqrt{2gh_4(t)} + \frac{\gamma_2 k_2}{A_2} v_2 \\ \frac{dh_3(t)}{dt} = -\frac{a_3}{A_3}\sqrt{2gh_3(t)} + \frac{(1-\gamma_2)k_2}{A_3} v_2 \\ \frac{dh_4(t)}{dt} = -\frac{a_4}{A_4}\sqrt{2gh_4(t)} + \frac{(1-\gamma_1)k_1}{A_4} v_1 \end{cases}$$

(2.1)

Where;

A_i: Cross sectional area of Tank i

a_i: Cross sectional area of the outlet pipe

$h_i(t)$: Water level

k_i: Pump constant

γ_i: Valve position.

The system is linearized around an operating point and by using the variables $x_i \coloneqq h_i - h_{i0}$ and $u_i \coloneqq v_i - v_{i0}$, the system can be represented in state space form as below:

$$\begin{cases} \frac{dx}{dt} = \begin{bmatrix} -\frac{1}{T_1} & 0 & \frac{A_3}{A_1T_3} & 0 \\ 0 & -\frac{1}{T_2} & 0 & \frac{A_4}{A_2T_4} \\ 0 & 0 & -\frac{1}{T_3} & 0 \\ 0 & 0 & 0 & -\frac{1}{T_4} \end{bmatrix} x + \begin{bmatrix} \frac{\gamma_1 k_1}{A_1} & 0 \\ 0 & \frac{\gamma_2 k_2}{A_2} \\ 0 & \frac{(1-\gamma_2)k_2}{A_3} \\ \frac{(1-\gamma_1)k_1}{A_4} & 0 \end{bmatrix} u \\ y = \begin{bmatrix} k_c & 0 & 0 & 0 \\ 0 & k_c & 0 & 0 \end{bmatrix} x \end{cases} \tag{2.2}$$

Where time constants are:

$$T_i = \frac{A_i}{a_i}\sqrt{\frac{2h_{i0}}{g}}, i = 1, \cdots, 4$$

and h_{i0} is the water level at each operating point. The transfer function matrix of the linearized plant is given as:

$$G(s) = \begin{bmatrix} \frac{\gamma_1 c_1}{1+sT_1} & \frac{(1-\gamma_2)c_1}{(1+T_3 s)(1+sT_1)} \\ \frac{(1-\gamma_1)c_2}{(1+T_4 s)(1+sT_2)} & \frac{\gamma_2 c_2}{1+sT_2} \end{bmatrix} \tag{2}$$

CHAPTER III

ADAPTIVE POLE PLACEMENT CONTROL AND PID CONTROL

3.1. Online Parameter Estimation

Identification of unknown or uncertain model parameters is a very important ideal in adaptive control design especially in self-tuning. The parameter update law in the adaptive control system can be achieved by using a gradient method which involve utilizing the result of the estimation. The identification process requires only the input and output signal of the system. In order to accomplish this, the system model is represented in Static Parametric Model (SPM) form in order to carry out the estimation [113]. The SPM form is given by:

$$z = \theta^* \varphi$$

(3.1)

Where,

z: signal output

φ: regressor vector

θ^*: parameters.

At time, $t, \theta^* = \theta(t)$ which implies

$$\hat{z} = \theta(t)\varphi$$

(3.2)

An estimation error ε is used because the parameter difference, $\tilde{\theta} = \theta - \theta^*$ is unknown and also normalized to guarantee that $\frac{\varphi}{m_s}$ is bounded [48].

$$\varepsilon = \frac{z-\hat{z}}{m_s^2}$$

(3.3)

$$m_s = 1 + \alpha\varphi^2, m_s = 1 + \varphi^t\varphi \qquad (3.4)$$

Equations (3.3) and (3.4) result with the following alternative error definition:

$$\varepsilon = -\frac{\hat{\theta}\varphi}{m_s^2} \tag{3.5}$$

For either a scalar regressor or vector regressor, in order to minimize the estimation error, we choose a cost function as:

$$J(\theta) = \frac{\varepsilon^2 {m_s}^2}{2} \tag{3.6}$$

Using the gradient method

$$\dot{\theta} = -\gamma \nabla J(\theta)$$
(3.7)

and the adaptation law is obtained as

$$\dot{\theta} = \gamma\varepsilon\varphi, \qquad \theta(0) = \theta_0$$
(3.8)

For the purpose of obtaining a stable adaptation law, the following assumptions should be valid for a feasible adaptive system:

Assumption 1. *The ratio of the regressor vector to the normalization signal must be bounded* [113].

Assumption 2. *The ratio of the regressor vector to the normalization signal must be persistently exciting* [113].

Theorem 1.

Considering Assumptions 1 and 2, using the parametric form in (3.1) and parameter estimation in (3.2), with the help of error definiton in (3.3) and cost function (3.6), update law in (3.7) guarantees stable adaptation with bounded system signals and evantually leads the estimation of parameters to converge their actual values.

Proof. Let us consider the following Lyapunov-like function:

$$\boldsymbol{V = \frac{\tilde{\theta}^2}{2\gamma}} \tag{3.9}$$

Time derivative of (3.9) yields:

$$\boldsymbol{\dot{V} = \frac{\tilde{\theta}}{\gamma}\frac{d\tilde{\theta}}{dt} = -\frac{\varphi^2}{m_s^2}\tilde{\theta}^2 = -\varepsilon^2 m_s^2 \leq 0} \tag{3.10}$$

Since $V > 0$ and $\dot{V} \leq 0$, it follows that $V \in L_\infty$which implies $\varepsilon \in L_\infty$ and $\tilde{\theta} \in L_\infty$. Considering V is a non-increasing and positive definite function, the following inequality holds:

$$-\int_0^t \dot{V}(\tau)d\tau \leq V(0) \rightarrow m_s^2 \int_0^t \|\varepsilon\|^2 \leq V(0) < 0 \tag{3.11}$$

This implies that $\|\varepsilon\| \in L_2 \cap L_\infty$ and since $\frac{\varphi(t)}{m_s}$ is bounded by definition, one can conclude that all signals in the system are bounded and estimation error asymptotically converges to zero. Furthermore, substituting (3.5) into (3.6), the update law can be written as

$$\dot{\hat{\theta}} = -\gamma \frac{\varphi^2}{m_s} \hat{\theta}\ ,\ \theta(0) = \theta_0 \tag{3.12}$$

The initial value problem in (3.12) has the solution

$$\hat{\theta}(t) = e^{-\gamma \int_0^t \frac{\varphi^2(\tau)}{m_s^2(\tau)} \hat{\theta}_0 d\tau} \tag{3.13}$$

If $\frac{\varphi(t)}{m_s}$ satisfies

$$\frac{1}{T}\int_0^t \frac{\varphi^2(\tau)}{m_s^2(\tau)} \hat{\theta}_0\, d\tau \geq \alpha_0 > 0 \tag{3.14}$$

$\forall t \geq 0$ with $T, \alpha_0 > 0$ are some constants, then $\hat{\theta}(t)$ converges exponentially to θ^*, which further implies that parameter estimate approaches its true value exponentially [112]. These results complete the proof.

3.2. Continuous-Time Adaptive Pole Placement Control (CT-APPC)

Similar to Discrete-Time Adaptive Pole Placement Control, CT-APPC is designed to satisfy desired closed loop requirements. The desired polynomial is represented by $A^*(s)$ [113], [114]. The desired closed loop requirements closely relate to the parameters of the controller to the online estimates of the plant. The control input is therefore guaranteed to satisfy the closed loop characteristics equation. Let us consider a SISO Linear Time Invariant (LTI) system described by the transfer function model in (3.15-3.17).

$$y_p = G_p(s)u_p, \qquad G_p(s) = \frac{Z_p(s)}{R_p(s)}$$

(3.15)

$$Z_p = b_n s^{n-1} + b_{n-1} s^{n-2} + \cdots + b_0$$

(3.16)

$$R_p = s^n + a_n s^{n-1} + \cdots + a_0 \tag{3.17}$$

Where y_p is the output signal, $G_p(s)$ is a proper transfer function, and u_p is the control input signal. The control objective is provided by the following assumptions about the system.

B1. $R_p(s)$ is a monic polynomial with known degree, n.

B2. $Z_p(s)$ is a polynomial with $n-1$ degree and coprime with R_p.

B3. $Q_m(s)$, $Z_p(s)$ are coprime.

The two assumptions make R_p, Z_p to be non-hurtwitz.

The control law is considered to be

$$Q_m(s)L(s)u_p = -P(s)y_p - M(s)y_m$$

(3.18)

Where $P(s)$, $L(s)$ are polynomials of degree $q+n-1$ and $n-1$ respectively while $Q_m(s)$ is the internal model of y_m as well as a known monic polynomial and should satisfy

$$Q_m(s)y_m = 0$$

(3.19)

Substituting (3.15) into (3.18),

$$y_p = \frac{Z_p(s)M(s)}{R_P(s)Q_m(s)L(s)+P(s)Z_P(s)}y_m$$

(3.20)

$P(s)$ and $L(s)$ are chosen to satisfy the desired monic hurwitz polynomial equation, $A(s)^*$ of degree $2n+q-1$.

$$R_P(s)Q_m(s)L(s) + P(s)Z_P(s) = A^*(s) \quad (3.21)$$

The solution for the coefficients of $L(s)$ and $P(s)$ can be obtained by the algebraic equation [115],

$$S_1\beta_1 = \alpha_l^* \quad (3.22)$$

Where S_1 is the Sylvester matrix of Q_m, Z_P, R_P of dimension of $2(n+q)\times 2(n+q)$.

$$\beta_1 = \left[l_q^T, p^T\right]^T, \alpha_l^* = \left[0, \dots 0,1, \alpha^{*T}\right]^T \quad (3.23)$$

$$l_q = [0, \dots 0,1, l^T]^T \epsilon R^{2n+q-1} \tag{3.24}$$

$$l = [l_{n-2}, l_{n-3 \dots\dots} l_1, l_0]^T \epsilon R^{n-1} \tag{3.26}$$

$$p = \left[p_{n+q-1}, l_{n+q-2 \dots\dots} p_1, p_0\right]^T \epsilon R^{n+q} \tag{3.27}$$

$$\alpha^* = \left[\alpha^*_{2n+q-2}, \alpha^*_{2n+q-3_{\dots\dots}} \alpha^*_1, \alpha^*_0\right]^T \epsilon R^{n+q-1} \tag{3.28}$$

l_i, p_i, α^*_i are coefficients of

$$L(s) = s^{n-1} + l_{n-2}s^{n-2} + \dots + l_1 s + l_0$$

(3.29)

$$P(s) = p_{n+q-1}s^{n+q-1} + p_{n+q-2}s^{n+q-2} + \dots + p_1 s + p_0 \tag{3.30}$$

$$A^*(s) = s^{2n+q-1} + \alpha^*_{2n+q-2}s^{2n+q-2} + \dots + \alpha^*_1 s + \alpha^*_0 \tag{3.31}$$

S_l is nonsingular because of the coprimeness of Q_m, Z_P, R_P. The coefficients of $P(s)$ and $L(s)$ can the be calculated from the equation

$$\beta_1 = S_l^{-1}\alpha^*_l \tag{3.32}$$

(3.20) can be written as

$$y_p = \frac{Z_p(s)M(s)}{A(s)^*} y_m \tag{3.33}$$

Substituting (3.15) into (3.33)

$$u_p = \frac{R_p(s)M(s)}{A(s)^*} y_m \tag{3.34}$$

When y_m is zero, (3.33) and (3.34) becomes zero. Which means that y_p and u_p converge to zero exponentially. When $y_m \neq 0$, the tracking error, $e = y_p - y_m$ is written as

$$e = \frac{Z_p(s)M(s) - A^*(s)}{A(s)^*} y_m$$

(3.35)

$$e = \frac{Z_p(s)(M(s) - P(s))}{A(s)^*} y_m - \frac{LR_p}{A(s)^*} Q_m y_m$$

(3.36)

The error becomes zero when $M(s) = P(s)$ and $Q_m y_m = 0$. As a result of the $\frac{Z_p}{A^*}, \frac{LR_p}{A^*}$ being proper with stable poles, the error converges exponentially to zero.

This shows the pole placement and the tracking objective can be achieved replacing $M(s) = P(s)$ into (3.18). The control law the becomes

$$Q_m(s)L(s)u_p = -P(s)(y_p - y_m)$$

(3.37)

A filter is added to guarantee that the polynomial equation of the controller remains as a Hurwizt polynomial because $L(s)$ is not necessary Hurwizt.

The control law in (3.18) can be rewritten with a filter

$$u_p = \frac{F(s)-L(s)Q_m(s)}{F(s)}u_p - \frac{P(s)}{F(s)}(y_p - y_m) \quad (3.38)$$

The control law is illustrated in figure 3.1.

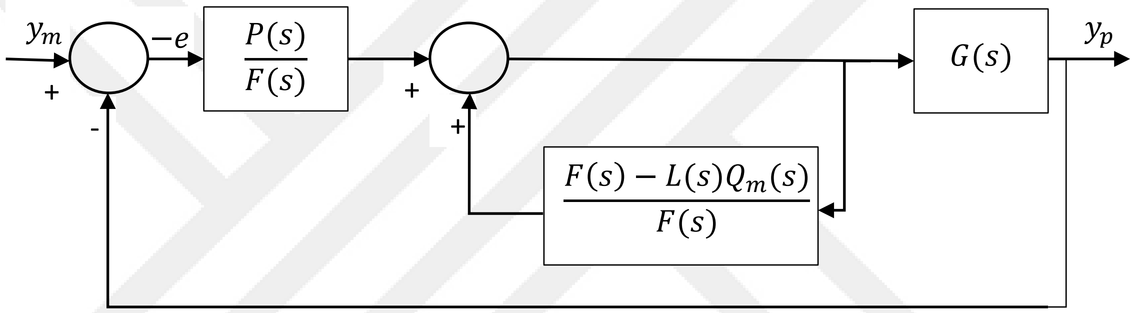

Figure 3.1 Block Diagram of Pole Placement control

3.3 PID

PID Controllers are widely used in many industries today. In the late 1930s, Taylor Instrument Company developed a new instrument called pre-act in addition to proportional and reset control action and later in the same period Foxboro Instrument Company also came out with the hyper-rest instrument. The pre-act and hyper-reset each provided control action proportional to the derivative of the error signal while the reset control action provided control action proportional to the integral of the error signal [133]. These instruments formed the PID controller. The parameters of these sets needed to be adjusted so as to control the desired input signal. J.G. Ziegler and N.B Nichols carried out experiment to find ways of choosing the optimum control setting of the PID. Finally, in 1942 and 1943, they have developed methods on how to obtain the parameters of the PID [134-135] and later in 1950, G.H Cohen and G.A Coon provided alternative tuning methods for certain kind of plants [136]. In the same year, Walter R. Evans developed the root locus method to allow the design for desired transient response [137]. The root locus method is used when the transfer function of the plant is known.

The control law of the PID is written as:

$$\boldsymbol{u(t) = K_p e(t) + K_i \int_0^t e(\tau) d\tau + K_d \frac{de(t)}{dt}}$$

(3.39)

Where $\boldsymbol{K}_p$ is the proportional gain, $\boldsymbol{K}_i$ is the integral, $\boldsymbol{K}_d$ is the derivative gain, $\boldsymbol{u(t)}$ is the control signal and $\boldsymbol{e(t)}$ is the error signal.

3.3.1 Root Locus Method

It is used to achieve the desired transient response by varying the loop gain which in turn adjust the location of the closed loop poles. The variation of the loop gain alone may not give the desired transient response thereby providing the space for compensation by adding zeros or poles to the closed loop system. This technic allows for the design of PID controllers using the root locus method. Below is a simple closed loop representation with the PID controller.

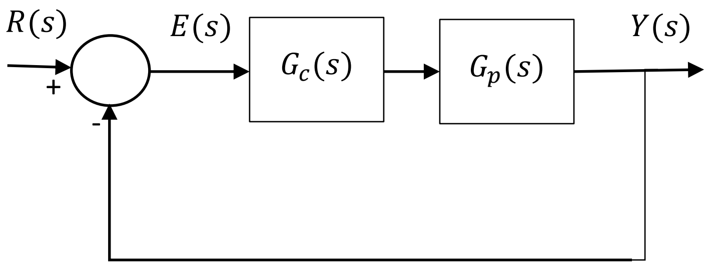

Figure 3.2 Block Diagram of PID control

$R(s)$: is the input signal

$Y(s)$: is the output signal

$G_C(s)$: is the PID controller

$G_p(s)$: is the transfer function of the plant

By taking the Laplace transform of (3.39)

$$G_c(s) = \boldsymbol{K_p} + \frac{\boldsymbol{K_i}}{s} + \boldsymbol{K_d}s$$

(3.40)

Where $\boldsymbol{K}_i = \frac{\boldsymbol{K_p}}{\boldsymbol{T_i}}$ and $\boldsymbol{K_d} = \boldsymbol{K_p T_d}$, then

$$G_c(s) = \boldsymbol{K_p} \frac{[1+T_i s+T_i T_d s^2]}{\boldsymbol{T_i s}} \tag{3.41}$$

$$G_{cp} = \frac{G_c(s)G_p(\boldsymbol{s})}{1+G_c(s)G_p(\boldsymbol{s})}$$

(3.42)

Where G_{cp} is the closed loop transfer function.

The design of PID controller using the root locus requires the location of the desired poles on the s plane based on desired transient requirements. The process is as follows:

1. The desired transient requirements are outlined in the form of settling time, t_s and percent overshoot, M_p.

2. The location of the desired closed loop are calculated by using the desired transient response. For a second order behavior

$$Desired\ poles = -\tau\omega_n \pm i\omega_n \sqrt[2]{1-\tau^2}$$

(3.43)

Where τ is the damping ratio and ω_n is the natural frequency.

$$\tau = \sqrt[2]{\frac{(\ln(M_p))^2}{\pi^2+(\ln(M_p))^2}}$$

(3.44)

$$\omega_n = \frac{4}{t_s\tau}$$

(3.45)

3. The desired poles are located on the s plane.

4. The poles and zeros of the PID control are also located on the s plane.

$G_c(s) = \boldsymbol{K_p}\frac{(s+a)(s+b)}{\boldsymbol{s}}$

(3.46)

Where a and b are the zeros of the PID to be located on the s plane.

5. First, PD controller is design and a which is associated with PD is located away from the desired closed loop poles. The characteristic equation of the closed loop system is obtained by equating the denominator of (3.42) to zero.

$$G_{PD}(s) = \boldsymbol{K_p}(s + a) \quad (3.47)$$

$G_{open}(s) = \boldsymbol{K_p}(s + a)G_{\boldsymbol{P}}$

(3.48)

$1 + G_{\boldsymbol{PD}}(s)G_{\boldsymbol{p}}(\boldsymbol{s}) = 0$

(3.49)

Angle condition

$/G_{\boldsymbol{PD}}(s)G_{\boldsymbol{p}}(\boldsymbol{s}) = \pm 180(2k + 1)\ where\ (k = 0,1,2..)$

(3.50)

Magnitude Condition

$\left|G_{\boldsymbol{PD}}(s)G_{\boldsymbol{p}}(s)\right| = 1$

(3.51)

The angle condition is used to calculate a by drawing the lines the zeros and poles of the system to meet at one of the conjugated poles on the s plane. The overall gain, $\boldsymbol{K}_{overall}$ is then obtained from the magnitude condition.

$\left|\boldsymbol{K_{overall}}(s + a)G_{\boldsymbol{p}}(\boldsymbol{s})\right| = 1$

(3.52)

If the numerator of the plant is 1, $\boldsymbol{K} = \boldsymbol{K}_{overall}$. However, if the numerator of $G_{\boldsymbol{p}}(\boldsymbol{s})$ is k_1, $\boldsymbol{K} = \frac{\boldsymbol{K_{overall}}}{\boldsymbol{k_1}}$.

6. The b of the PID controller is located close to the origin of the s plane so that it will cancel the pole of the PID controller.

7. In comparing (3.41) and (3.46), T_i and T_d are calculated.

$$T_d = \frac{1}{a+b}$$

(3.53)

$$T_i = \frac{1}{T_i ab}$$

(3.54)

CHAPTER IV

ROBUST CONTROL

Robust control is a control design method that involves taking into account the resilience of the controller to disturbances, un-modelled dynamics and parameter uncertainties. Over the years, they have been many techniques developed to achieve a very good robust controller. Some of these methods are H-infinity, SMC, Qualitative Feedback Theory, Passivity Based Control. The two commonly known robust controllers are H-infinity and SMC. H-infinity control is very complex and requires the knowledge of high optimization computation [120]. On the other hand, SMC is simple and easily implementable controller. As a result, the focus of this topic is going to be on SMC.

SMC was developed half century ago by S.V. Emelyanov and other researchers to solve the control problem of a noisy plant with bounded unknown varying parameters [121]. Today, it has been applied to many practical systems from motor control [122-127] to robot control. Research into robot manipulators dates back to the late 1970's [121]. There has also been application of SMC to LP [128-130]. This wide spread usage of SMC made it a powerful tool in control design.

4.1. Sliding Mode Controller

Sliding Mode Controller is a variable structure controller that uses a switching function to control the system. The switching function forces the system trajectories to move on to the sliding surface and keep them on the surface. Hence, the sliding surface is said to be in sliding mode when the surface approaches zero and continuous to remain at that position. The transition period of the sliding mode is called reaching mode. The sliding surface is also called the switching surface. It is defined as a differential equation of the system's states variables. It is applicable to linear and non-linear system.

$$S(x,t) = (\frac{d}{dt} + c)^{n-1}x \qquad (4.1)$$

Where n is the order of the system and $c > 0$. If $n = 2$, then

$S = \dot{x} + cx$

(4.2)

At the sliding manifold, $S = 0$, then

$\dot{x} = -cx$

(4.3)

$x = x(0)e^{-ct}$

(4.4)

$\dot{x} = -cx(0)e^{-ct}$ (4.5)

$x(t) \rightarrow 0$ exponentially as $t \rightarrow \infty$.

As we can see the trajectories of the system becomes independent of the parameter uncertainties and disturbances.

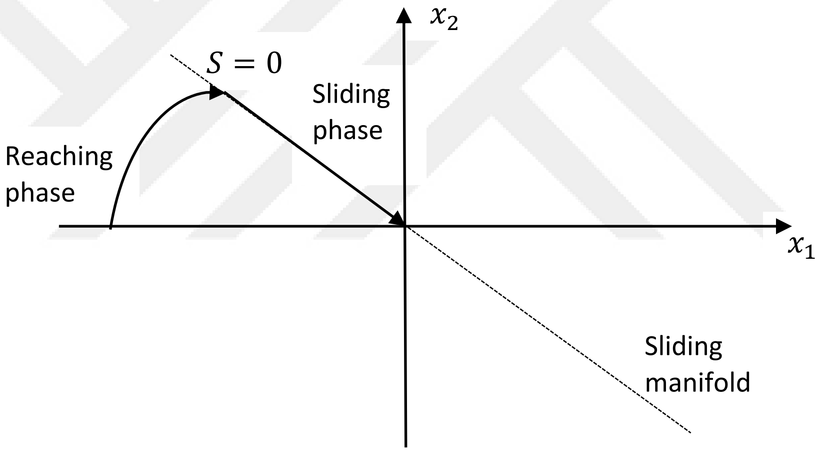

Figure 4.1 Sliding Surface Motion

The order of the sliding surface is lower than the order of the system. A switching function generates the control signal that is used to the drive the states outside the sliding surface to reach the sliding surface in finite time [118].

Switching Function is selected as,

$$u(x,t) = \begin{cases} u^{+}(x,t)\ when\ S > 0 \\ u^{-}(x,t)\ when\ S < 0 \end{cases} \quad (4.6)$$

Such that the reaching modes satisfy the reaching condition.

4.1.1 Reaching Condition

Reaching condition is the condition that causes the variable states to get to the sliding surface. There are many various ways to specify the reaching conditions [118].

1. Direct switching Approach

This approach was the first proposed reaching condition. [121].

$\dot{S} > 0 \; when \; S < 0$

(4.7)

$\dot{S} < 0 \; when \; S > 0$

(4.8)

Or, equivalently

$S\dot{S} < 0$

This reaching condition may not always arrive at sliding surface in a finite time.

2. Lyapunov Function Approach

A Lyapunov function candidate is chosen [131].

$$V = \frac{S^2}{2} \tag{4.9}$$

$\dot{V} < 0$ for $S \neq 0$

(4.10)

A finite time is achieved when a value is given,

$\dot{V} < -\epsilon, \;\; S \neq 0$, where ϵ is positive

(4.11)

3. Rate Reaching Law Approach

This a new approach in sliding condition. There are different rate reaching law methods namely,

a. The constant rate reaching law

$$\dot{S} = -k sign(S) \tag{4.12}$$

b. The constant plus proportional rate reaching law

$$\dot{S} = -k_1 sign(S) - k_2$$

(4.13)

c. Power rate reaching law

$$\dot{S} = -k|S|^{\alpha} sign(S) \; 0 < \alpha < 1 \tag{4.14}$$

This rate reaching law also indicates the dynamic behavior of the system during the sliding phase. Moreover, it provides a way of reducing chattering [118].

Consider a given second order plant

$$\begin{cases} \dot{x}_1 = x_2 \\ \dot{x}_2 = f(x_1, x_2, t) + g(x_1, x_2, t)u + d(t) \end{cases}$$

(4.15)

Where f and g are known nonlinear functions, $d(t)$ is the bounded disturbance input with $|d(t)| \leq D$ [114]. The SMC law based on feedback linearization is given by

$$u = \frac{v - f(x_1, x_2, t)}{g(x_1, x_2, t)} \tag{4.16}$$

$$v = \ddot{x}_d - c\dot{e} - ksgn(S) \tag{4.17}$$

$$S(t) = ce + \dot{e} \tag{4.18}$$

$$e = x - x_d \tag{4.19}$$

Where $x = x_2$ is the plant output that is the controlled variable, x_d is the desired output, S is the sliding surface and k and c are positive real numbers. By using a proper Lyapunov function, stability of the system can be determined by Lyapunov theory of stability [20]-[24], [116], [138]. The Lyapunov function candidate, $V(t)$ is selected as a positive definite function of time, expressed in terms of the sliding surface S and for global asymptotic stability the time derivative of V should be negative definite. Therefore, the Lyapunov function candidate and its derivative are expressed as,

$$V = \frac{S^2}{2} \tag{4.20}$$

$$\dot{V} = S\dot{S}$$

(4.21)

Using (4.7) we can rewrite (4.8) as,

$$\dot{V} = S(c\dot{e} + \ddot{e})$$
(4.22)

$$\dot{V} = S(c\dot{e} + \ddot{x} - \ddot{x}_d)$$
(4.23)

Substituting closed-loop dynamics (4.15-4.17) into (4.23) and performing cancellation of terms we reach,

$$\dot{V} = S\left(c\dot{e} + f(x_1, x_2, t) + g(x_1, x_2, t)\left[\frac{\ddot{x}_d - c\dot{e} - ksgn(S) - f(x_1,x_2,t)}{g(x_1,x_2,t)}\right] + d(t) - \ddot{x}_d\right)$$
(4.24)

$$\dot{V} = S(-ksgn(S) + d(t))$$
(4.25)

$$\dot{V} = -kSsgn(S) + Sd(t)$$
(4.26)

$$\dot{V} = -k|S| + Sd(t) \tag{4.27}$$

Recalling that $|d(t)| \leq D$, the following inequality is obtained,

$$\dot{V} \leq -k|S| + |S|D \tag{4.28}$$

$$\dot{V} \leq -(k - D)|S| \tag{4.29}$$

Which is a negative quantity provided that $(k - D) > 0$. Stability of the SMC rule with feedback linearization given in (4.16-4.19) for the plant in (4.15) is thus verified with the fact that $\dot{V}$ is negative definite with a gain k selected to be greater in magnitude than the maximum possible disturbance input, consequently the system under SMC is stabilizable for any bounded disturbance input. In standard SMC design, a proper selection would be $\dot{V} = -k|S|$ for the disturbance free case, which is consistent with the stability proof provided above [117].

As it has been indicated, SMC can guarantee stability as well as handle disturbances and nonlinerities effectively. However, in the operation process, the nonlinear control part of the SMC generates high frequencies which is known as chattering. The chattering phenomenon creates huge oscillations rendering the output signal very rough and high error. In fact, this can make the SMC unsuitable for controlling signals that require a fixed unoscillating and precise responses, for example in LLP and voltage systems. Since the control system in this case is a WLP, the SMC need to be design in a way that will alleviate chattering and ensuring a much smooth output signal. The proposed controller, ERL is a modified version of SMC.

4.2 The Proposed Exponential Reaching Law

One approach to reduce chattering in the literature is to adjust the control gain. This action has tremendeous effect on the reaching law. The adjustment process involves by intuitively tuning the switching gain manually so as to obtain a less chattered signal. Moreover, the another approach is to make the discontinuous gain a function of sliding surface. This strategy has been used to develop Power Rate Reaching Law (PRRL) and ERL [110],[118]. PRRL reduces the robustness of the controller and increases the reaching time due to the rapid reduction of the fractional power within the controller. With the development of ERL, the problems posed by the PRRL has been minimised with the help of the exponential which adjust smoothly to the variation of the sliding surface [110].

$$\dot{S} = -\frac{k}{N(S)} sgn(S) \quad and\ k > 0$$

(4.30)

Where

$$N(S) = \delta_0 + (1 - \delta_0)e^{-\propto|S|^p}$$

(4.31)

Where δ_0 is strictly positive offset between the range of zero and one, while p and α are strictly positive integer and strictly positive respectively. We can see from (4.30), if $|S|$ increases, (4.31) approaches δ_0, and therefore, the switching gain becomes $\frac{k}{\delta_0}$, which is greater than k. This makes the controller reach the sliding phase faster. On the contrary, if $|S|$ decreases, (4.31) approaches one, and the overall control gain behaves like normal SMC which is k. In this case, k decreases gradually to eliminate chattering. This means that ERL has the capability to dynamically alter the variation of the switching function within the range of k and $\frac{k}{\delta_0}$. If δ_0 was equal to one, the ERL would resemble the conventional SMC. The same behaviour occurs when δ_0 is greater than one.

***Remark 1*:** For $\delta_0 \geq 1$, $\dot{S} = -\frac{k}{N(S)} sgn(S) \approx -ksgn(S) \;\; and \; k > 0$. Therefore, in order to achieve an ERL, δ_0 shoud be within the range, $0 < \delta_0 < 1$.

***Proposition 1*:** ERL has smaller reaching time than SMC due to higher switching function.

***Proof*:** Let's calculate and compare the reaching time, t_r of both controllers by using the nonlinear control part [110].

$$\dot{S} = -ksgn(S) \; and \; k < 0$$

(4.32)

Integrating both sides of the (4.32) results in :

$$t_{rs} = \frac{|S(0)|}{k}$$

(4.33)

Where t_{rs} is the reaching time of SMC.

From (4.30) and (4.31), the discontinuous function can be rewritten as :

$$\delta_0 \dot{S} + (1 - \delta_0) e^{-\propto |S|^p} \dot{S} = -ksign(S)$$

(4.34)

Integrating from zero to t_{re}. At $t = t_{re}, \; S(t_{re}) = 0$.

$$t_{re} = \frac{1}{k}\left[\delta_0 |S(0)| + (1 - \delta_0) \int_0^{S(0)} sign(S) e^{-\propto |S|^p} . dS\right]$$

(4.35)

Where t_{re} is the reaching time of ERL.

If $S \leq 0$ for $t \leq t_{re}$, then

$$\int_0^{S(0)} sgn(S) e^{-\propto |S|^p} . dS = \int_0^{S(0)} -e^{-\propto |S|^p} . dS = \int_0^{-S(0)} e^{-\propto |S|^p} . dS$$

(4.36)

However, if $S \geq 0$ for $t \leq t_{re}$, then

$$\int_0^{S(0)} sgn(S) e^{-\propto |S|^p} . dS = \int_0^{S(0)} e^{-\propto |S|^p} . dS$$

(4.37)

In combining (4.35) and (4.36), then

$\int_0^{S(0)} sgn(S)e^{-\propto|S|^p}.dS = \int_0^{|S(0)|} e^{-\propto|S|^p}.dS$

(4.38)

Replacing (4.37) into (4.34), then

$t_{re} = \frac{1}{k}\left[\delta_0|S(0)| + (1-\delta_0)\int_0^{|S(0)|} e^{-\propto|S|^p}.dS\right]$

(4.39)

Using inequalities, $|S(0)| > \delta_0|S(0)| > 0\, for\ 0 < \delta_0 < 1$ and $\int_0^{|S(0)|} e^{-\propto|S|^p}.dS < (1-\delta_0)\int_0^{|S(0)|} e^{-\propto|S|^p}.dS < 0$ because of the exponential function, which implies that $\delta_0|S(0)| > \int_0^{|S(0)|} e^{-\propto|S|^p}.dS.$ Therfore, $\delta_0|S(0)| + (1-\delta_0)\int_0^{|S(0)|} e^{-\propto|S|^p}.dS < |S(0)|.$

As a result in comparing (4.33) and (4.39), $t_{re} < t_{rs}$.

4.2.1 Systems Without Parameter Uncertainties

The absence of an uncertainty makes it easy to achieve the desired reaching time. This is one good thing about ERL. By using a symbolic software from the appendix in [110].

(4.39) can be written as

$$t_{re} \leq \frac{1}{k}\left[\delta_0|S(0)| + \frac{(1-\delta_0)}{\alpha^{\frac{1}{p}}}\right] \quad (4.40)$$

If we choose

$t_{rs} = \frac{1}{k}\left[\delta_0|S(0)| + \frac{(1-\delta_0)}{\alpha^{\frac{1}{p}}}\right]$

(4.41)

We can be rest assured the reaching time, t_{re} is going to be less than the desired reaching time, t_{rs}. If α is bigger in the given bound

$$\alpha \gg \left(\frac{1-\delta_0}{\delta_0|S(0)|}\right)^{\frac{1}{p}} \quad (4.42)$$

$$k \approx \frac{\delta_0|S(0)|}{t_{rs}} \quad (4.43)$$

This shows that the gain can be adjusted to a desired value.

4.2.2 Systems With Disturbances

As it has been shown in (4.28), $K > D$ is chosen so as to ensure stability. In the case of ERL, the control law for the second order system in (4.15) is derived by using putting (4.30) into (4.16).

$$u = \frac{\ddot{x}_d - c\dot{e} - \frac{k}{N(S)} sgn(S) - f(x_1, x_2, t)}{g(x_1, x_2, t)} \tag{4.44}$$

Where $N(S) = \delta_0 + (1 - \delta_0)e^{-\propto|S|^p}$

From (4.17)

$$\dot{S} = -\frac{k}{\delta_0 + (1-\delta_0)e^{-\propto|S|^p}} sgn(S) + D \tag{4.45}$$

$$k > D\delta_0 + D(1 - \delta_0)e^{-\propto|S|^p} \tag{4.46}$$

Condition (4.46) is need for the sliding surface to converge to zero.

4.2.3 Systems With Parameter Uncertainties

$$\ddot{x} = f\dot{x} + u \tag{4.47}$$

Where β is unknown. $L_{MAX} = Sup\left|fx - \widehat{f}x\right|$

$$u = -c\dot{e} - \beta x + \ddot{x}_d - Ksgn(S) \tag{4.48}$$

From (4.17)

$$\dot{S} = fx - \hat{f}x - Ksgn(S) \tag{4.49}$$

$$K > fx - \hat{f}x \tag{4.50}$$

$$K > L_{MAX} \tag{4.51}$$

This is hold true for a convention sliding mode control.

For a ERL, the control law

$$u = -c\dot{e} - fx + \ddot{x}_d - \frac{k}{\delta_0 + (1-\delta_0)e^{-\propto|S|^p}} sgn(S) \tag{4.51}$$

From (4.17)

$$\dot{S} = fx - \hat{f}x - \frac{k}{\delta_0 + (1-\delta_0)e^{-\propto|S|^p}} sgn(S) \tag{4.52}$$

$k > L_{MAX}\delta_0 + L_{MAX}(1-\delta_0)e^{-\propto|S|^p}$
(4.53)

The gain is selected based on this so that the sliding surface approach zero in a finite time. This analysis shows that the reaching time of the ERL is smaller than the reaching time of SMC. $k = 0.5, \delta_0 = 0.8, \alpha = 0.1, p = 1.$

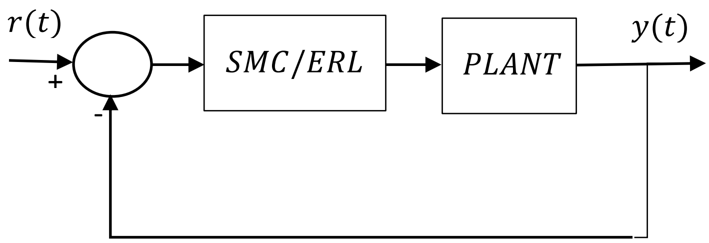

Figure 4.2 Block Diagram of Closed Loop SMC or ERL

CHAPTER V

SIMULATION TESTS

5.1 System Identification

A filter with the same denominator as the transfer function of the plant is needed to ensure that estimated parameters are good enough to be considered as the real values of the system dynamics. An open loop simulation is carried out on the system with the saturation block being added to limit the size of the control signal entering the plant within the range of 0 to 10.

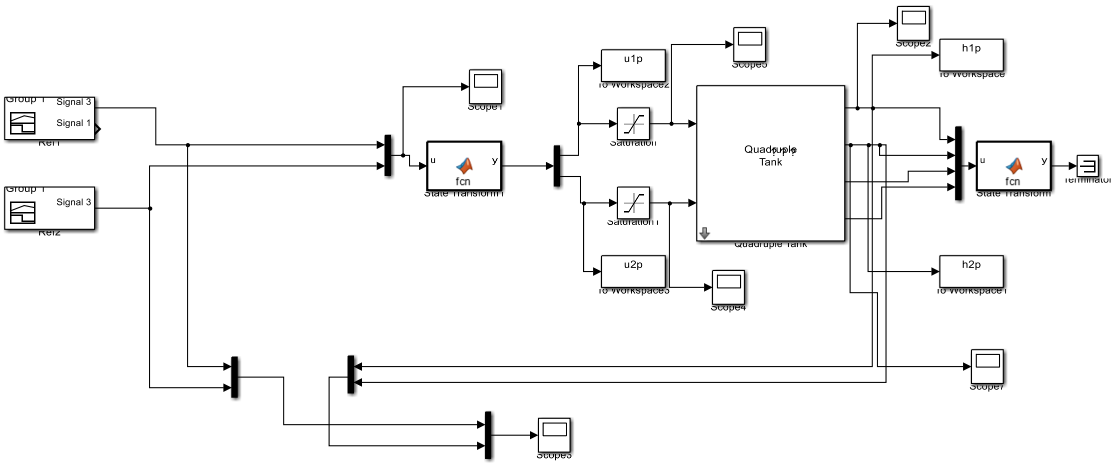

Figure 5.1 Open Loop Simulation of QTP

An identification toolbox has been used to generate the transfer function of each of the two outputs (y_1, y_2) with respect to their individual inputs (r_1, r_2). Below are the respective transfer functions after the simulation by assuming the plant is second order. A first order can also be used for system identification. A Pseudorandom Noise signal is used as the input signal in an open loop simulation because it is sufficiently rich to provide more parametric information about the plant. The code in the Appendix generates the object data to be uploaded and imported to the identification platform for the transfer function of the system to be identified. The transfer functions have been obtained for both the minimum and non-minimum phase of the QTP. From Figure 5.1, we obtained

Minimum Phase

$$G_1(s) = \frac{Y_1}{R_1} = \frac{67.98s+13.81}{s^2+10.31s+2.177} \tag{5.1}$$

$$G_2(s) = \frac{Y_2}{R_2} = \frac{12.86s+156.6}{s^2+11.86s+4.18}$$

(5.2)

Therefore, the corresponding filters are:

$$F_1(s) = s^2 + 10.31s + 2.177 \tag{5.3}$$

$$F_2(s) = s^2 + 11.86s + 4.18 \tag{5.4}$$

Non-minimum Phase

$$G_1(s) = \frac{Y_1}{R_1} = \frac{64.23s+17.66}{s^2+10.54s+2.983} \tag{5.5}$$

$$G_2(s) = \frac{Y_2}{R_2} = \frac{71.91s+1.012*10\text{^}4}{s^2+10.02s+239.6} \tag{5.6}$$

Therefore, the corresponding filters are also:

$$F_1(s) = s^2 + 10.54s + 2.983 \tag{5.7}$$

$$F_2(s) = s^2 + 10.02s + 239.6 \tag{5.8}$$

5.2. Adaptive SMC and ERL Design

The model of the QTP is considered to be second order. The polynomials of the transfer function are estimated using the gradient method.

$$y_P(s) = \frac{b_1s+b_0}{s^2+a_1s+a_0}u_P(s)$$

(5.9)

Both sides of (5.9) are divided by a filter, $F_1(s) = s^2 + 10.31s + 2.17$ and $F_2(s) = s^2 + 11.86s + 4.18$ represent the denominators of the second order transfer functions of QTP obtained through an open loop simulation of the system and the response signals are then imported to identification toolbox where the transfer functions of QTP are being estimated. Using a filter with similar parameters as the system is an easy way of choosing a good filter without randomly going through many filters which may not actually work. The coefficients of the filters are multiplied by a factor of 10^{-2} for smoother responses as depicted in Figures 5.4, 5.9 and 5.14.

$$\frac{y_p}{F}s^2 = [b_1\ \ b_0\ \ a_1\ \ a_0]\left[\frac{u_p s}{F}\ \frac{u_p}{F}\ \ \frac{-y_p s}{F}\ \ \frac{-y_p}{F}\right]^T$$

(5.10)

Where $z = \frac{y_p}{F}s^2$, $\theta_p^* = [b_1\ \ b_0\ \ a_1\ \ a_0]$, $\varphi = \left[\frac{u_p s}{F}\ \frac{u_p}{F}\ \ \frac{-y_p s}{F}\ \ \frac{-y_p}{F}\right]^T$, $F(s) = s^2 + f_1 s + f_0$ which implies that the estimated parameters can be written as:

$$\dot{\theta}_p = \gamma\varepsilon\varphi, \qquad \theta(0) = \theta_0 \tag{5.11}$$

$$\varepsilon = \frac{z-\theta_p\varphi}{m_s}, \qquad m_s^2 = 1 + \varphi^T\varphi$$

(5.12)

Where $\gamma = \gamma^T > 0$ is the adaptation gain and $\theta_p = \left[\hat{b}_1\ \ \hat{b}_0\ \ \hat{a}_1\ \ \hat{a}_0\right]^T$. By using the certainty equivalence principle, the estimated parameters of the plant are replaced instead of the actual parameters. The parameters of the controller then become: $\hat{P}(s) = \hat{p}_2 s^2 + \hat{p}_1 s + \hat{p}_0$, $L(s) = s + \hat{l}_0$, $A^* = (s+1)^4$ and $Q_m = s$. These coefficients satisfy the Diophantine equation below.

$$(s + l_0)(s^2 + a_1 s + a_0) + (p_2 s^2 + p_1 s + p_0)(b_1 s + b_0) = (s + 1)^4 \tag{5.13}$$

Solving (5.13) using Sylvester's equation yields [115]:

$$\begin{cases} \hat{l}_0 = \frac{\hat{b}_0^2\hat{b}_1(\hat{a}_0-6)+\hat{b}_0^3(4-\hat{a}_1)+4\hat{b}_1^2\hat{b}_0-\hat{b}_1^3}{\hat{b}_0^3-\hat{a}_1\hat{b}_1\hat{b}_0^2+\hat{a}_0\hat{b}_1^2\hat{b}_0} \\ \hat{p}_2 = \frac{4-\hat{a}_1-\hat{l}_0}{\hat{b}_1} \\ \hat{p}_1 = \frac{\hat{b}_0\left(4-\hat{a}_0\hat{l}_0\right)-\hat{b}_1}{\hat{b}_0^2} \\ \hat{p}_0 = \frac{1}{\hat{b}_0} \end{cases}$$

(5.14)

The control law can be written as:

$$u_{pi} = \frac{s^2+f_1 s+f_0-s(s+\hat{l}_0)}{s^2+f_1 s+f_0}u_p - \frac{\hat{p}_2 s^2+\hat{p}_1 s+\hat{p}_0}{s^2+f_1 s+f_0}(y_p - r)$$

(5.15)

and that of ASMC can also be written as:

$u_i = \frac{1}{\hat{b}_0}\left(-c\dot{e} + \hat{a}_1 x_2 + \hat{a}_0 x_1 - \hat{b}_1 u_2 + \ddot{x}_d - ksat\left(\frac{S}{\delta}\right)\right)$

(5.16)

and also ERL-ASMC can be illustrated as:

$$u_i = \frac{1}{\hat{b}_0}\left(-c\dot{e} + \hat{a}_1 x_2 + \hat{a}_0 x_1 - \hat{b}_1 u_2 + \ddot{x}_d - \frac{k}{\delta_0 + (1-\delta_0)e^{\propto|S|^p}} sgn(S)\right) \quad (5.17)$$

Where $\dot{V} = -k|S| < 0$, which guarantees the stability of the closed-loop system. By changing the control gain, k we reduce the sharpness of the output responses of the sliding mode controller in order to make them smooth as shown in Figures 5.4, 5.5 and 5.6.

5.3 PID Control Design

The Employed PID control law is given by:

$$u(t) = K_c e(t) + K_i \int_0^t e(\tau)d\tau + K_d \frac{de(t)}{dt} \quad (5.18)$$

Where $e(t)$ represents the feedback error, $u(t)$ represents the control signal, and PID parameters of respective decentralized controllers are given in Table 5.1.

Table 5.1 Control parameters of decentralized control loops under PID control given in Figure 5.2

	PID 1	PID 2
Proportional gain K_c	3.0	2.7
Integral gain K_i	0.1	0.0625
Derivative gain K_d	4.0	5

The decentralized ASMC and ERL are similar to the decentralized APPC in structure, except that the control law in the APPC is replaced by the SMC law in (5.16) for ASMC and ERL control input in (5.17) for ERL. Simulation tests are performed and results are analysed for the three cases of robustness to set point variations, disturbance rejection, and robustness to parametric uncertainty. The simulation is run for 250 seconds for each case.

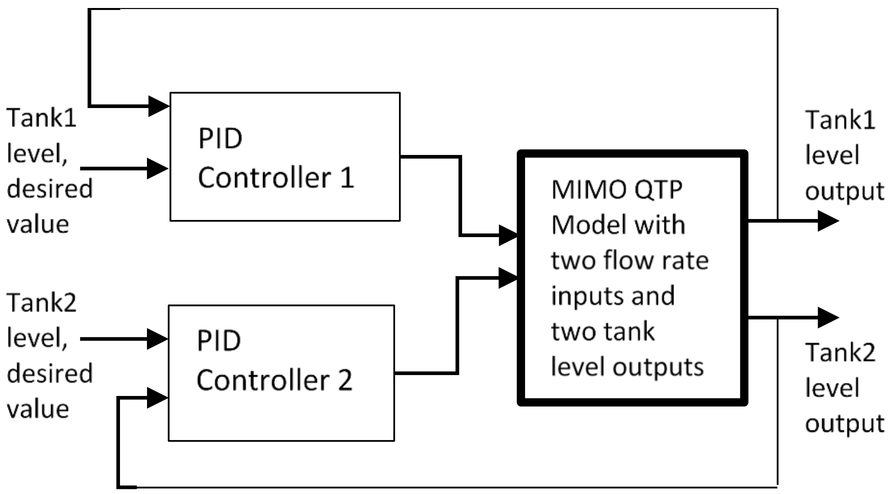

Figure 5.2 Block Diagram of Closed Loop Decentralized PID Control of QTP.

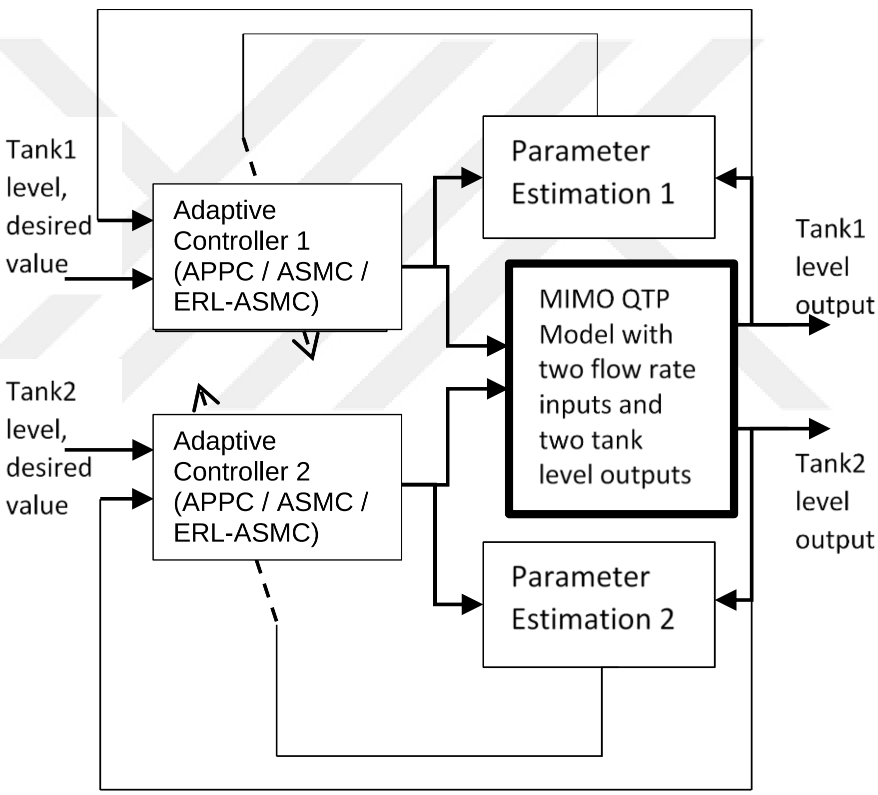

Figure 5.3 Diagram of Closed Loop Decentralized Control of APPC or ASMC or ERL-ASMC of QTP.

Mean Square Error (MSE), Integral Square Error (ISE), Integral Absolute Error (IAE), and Integral of Time Weighted Absolute Error (ITAE) performance indices formulated in (5.19-5.22) are calculated for each case in order to analyze the performance of each controller.

$$MSE = \frac{1}{N}\int_0^{infinity} e^2(t)dt \tag{5.19}$$

$$ISE = \int_0^{infinity} e^2(t)dt \tag{5.20}$$

$$IAE = \int_0^{infinity} |e(t)|dt \tag{5.21}$$

$$ITAE = \int_0^{infinity} t|e(t)|dt \tag{5.22}$$

The performance indices are presented in Tables 5.2-5.4, where the values in bold fonts indicate the lowest index value in each case.

The perfomances of the controllers can also be evaluated based on their transient response specifications. The transient response can exhibit either first order or second order behaviour before reaching the steady state. The first order behaviour has no overshoots but sluggish while the second order behaviour tends to have overshoots however it is faster in arriving at the desired reference input. There are various ways to characterise the transient response of the system. These specifications include delay time, dead time, peak time, maximum overshoot and settling time especially for a second order behaviour. The main specifications that are going to be used to analyse the performance of the controller are [132]:

1. Settling Time, t_s

It is the time it takes for the output response to reach 95% or 98% of its desired value. The smaller the settling time, the faster the response.

2. Peak Time, t_p

It is the time it takes for the response to reach the first peak of the overshoot.

3. Maximum Overshoot

It is the maximum peak value of the response signal which is measured from the desired reference signal. It is sometimes defined in terms of percentage if the desired reference input is different than unity.

$$Maximum\ percent\ overshoot = \frac{y(t_p) - y(\infty)}{y(\infty)}$$

(5.23)

The smaller the maximum percent overshoot, the better the performance of the designed controller.

5.4. Robustness to Set Point Variations

In order to reveal the robustness properties of PID, APPC, ASMC and ERL-ASMC control strategies with respect to set point variations, three simulation tests are implemented with the set point values of 12.8, 15.8, 9.8 centimeters for Tank1, and 14, 17, 11 centimeters for Tank2. Simulation results are presented for the three sets of set point values in Figures 5.4, 5.9, and 5.14, respectively. Performance indices are tabulated in Tables 5.2, 5.4 and 5.6. ERL is short form of ERL-ASMC.

Table 5.2 Performance indices of PID, APPC, ASMC and ERL with 12.8 and 14 cm reference inputs

	Tank1				Tank2			
	PID	APPC	ASMC	ERL	PID	APPC	ASMC	ERL
MSE	2.5×10^{-3}	$\mathbf{8.5451\times 10^{-7}}$	9.0×10^{-4}	1.6400×10^{-4}	0.0474	0.0442	**0.0189**	**0.0273**
ISE	630.5795	**2.6941**	222.0008	40.999	1.18×10^{4}	1.3939×10^{5}	$\mathbf{4.720\times 10^{3}}$	6.8202×10^{3}
IAE	6.06×10^{3}	**620.4401**	956.9577	$\mathbf{1.1587\times 10^{3}}$	1.91×10^{4}	2.3161×10^{5}	$\mathbf{1.072\times 10^{4}}$	$\mathbf{9.9052\times 10^{3}}$
ITAE	3.80×10^{8}	5.412×10^{8}	$\mathbf{1.406\times 10^{7}}$	1.4606×10^{8}	1.20×10^{9}	1.8562×10^{11}	1.089×10^{9}	$\mathbf{8.2495\times 10^{8}}$

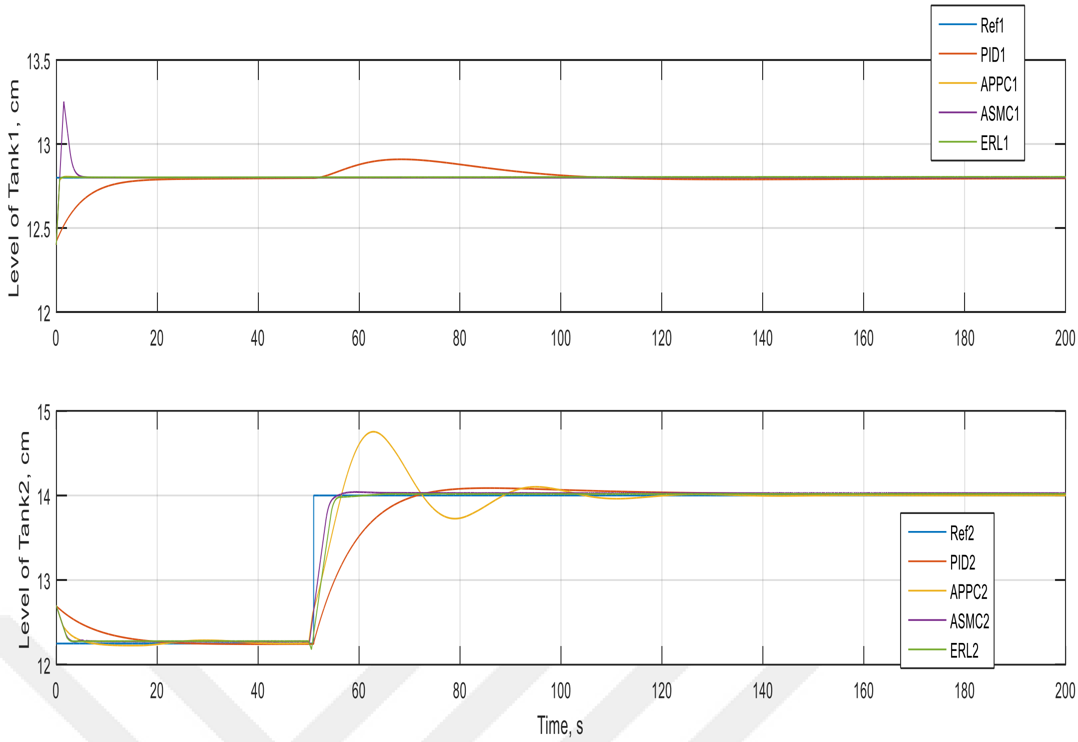

Figure 5.4 Closed Loop Responses of PID (red), APPC (yellow), ASMC (purple) and ERL-ASMC (green) of QTP in Minimum Phase with 12.8 and 14 cm reference inputs (blue).

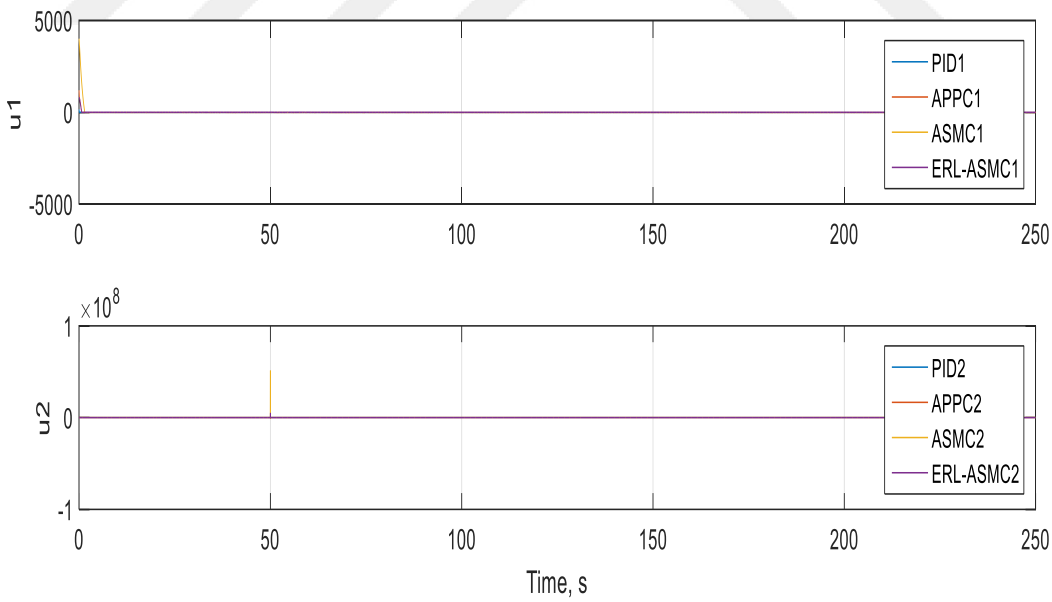

Figure 5.5 Control signal of PID (blue), APPC (red) , ASMC (yellow) and ERL-ASMC (purple) of QTP in Minimum Phase with 12.8 and 14 cm reference inputs.

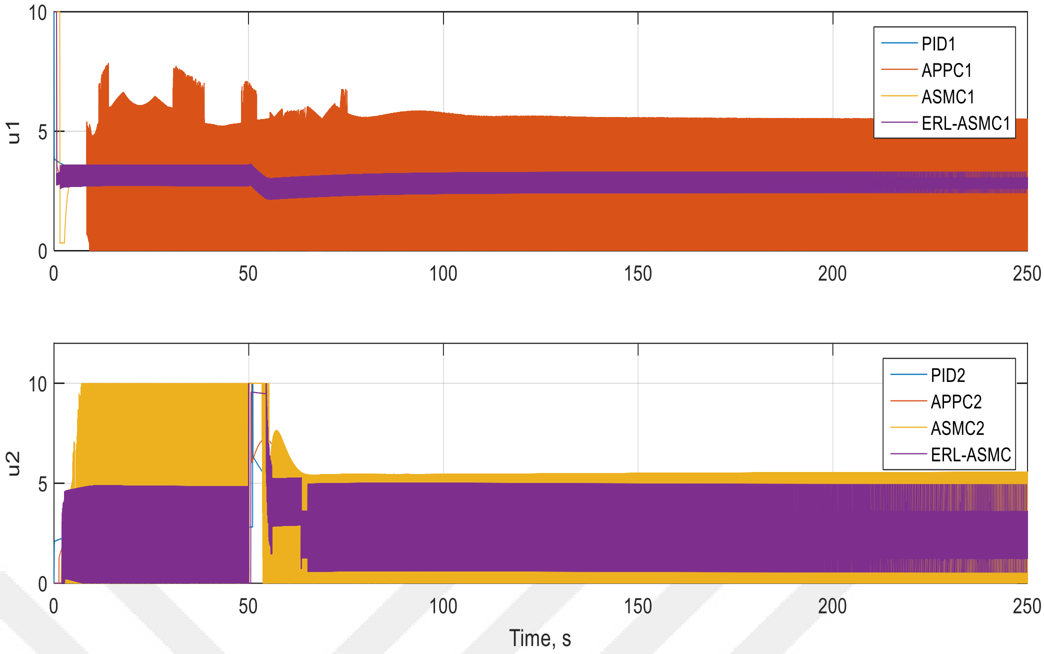

Figure 5.6 Control signal of PID (blue), APPC (red) , ASMC (yellow) and ERL-ASMC (purple) of QTP in Minimum Phase with 12.8 and 14 cm reference inputs after saturation.

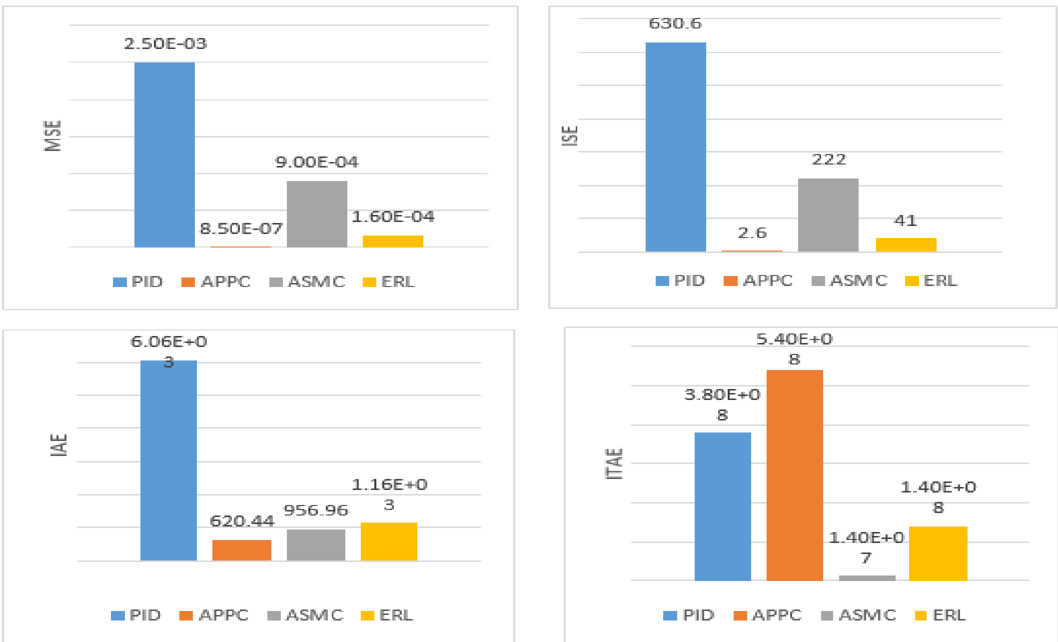

Figure 5.7 Performance indices of Tank1 with 12.8 cm reference input

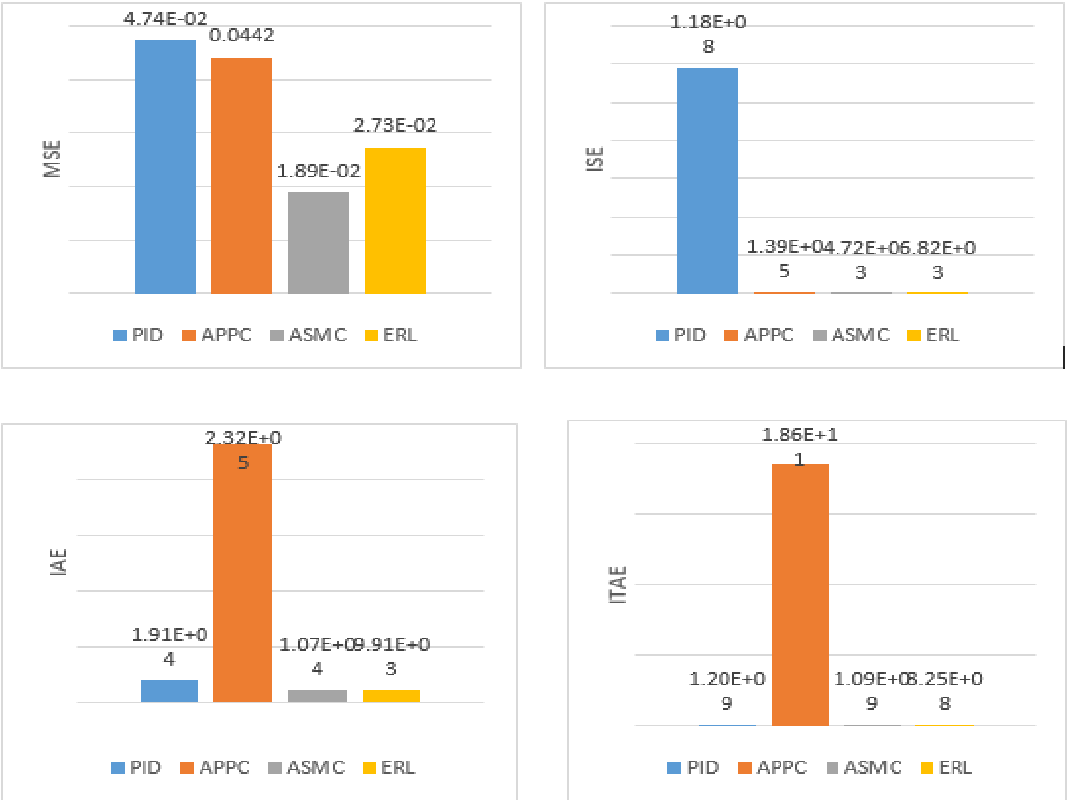

Figure 5.8 Performance indices of Tank2 with 14 cm reference input

Table 5.3 Transient Response Specification of PID, APPC, ASMC and ERL with 12.8 and 14 cm reference inputs

	Tank1				Tank2			
	PID	APPC	ASMC	ERL	PID	APPC	ASMC	ERL-ASMC
Settling Time	159.84	0.85	4.81	**0.67**	121.62	113	62.57	**55.53**
Maximum Overshoot (%)	0.83	0.05	3.54	**0.04**	0.62	5.4	0.29	**0.14**
Peak Time	68.3	2.1	1.49	250	85.58	62.85	**59.43**	249.74

The output responses of PID, APPC, ASMC and ERL-ASMC with set point values of 12.8 and 14 cm for Tank1 and Tank2, respectively are shown in Figure 5.4. In this figure, ERL-ASMC has the fastest response time of 0.6730 s for Tank1 and 55.53 s for Tank2 after an initial delay of 50 s for Tank2. APPC has faster response time of 0.85 s for Tank1 and 113 s for Tank2, while ASMC has satisfactory response time of

4.81 s for Tank1 and 62.57 for Tank2 with a delay of 50 s for Tank2. PID has the worst response time of 159.84 s for tank1 and 1 s after a delay of 121.62 s for Tank2.

The performance indices of Tank1 with 12.8 cm and 14 cm step input are represented in Table 5.2, Figure 5.7 and 5.8. In both figures, the proposed ERL-ASMC has the smallest values for the performance indices for the IAE and ITAE performance indices of Tank2. The proposed ERL-ASMC underperforms in these performance indices shown in Table 5.2 due to the accumulation of small insignificant steady-state errors in the output responses of the ERL-ASMC that are persistent over a long period of time. Small values of the performance indices indicate that the controller has a good performance. APPC has the lowest performance indices in tank1 and the highest performance indices except for its MSE in tank2. This is because of the huge overshoots caused by the time delay. ASMC tends to have the lowest performance indices in tank2. PID has the largest performance indices in tank1 due to the high settling in Table 5.3. The smallest values in each performance index relating to the controllers are indicated in Table 5.2, Figure 5.7 and 5.8. The control signals generated by the adaptive controllers appeared to huge compared to the PID as indicated in Figure 5.5. Even after saturation block is being used, the adaptive controls produced boundary layers as depicted in Figure 5.6. The proposed ERL-ASMC has lower control signals compared to APPC and ASMC.

Table 5.4 Performance indices of PID, APPC, ASMC and ERL-ASMC with 15.8 and 17 cm reference inputs

	Tank1				Tank2			
	PID	APPC	ASMC	ERL	PID	APPC	ASMC	ERL-ASMC
MSE	0.1205	0.1615	**0.0897**	0.0973	0.1283	0.2303	0.0676	**0.0668**
ISE	3.0113×10^4	**2.6941**	2.2414×10^4	2.4314×10^4	3.2086×10^4	1.3939×10^5	1.6894×10^4	$\mathbf{1.6708\times 10^4}$
IAE	2.7452×10^4	2.5663×10^4	$\mathbf{1.0782\times 10^4}$	1.2438×10^4	3.9106×10^4	4.6354×10^4	1.2114×10^4	$\mathbf{1.1801\times 10^4}$
ITAE	7.4686×10^8	2.3586×10^8	4.1516×10^7	$\mathbf{11.8377\times 10^3}$	1.7670×10^9	1.1851×10^9	$\mathbf{2.4561\times 10^8}$	3.0994×10^8

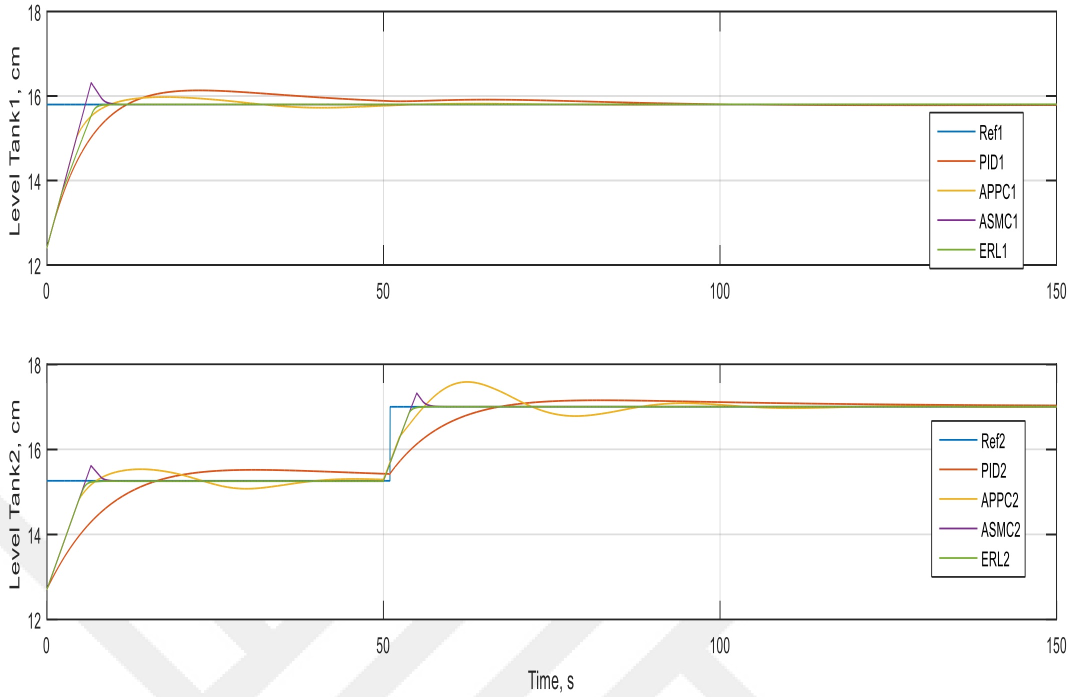

Figure 5.9 Closed Loop Responses of PID (red), APPC (yellow), ASMC (purple) and ERL-ASMC (green) of QTP in Minimum Phase with 15.8 and 17 cm reference inputs (blue).

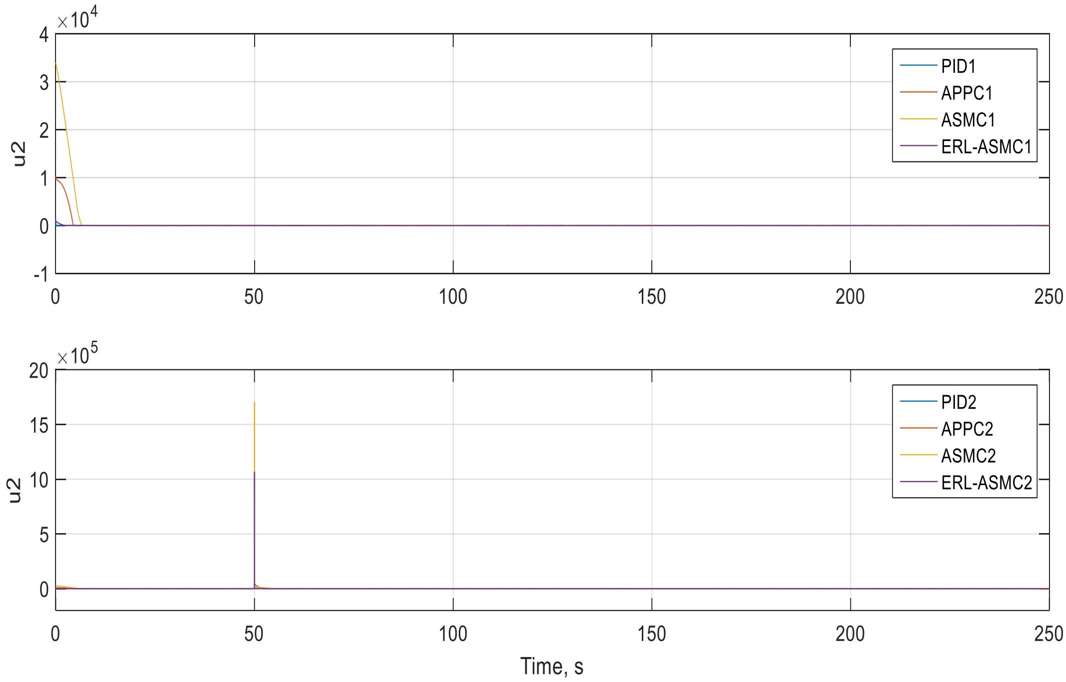

Figure 5.10 Control signal of PID (Blue), APPC (red) , ASMC (yellow) and ERL-ASMC (purple) of QTP in Non-minimum Phase with 15.8 and 17 cm reference inputs

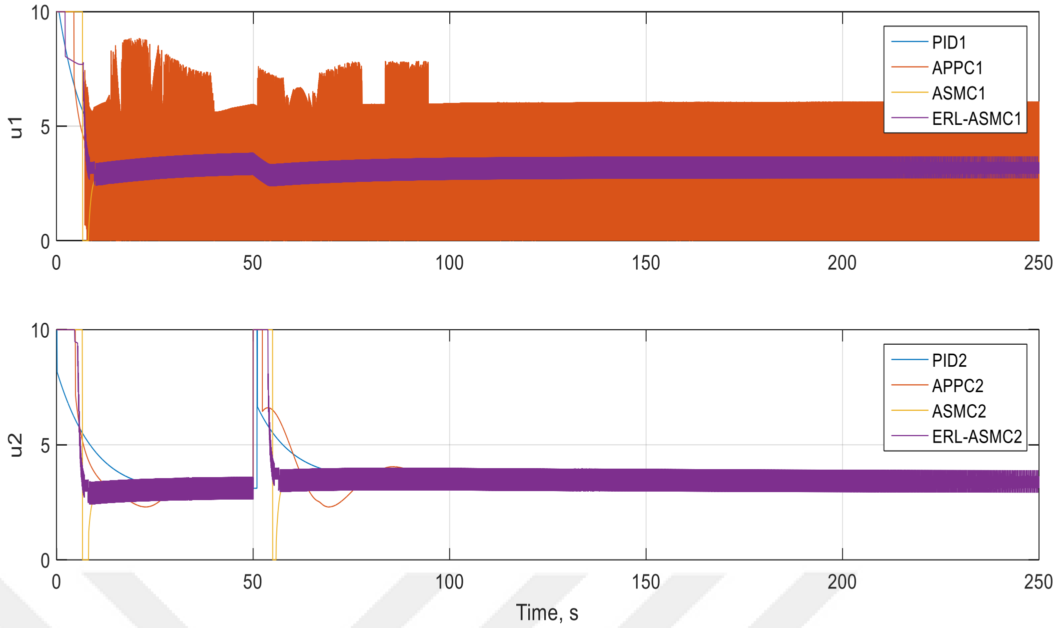

Figure 5.11 Control signal of PID (blue), APPC (red) , ASMC (yellow) and ERL-ASAMC (purple) of QTP in Non-minimum Phase with 15.8 and 17 cm reference inputs after saturation.

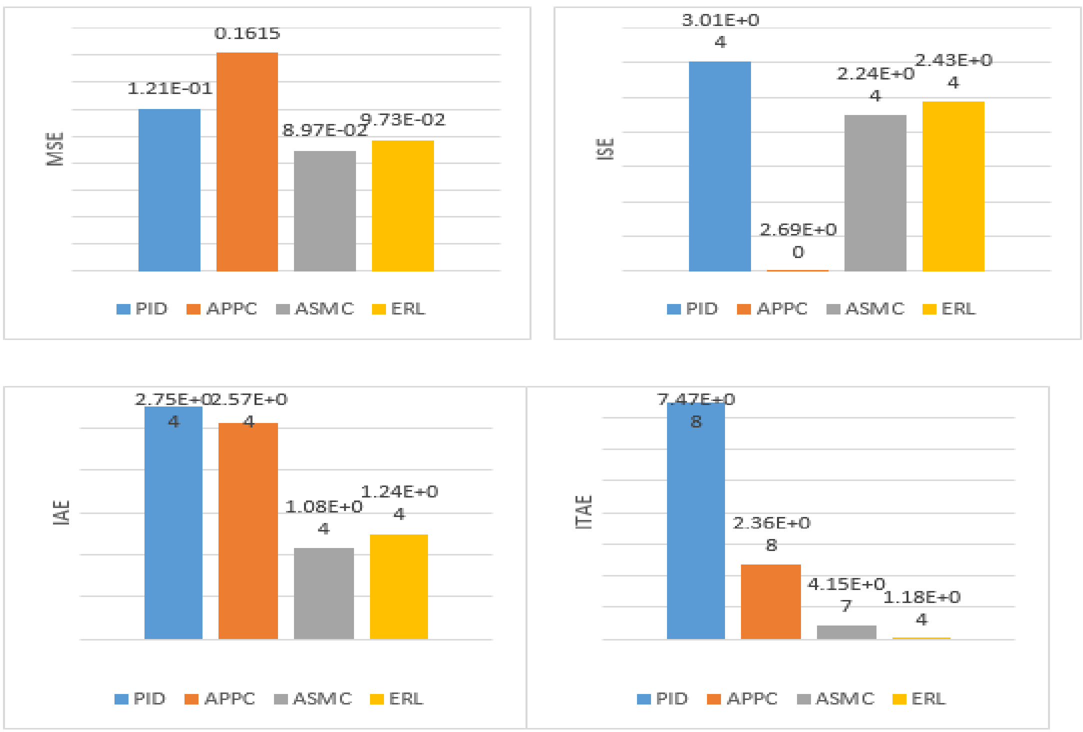

Figure 5.12 Performance indices of Tank1 with 15.8 cm reference input

Figure 5.13 Perfo rmance indices of Tank2 with 17 cm reference input

Table 5.5 Transient Response Specification of PID, APPC, ASMC and ERL-ASMC with 15.8 and 17 cm reference inputs

	Tank1				Tank2			
	PID	APPC	ASMC	ERL	PID	APPC	ASMC	ERL-ASMC
Settling time	81.0	44.08	8.62	**7.32**	108.82	85.17	56.11	**54.08**
Maximum Overshoot (%)	2.11	1.12	3.25	**0.04**	0.90	3.44	1.89	**0.03**
Peak Time	22.64	17.48	**6.59**	249.6	82.23	62.45	**54.95**	249.7

The output responses of PID, APPC, ASMC and ERL-ASMC with 15.8 cm reference input for Tank1 and 17 cm reference input for Tank2 are shown in Figure 5.9. It is clear from this figure that ERL-ASMC has the smallest settling time of 7.32 s for

Tank1 and 54.08 s with an initial delay of 50 s for Tank2, followed by ASMC which has a settling time of 8.62 s for Tank1 and 56.11 s with a delay of 50 s for Tank2. PID control exhibits the biggest settling time of 81 s for Tank1 and 108.92 s with a delay of 50 s for Tank2.

Table 5.4, Figure 5.12 and 5.13 represent the performance indices of Tank1 and Tank2. In both figures, the proposed ERL-ASMC and ASMC have the smallest value for each performance index than APPC and PID except in Tank1 where the ISE of APPC has the lowest value. It is also shown clearly in both figures that PID has a smaller value for each performance index than APPC except for ISE, IAE and ITAE performance indices in Tank1. This is because of the huge overshoots that are being exhibited by the output responses of Tank1. Similar to previous level response, APPC has the biggest errors in tank2 because of the time delay.

The control signals represented in Figure 5.10 have higher values except for the proposed ERL-ASMC. And it is even more clearly shown in Figure 5.11. However, it has a visible boundary layer.

Table 5.6 Performance indices of PID, APPC, ASMC and ERL-ASMC with 9.8 and 11 cm reference inputs

	Tank1				Tank2			
	PID	APPC	ASMC	ERL	PID	APPC	ASMC	ERL-ASMC
MSE	0.1121	0.1371	**0.0935**	0.0940	0.3737	0.5492	**0.2988**	0.3029
ISE	2.8031×10^4	3.4270×10^4	2.3386×10^4	$\mathbf{2.2490\times 10^4}$	9.3414×10^4	1.3729×10^5	$\mathbf{1.6894\times 10^4}$	7.5719×10^4
IAE	2.9282×10^4	2.4811×10^4	$\mathbf{1.3509\times 10^4}$	1.8439×10^4	6.1250×10^4	7.6483×10^4	$\mathbf{3.4377\times 10^4}$	3.8139×10^4
ITAE	7.0774×10^8	2.4803×10^8	$\mathbf{5.2029\times 10^7}$	7.0743×10^8	1.8037×10^9	1.9387×10^9	$\mathbf{3.6252\times 10^8}$	8.2523×10^8

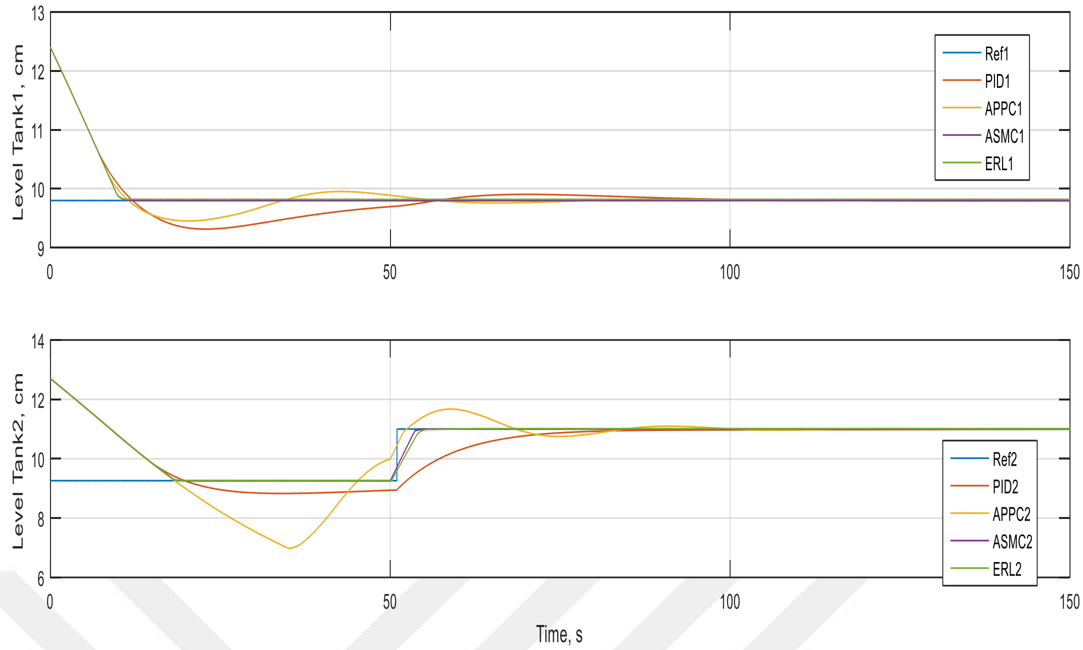

Figure 5.14 Closed Loop Responses of PID (red), APPC (yellow), ASMC (purple) and ERL-ASMC (green) of QTP in Minimum Phase with 9.8 and 11 cm reference inputs (blue).

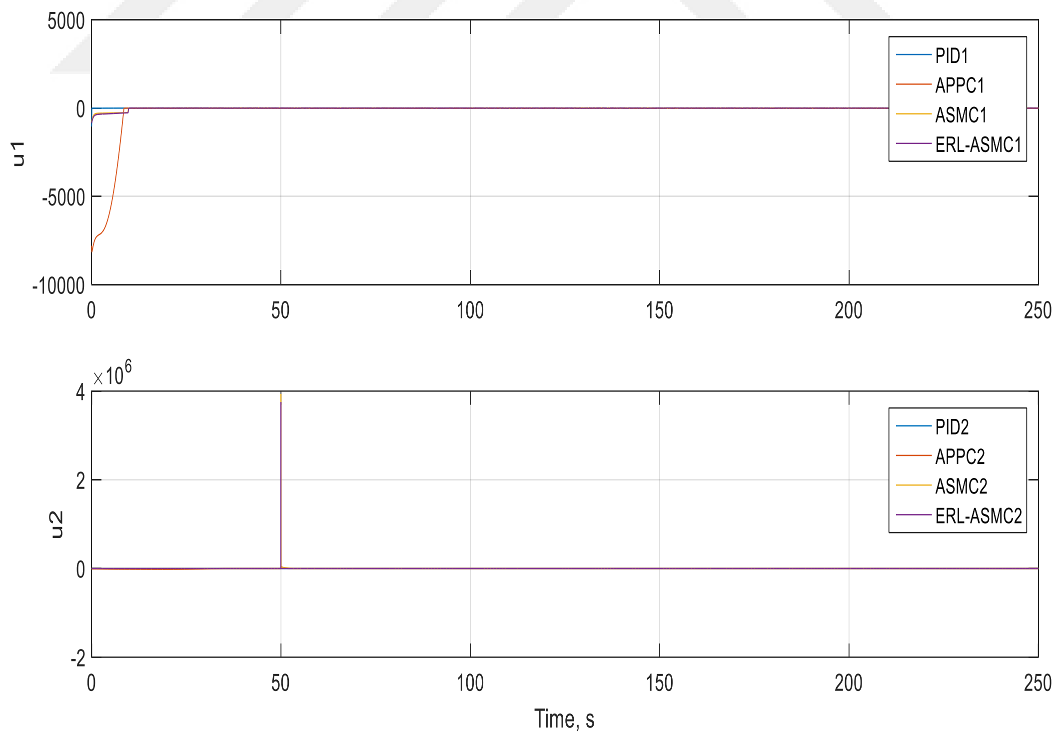

Figure 5.15 Control signal of PID (blue), APPC (red) , ASMC (yellow) and ERL (purple) of QTP in Non-minimum Phase with 9.8 and 11 cm reference inputs.

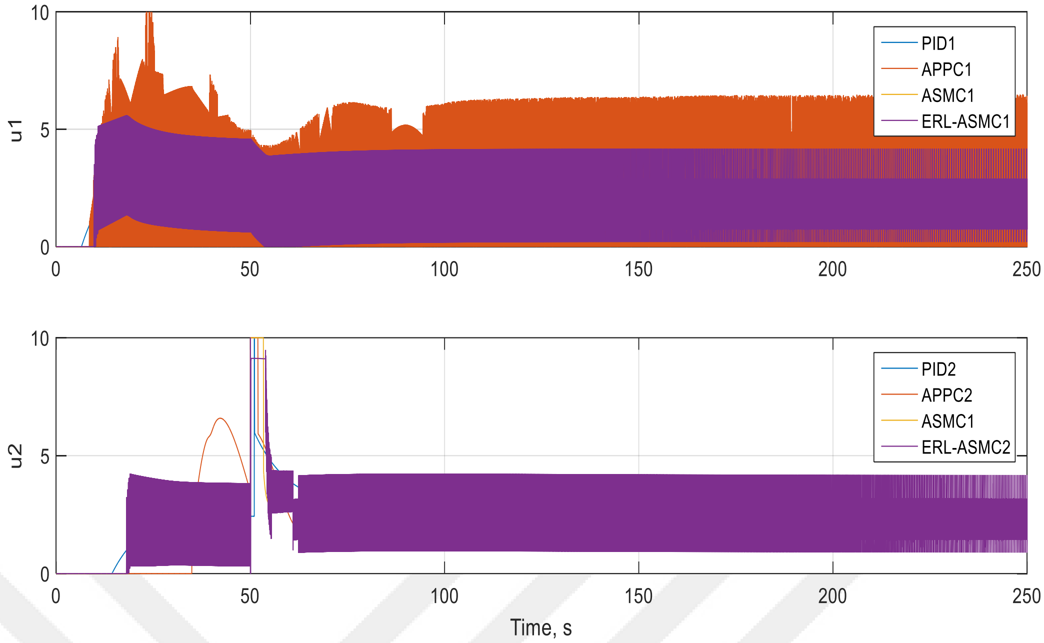

Figure 5.16 Control signal of PID (blue), APPC (red) , ASMC (yellow) and ERL-ASMC (purple) of QTP in Non-minimum Phase with 9.8 and 11 cm reference inputs after saturation.

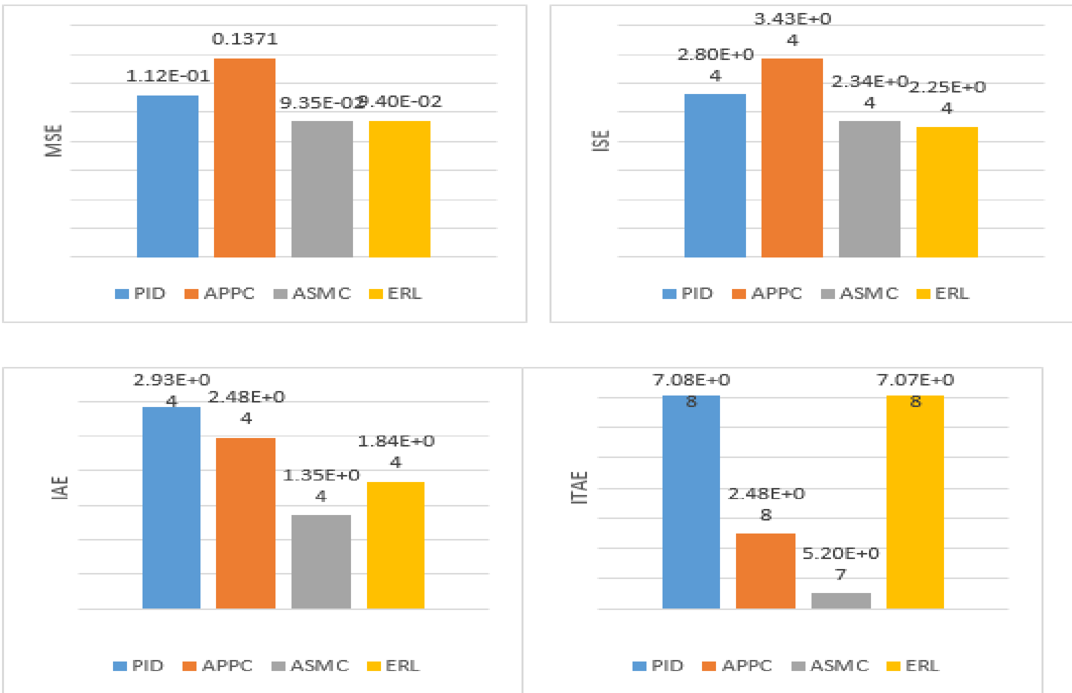

Figure 5.17 Performance indexes of Tank1 with 9.8 cm reference input

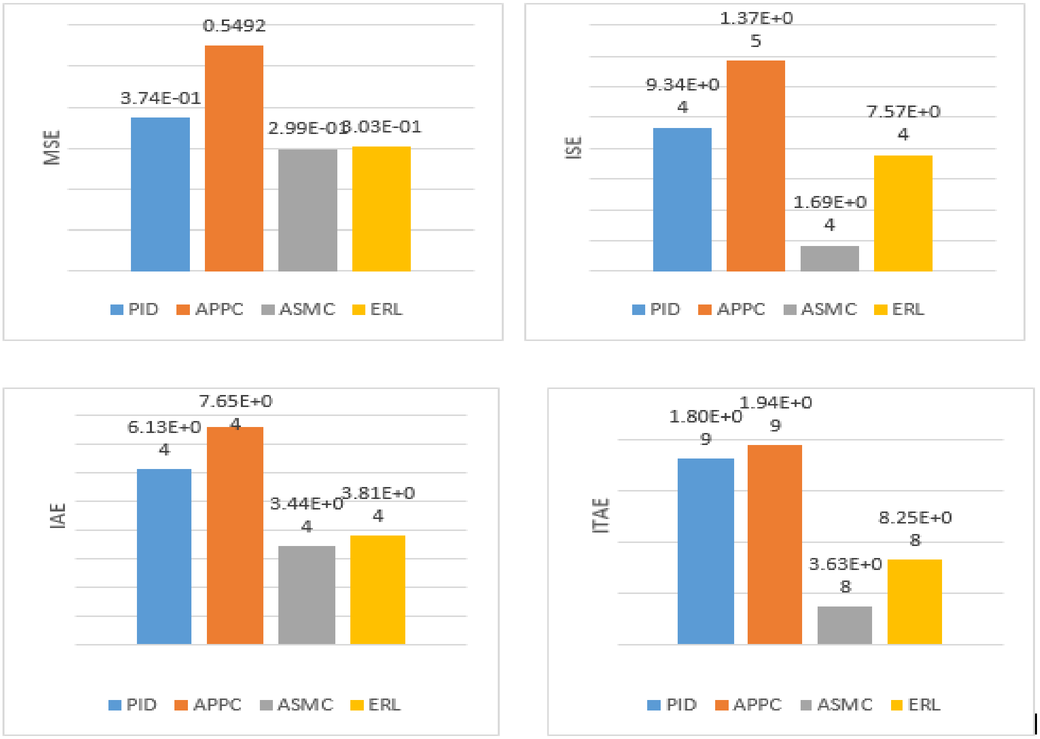

Figure 5.18 Performance indexes of Tank2 with 11 cm reference input

Table 5.7 Transient Response Specification of PID, APPC, ASMC and ERL-ASMC with 9.8 and 11 cm reference inputs

	Tank1				Tank2			
	PID	APPC	ASMC	ERL	PID	APPC	ASMC	ERL-ASMC
Settling time	87.86	52.66	**10.25**	10.28	87.27	94.03	**53.98**	54.94
Maximum Overshoot (%)	26.53	26.53	0.00	0.00	0.00	15.45	0.00	0.00
Peak Time	65.00	40.00	0.00	0.00	0.00	62.0	0.00	0.00

The output responses of PID, APPC, ASMC and ERL-ASMC with a signal input of 9.8 cm for Tank1 and 11 cm signal input for Tank2 are shown in Figure 5.14. In this figure, ASMC and ERL-ASMC are the quickest to reach the desired inputs with almost the same settling time at 10 s for Tank1 and at 54 s with a delay of 50 s for Tank2. APPC takes 52.66 s to reach the desired input for tank1 and 94.03 s with a delay of 50 s to arrive at the desired input of Tank2 which is faster than PID in Tank1 which takes a longer time of 87.86 s to reach the desired signal input of Tank1 and slower than PID in Tank2 at 87.27 s with an initial delay of 50 s to reach the desired input of Tank2.

The performance indices of Tank1 with 9.8 cm reference input and that of Tank2 with 11 cm reference input are represented in Table 5.6, Figure 5.17 and 5.18. In Table 5.6, ASMC has the lowest values for the performance indices of Tank1 and Tank2 with the exception of ISE where ERL has the smallest values. This is followed by the proposed ERL with values close to the values as ASMC. PID has smaller values for the performance indices in Table 5.6 than the APPC except IAE and ITAE performance indices for Tank1 in which the PID has the larger value of the performance indices.

In this simulation, the controllers have small control signals as depicted in both Figure 5.15 and 5.16. This is maybe attributed to the small reference inputs that are being used.

5.5. Disturbance Rejection

In order to test robustness of the designed controllers to disturbance inputs, a low frequency square wave signal with the frequency of 0.05 rad/s is superimposed onto the two level outputs of the QTP.

$$y_{ci} = y_i + d \tag{5.24}$$

Where y_{ci} denotes the total output, y_i is the disturbance-free output and d is the square wave disturbance input with unity amplitude given in Figure 5.19.

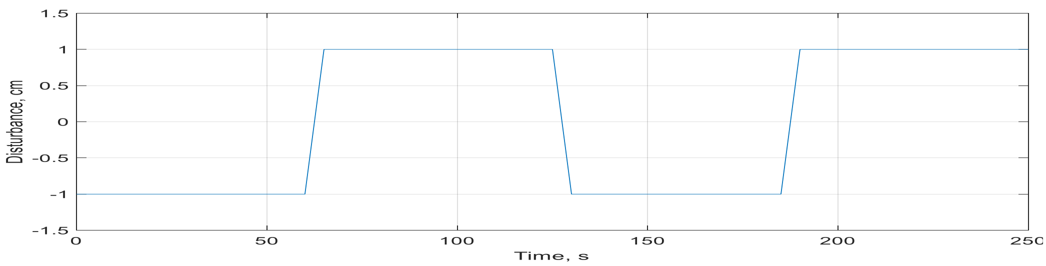

Figure 5.19 Disturbance signal that is assumed to corrupt the level output measurements

Table 5.8 Disturbance rejection of PID (red), APPC (yellow), ASMC (purple) and ERL-ASMC (green) of QTP in Minimum Phase with 12.8 and 14 cm reference inputs

	Tank1				Tank2			
	PID	APPC	ASMC	ERL	PID	APPC	ASMC	ERL-ASMC
MSE	1.853×10^{-1}	1.747×10^{-1}	1.121×10^{-1}	1.103×10^{-1}	2.032×10^{-1}	3.919×10^{-1}	1.444×10^{-1}	$\mathbf{1.427 \times 10^{-1}}$
ISE	4.6329×10^{4}	2.8020×10^{4}	$\mathbf{2.3386\times 10^{4}}$	2.7566×10^{4}	5.0809×10^{4}	9.7179×10^{4}	3.6105×10^{4}	$\mathbf{3.5677\times 10^{4}}$
IAE	5.7380×10^{4}	4.4348×10^{4}	2.3111×10^{4}	$\mathbf{2.2248\times 10^{4}}$	6.2706×10^{4}	8.8774×10^{4}	2.9646×10^{4}	$\mathbf{2.8102\times 10^{4}}$
ITAE	6.7556×10^{9}	5.3096×10^{8}	2.6305×10^{9}	$\mathbf{2.6065\times 10^{9}}$	7.6315×10^{9}	1.0496×10^{10}	33.3710×10^{9}	$\mathbf{3.2960\times 10^{9}}$

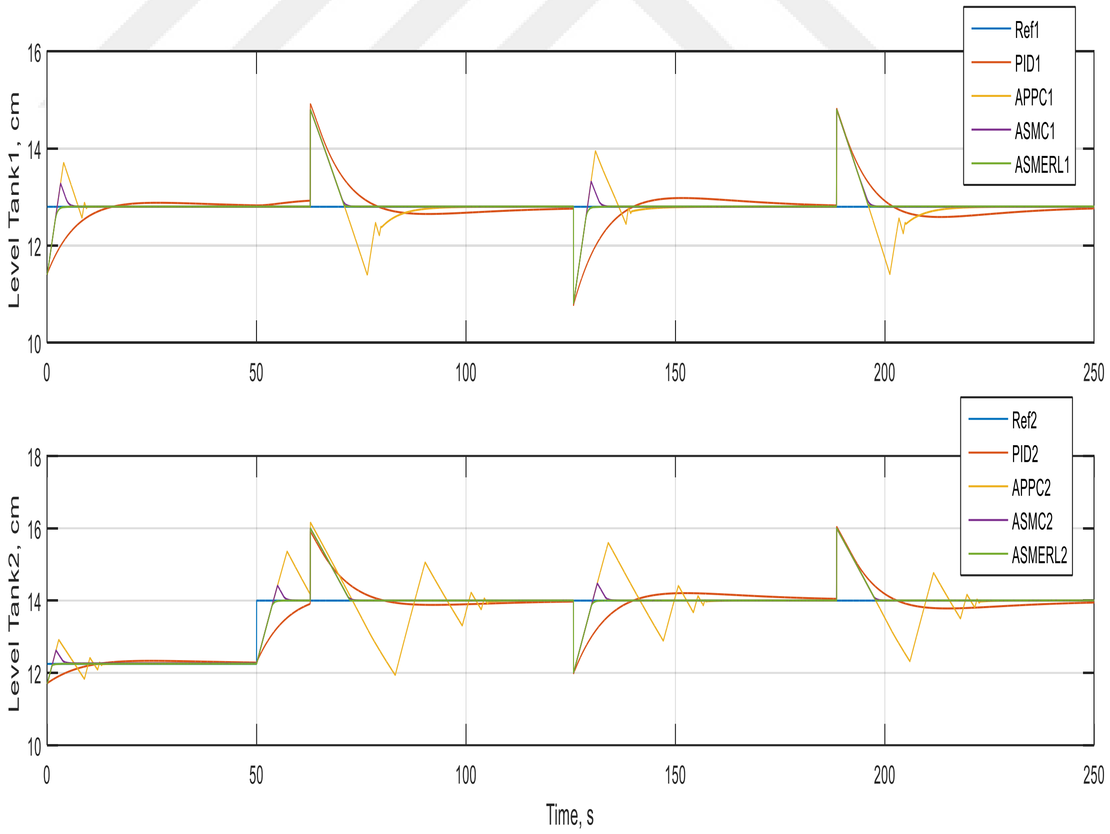

Figure 5.20 Closed Loop Responses of PID (red), APPC (yellow) , ASMC (purple) and ERL-ASMC (green) of QTP in Minimum Phase with 12.8 and 14 cm reference inputs (blue).

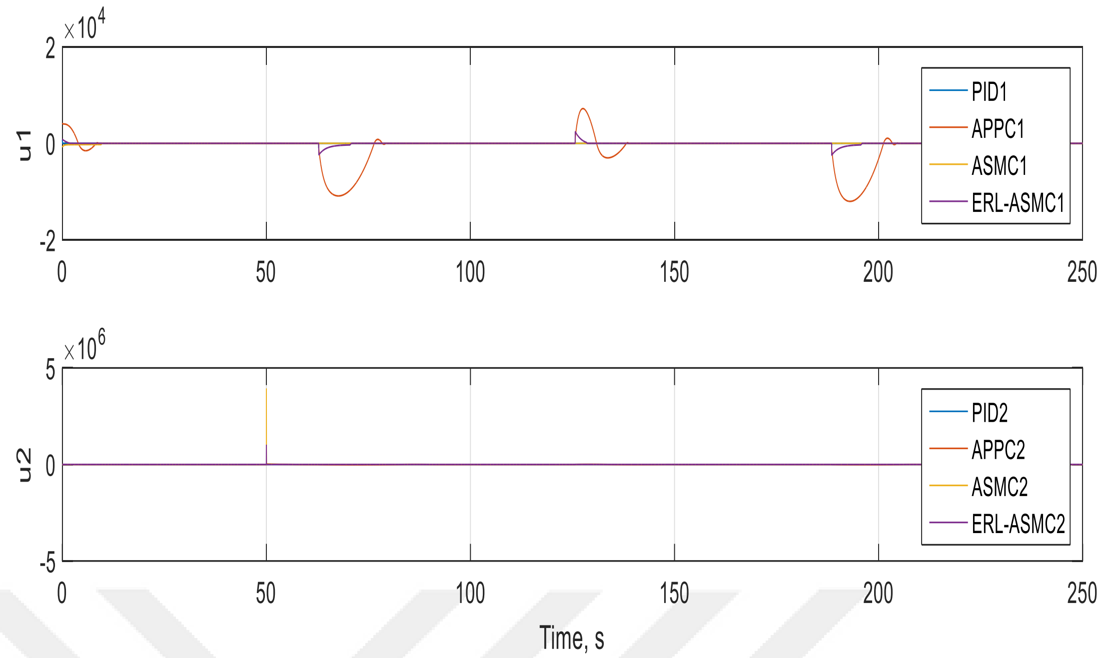

Figure 5.21 Control signal of PID (blue), APPC (red) , ASMC (yellow) and ERL-ASMC (purple) of QTP in Non-minimum Phase with 12.8 and 14 cm reference inputs.

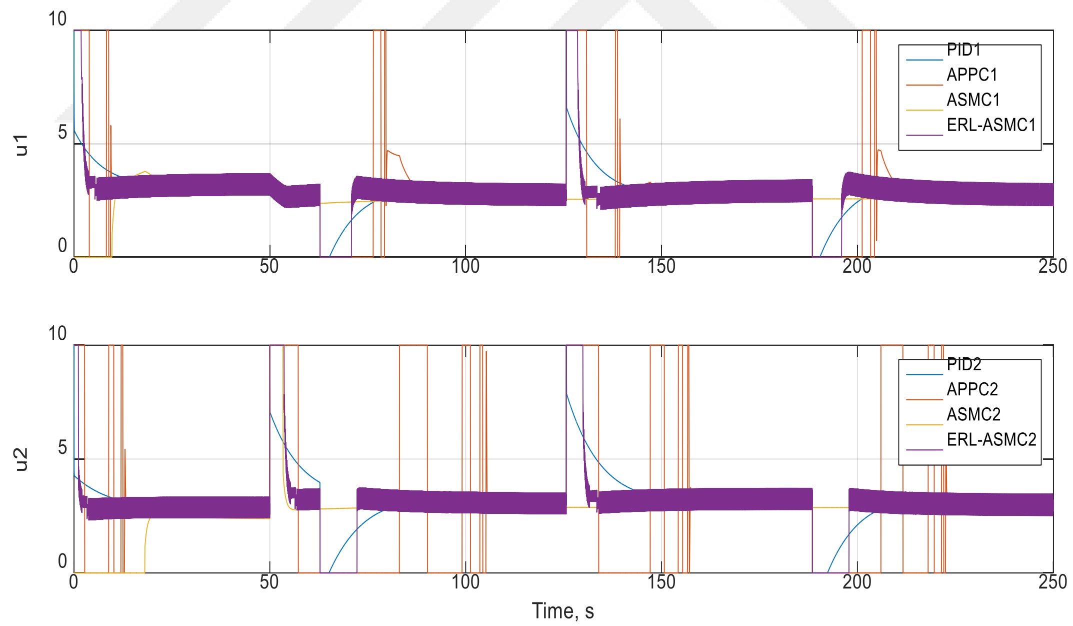

Figure 5.22 Control signal of PID (blue), APPC (red) , ASMC (yellow) and ERL-ASMC (purple) of QTP in Non-minimum Phase with 12.9 and 6.2 cm reference inputs after saturation.

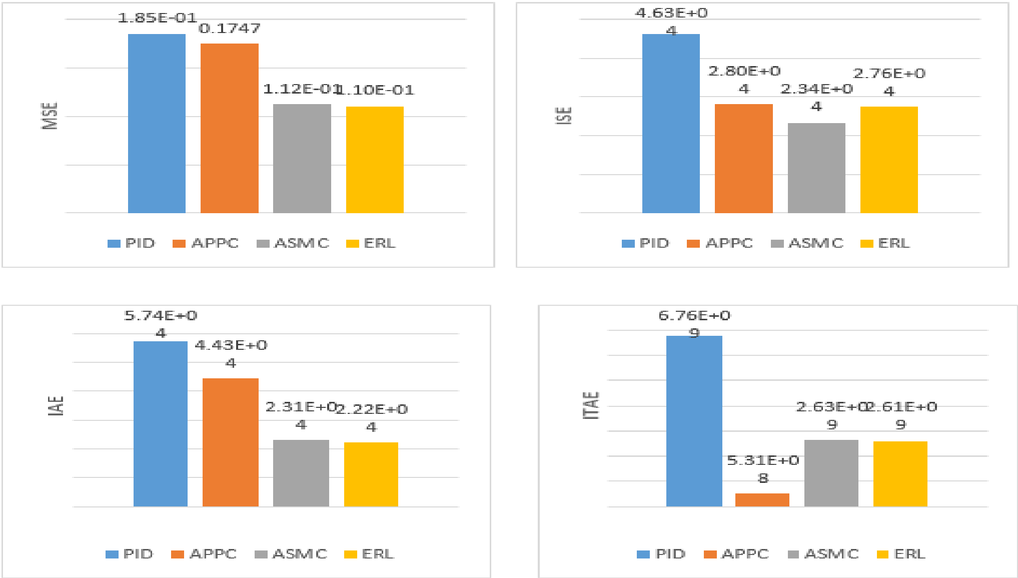

Figure 5.23 Performance indices of Disturbance on Tank1 with 12.8 cm reference input

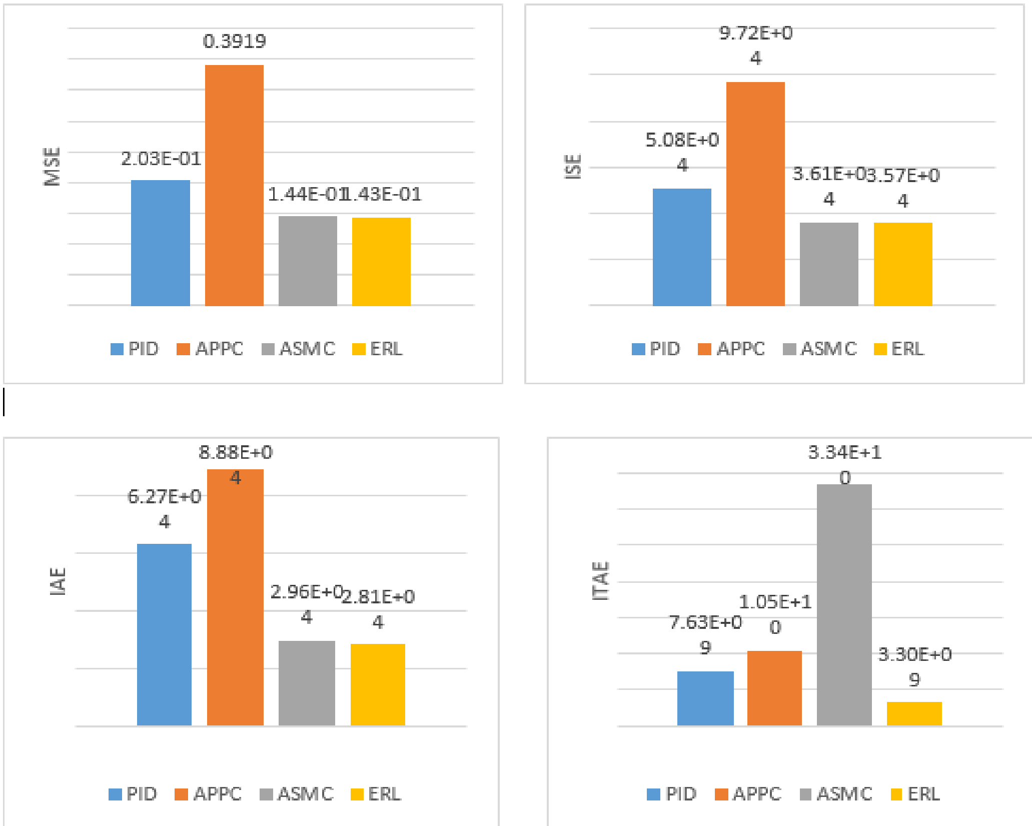

Figure 5.24 Performance indexes of Disturbance on Tank2 with 14 cm reference input

As shown in Figure 5.20, the three controllers are capable of dealing with the effects of the low-frequency square wave disturbance signals acting on the level outputs of Tank1 and Tank2. The disturbance starts at the same time as the outputs of the two tanks. At 62, 125 and 188 s, there are changes in the in the behavior of the output signals due to the nature of the square wave signal. At each signal level change, the Parameter Estimation with SMC rejects the disturbance much faster than APPC. PID takes a longer time to reject the disturbance compared to ASMC, ERL-ASMC and APPC.

As the disturbances are being added, the PID reacted with large control signals compared to the others as represented in Figure 5.21 and 5.22.

With regard to the control performance indices in Table 5.8, Figure 5.23 and 5.24. ERL-ASMC also has the lowest errors with the exception of ISE followed by ASMC which also has lower errors than APPC. In the Table, APPC has smaller errors than PID in tank1 but in tank2, it has the largest errors. This is because the level output of Tank2 has larger overshoots than the level output of Tank1.

5.3. Uncertainty Rejection

As a source of uncertainty in the plant model, the value of a_1 in (1) is varied between 0.061 to 0.081 by using a uniform random input in order to find out if the designed controllers can compensate for parametric uncertainties within the plant. This corresponds to an uncertainty in the cross-sectional area of the outlet pipe from Tank1. The results are presented in Figures 5.25 and Table 5.9.

Table 5.9 Performance indices of PID, APPC, ASMC and ERL-ASMC with 12.8 cm reference input in the case of parametric uncertainty

	PID	APPC	ASMC	ERL-ASMC
MSE	2.5×10^{-3}	1.2×10^{-3}	9.076×10^{-4}	$\mathbf{1.4660\times 10^{-4}}$
ISE	6.2980×10^{2}	2.9396×10^{2}	2.26789×10^{2}	$\mathbf{3.6649 \times 10^{1}}$
IAE	6.07×10^{3}	1.14×10^{3}	9.6086×10^{2}	$\mathbf{2.3955 \times 10^{2}}$
IATE	3.78×10^{8}	$\mathbf{5.90\times 10^{6}}$	1.3931×10^{7}	1.0799×10^{7}

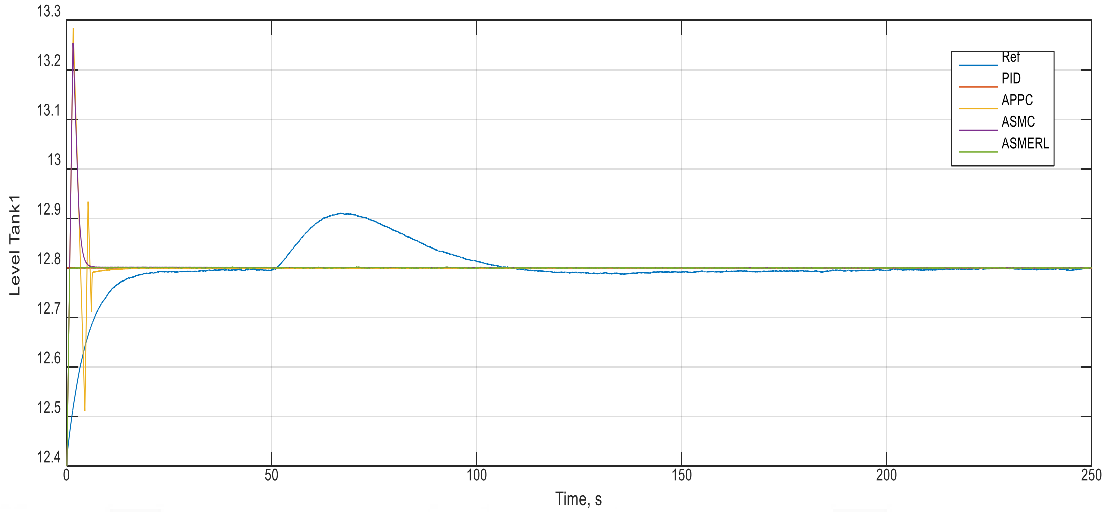

Figure 5.25 Uncertainty Rejection of PID (red), APPC (yellow), ASMC (purple) and ERL-ASMC (green) of QTP in Minimum Phase with 12.8 reference input (blue)

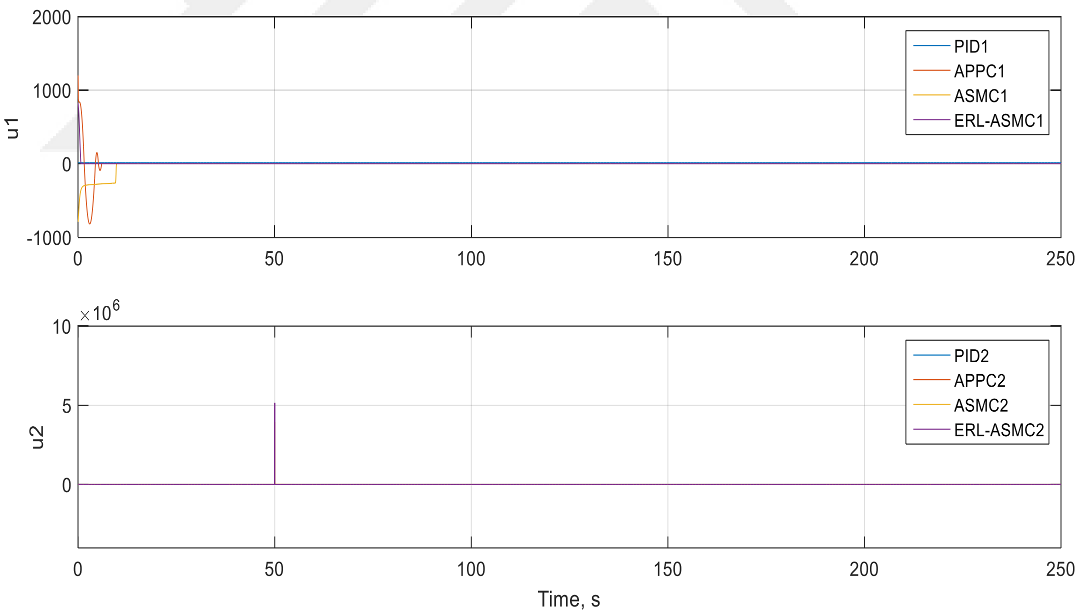

Figure 5.26 Control signal of PID (blue), APPC (red) , ASMC (yellow) and ERL-ASMC (purple) of QTP in Non-minimum Phase with 12.9 and 6.2 cm reference inputs

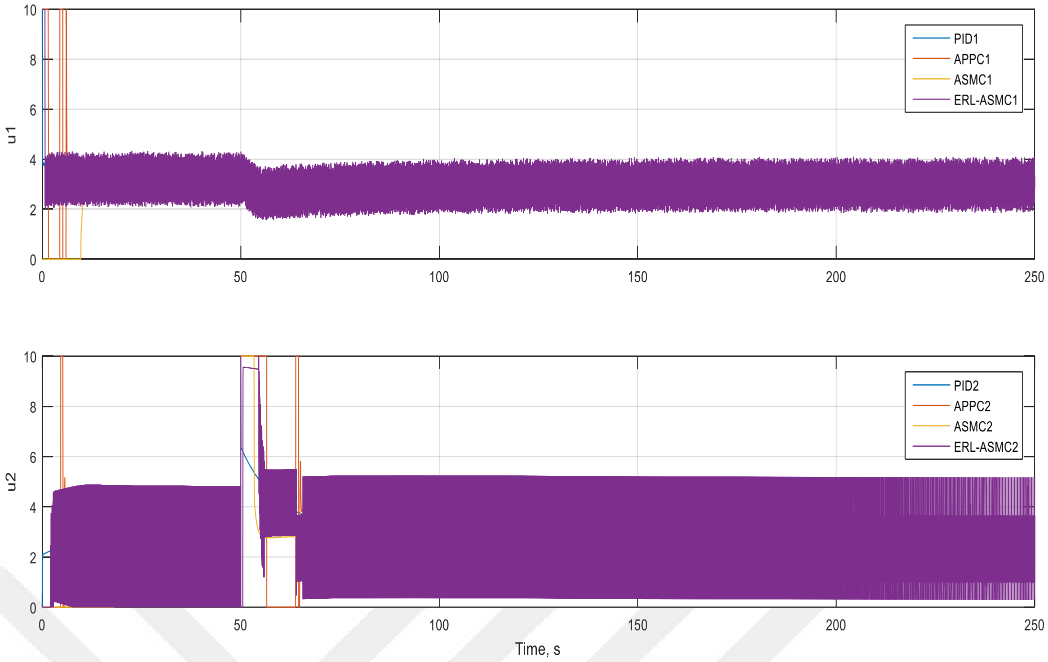

Figure 5.27 Control signal of PID (blue), APPC (red) , ASMC (yellow) and ERL-ASMC (purple) of QTP in Non-minimum Phase with 12.8 and 14 cm reference inputs after saturation.

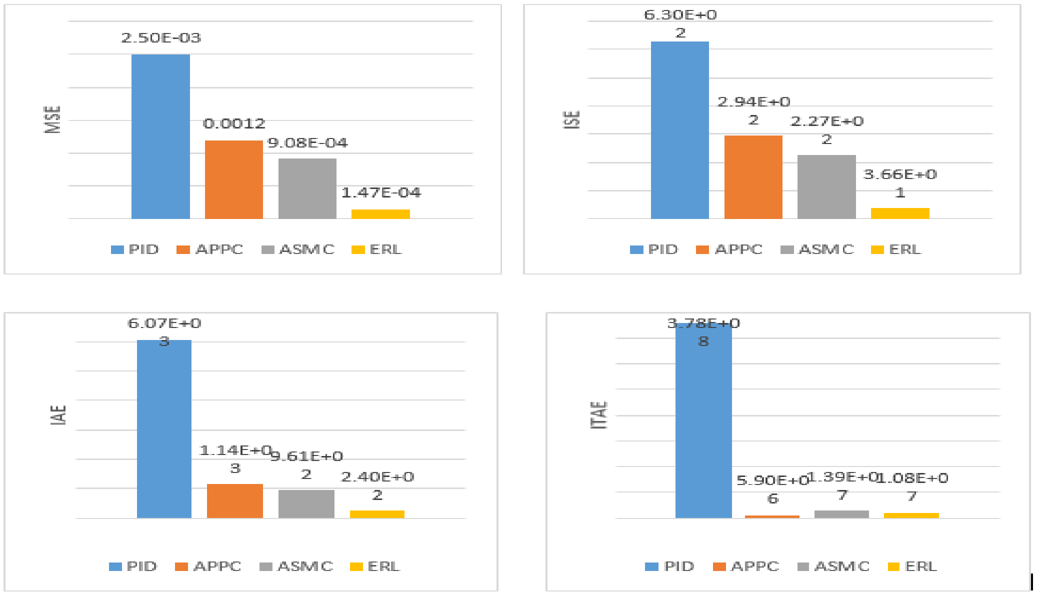

Figure 5.28 Performance indices of Uncertainty on Tank1 with 12.8 cm reference input

In Figure 5.25, it is obvious that both APPC and ASMC are capable of dealing with the uncertainty well by reducing the effects of the parameter variation resulting from the parameter change within the QTP model. In response to the introduction of this random parametric variation within ±0.01 uncertainty, the PID performs poorly in minimizing the oscillations in the pipe outlet completely. Performance indices of the uncertainty on the Tank1 are shown in Table 5.9 and Figure 5.28. PID has the highest errors for each performance index than APPC, ASMC and ERL-ASMC. Apart from ITAE, the proposed ERL-ASMC and ASMC has lower errors in each performance index than APPC.

As it has been shown in Figure 5.26 and 5.27, the controllers generated huge overshoots

CHAPTER VI

EXPERIMENT TESTS

The experiments are carried out by using a real QTP in the control systems laboratory. The physical QTP has valves to regulate the amount of water entering into the tanks. The objective of the experiment is to find out how the controllers we designed based on the mathematical mode of the system will perform on the real system. The designed controllers are being tested with different reference input, disturbances and uncertainties. As it has been indicated in the simulation results, the controllers turn to generate high control signals which could not be used by the QTP. Similar to the simulations, a saturation block is being added to limit the amount of voltage entering the pumps of the physical system. The saturation limits ranges from -2.5 to 2.5 volts for pump 1 and from -2.9 to 2.9 volts for pump 2. However, the saturated control signals are not being illustrated. Only the raw control signals are depicted.

The valves in the plant are indicated in Figure 6.1. The red valves allow water to enter Tank1, Tank2 and Tank3 while the blue valves allow water to enter Tank1, Tank3 and Tank4 as labeled on the real QTP. The yellow valves also allow water to enter Tank2 and Tank4. Each valve can rotate between 0 and 90 degrees. 90 degrees means that the tank is fully open and more water is being allowed to pass through whereas zero degrees shows that no water is being allowed to pass through. Throughout the experiment, v_{c2} , v_{c3} and v_{b1} are fully opened while v_{a1} is half opened. The rest of the valves are changed depending on which kind of phase or state the system is to be operated. The experiment is being ran for 1000 s. The first 300 s is being ran at operation points of 2.5 and 2.9 volts for tank 2 and tank 4 respectively. This is being done without activating the controllers. After 300 s, the controllers are being enabled are the same time with the reference inputs. The figures below represent the results of the experiment for the rest of the 700 s. Therefore, the results of the first 300 s have been removed because the controllers were not in operation during that period.

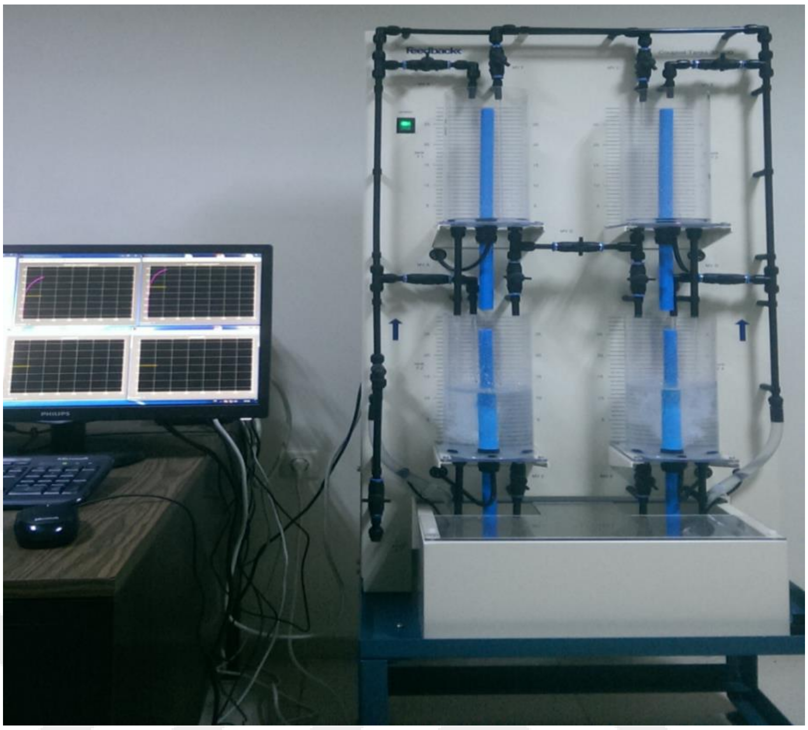

Figure 6.1 Physical QTP in the laboratory

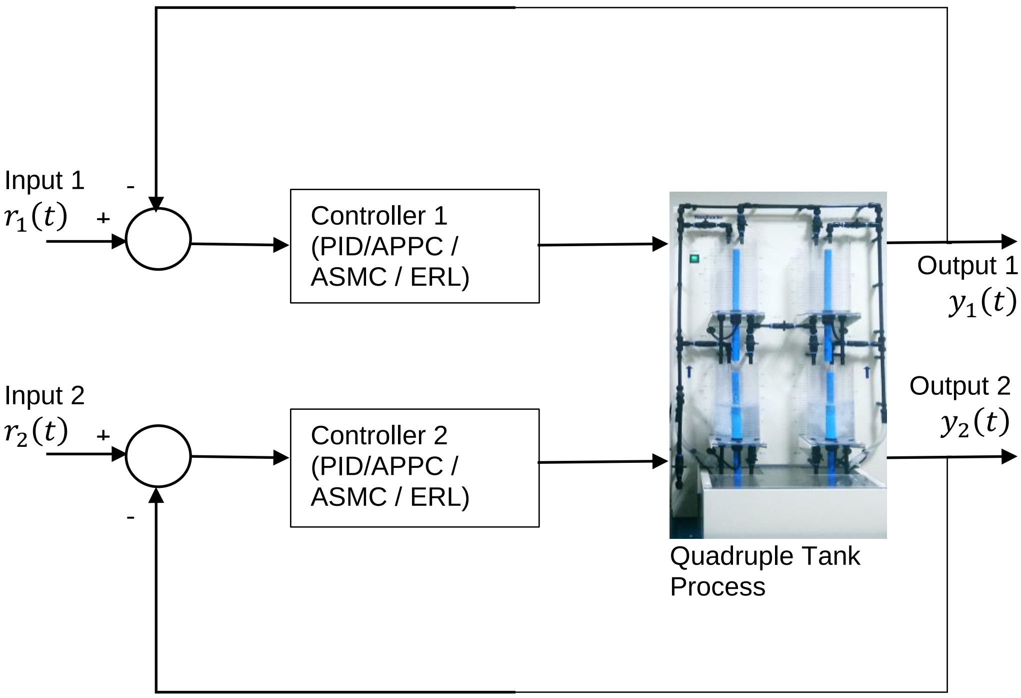

Figure 6.2 Block Diagram of Decentralized Closed loop control of the Physical QTP.

6.1 Set points Variations

The QTP is operated as a linear system by allowing less amount of water into the tanks. This is being done by opening v_{a3} and v_{b3} half of its maximum position. The experiment is carried for different reference levels of 6.4, 8.6 and 6.8 cm for Tank2 and 16.4, 16.4 and 17.7 cm for Tank4. The operating points are 2.4, 6.6 and 2.8 cm for Tank2 and 13.4, 15.4 and 17.7 cm for Tank4 respectively. In figure, Tank1 corresponds to Tank2 while Tank2 correspond to Tank4 of the physical QTP. The experimental results are depicted for the three different reference inputs in Figure 6.3-6.8. The MSE values are also represented in Table 6.1-6.3.

Table 6.1 MSE of PID, APPC, ASMC and ERL-ASMC for 6.4 and 16.4 cm reference inputs

	Tank1	Tank2
PID	**0.1059**	0.1668
APPC	0.2636	**0.1492**
ASMC	0.1510	0.2684
ERL	0.3749	2.2176

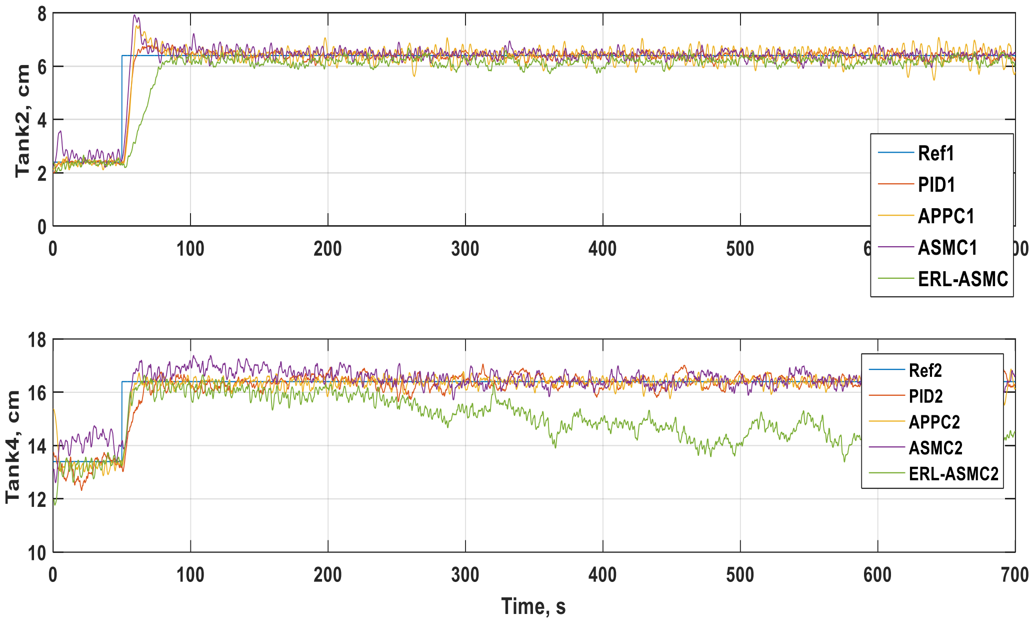

Figure 6.3 Level of Tanks of PID (red), APPC (yellow) , ASMC (purple) and ERL-ASMC (green) of QTP in Minimum Phase with 6.4 and 16.4 cm reference inputs (blue).

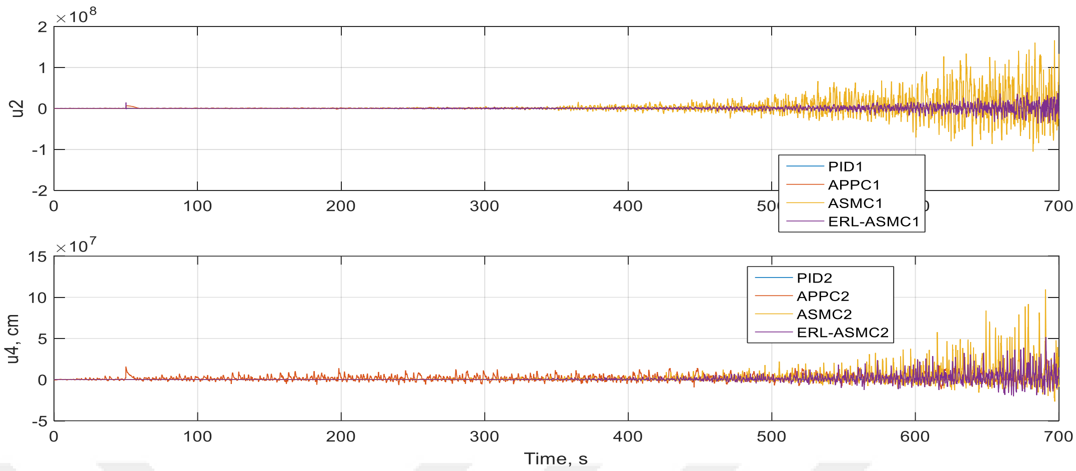

Figure 6.4 Control signal of PID (blue), APPC (red) , ASMC (yellow) and ERL-ASMC (purple) of QTP in Minimum Phase with 6.4 and 16.4 cm reference inputs.

The output responses of Tank2 with 6.4 cm level and Tank4 with 16.4 cm level are shown in Figure 6.3. It can be seen that the output response of the proposed ERL-ASMC in the figure has started to diverge from the desired level after 250 s in Tank4 though it has the least response time. This causes the error to increase especially in Tank4 thereby making its MSE values the highest as indicated in Table 6.1. Moreover, it has the slowest settling time with regard to Tank2. The rest of the other controllers have almost the same response time. However, MSE of the PID has the lowest in Tank2 whereas the MSE of APPC is the smallest in Tank4. It is obvious that in Figure 6.4, ASMC generates the largest control signal which is not ideal when dealing with certain electrical components.

Table 6.2 MSE of PID, APPC, ASMC and ERL-ASMC for 8.6 and 16.4 cm reference inputs

	Tank1	Tank2
PID	0.2217	1.3304
APPC	0.2812	1.0064
ASMC	**0.1084**	0.6390
ERL	0.2436	**0.3362**

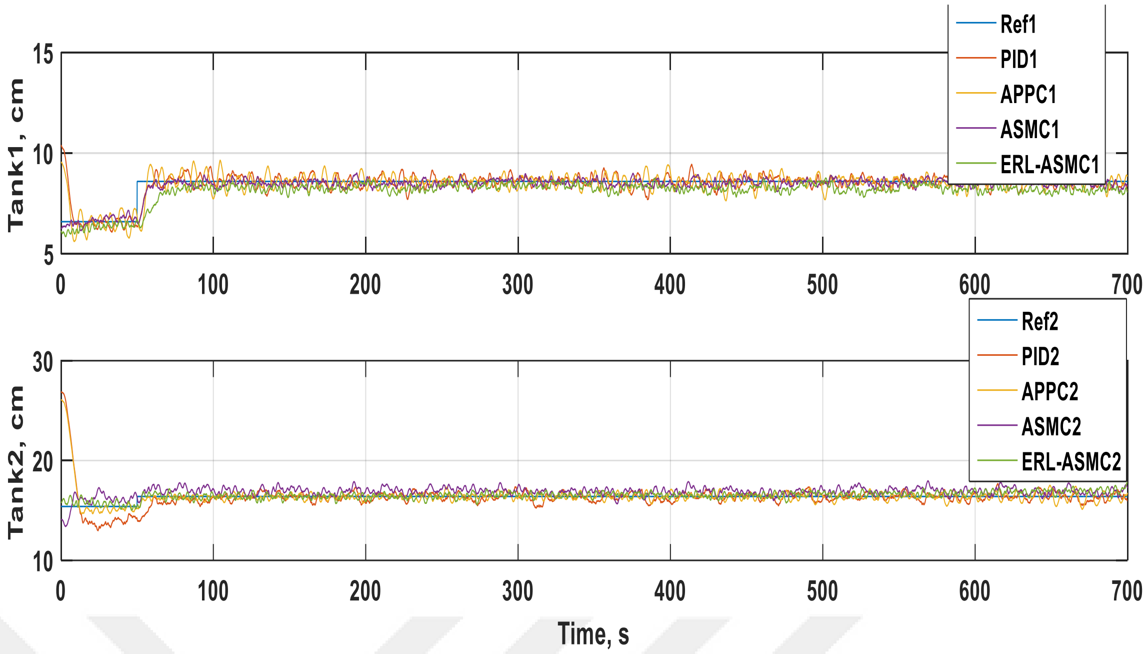

Figure 6.5 Level of Tanks of PID (red), APPC (yellow) , ASMC (purple) and ERL-ASMC (green) of QTP in Minimum Phase with 8.6 and 16.4 cm reference inputs (blue).

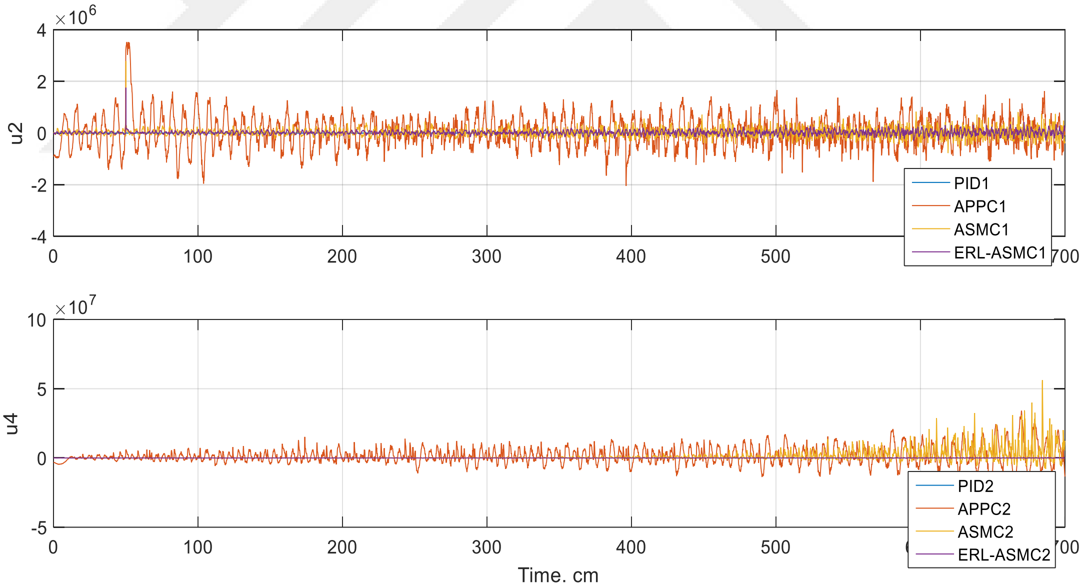

Figure 6.6 Control signal of PID (blue), APPC (red) , ASMC (yellow) and ERL - ASMC(purple) of QTP in Minimum Phase with 8.6 and 16.4 cm reference inputs.

The level responses of Tank2 with 8.6 cm and Tank4 with 16.4 cm are represented in Figure 6.5. In the Figure, all the controllers have almost the same settling time even though the proposed ERL-ASMC appeared to be little slower in Tank2 and the quickest in Tank4. MSE of ASMC has the smallest in Tank2 but with a very high control input in Figure 5.14 while MSE of ERL-ASMC has the lowest in Tank4 in Table 6.2.

Table 6.3 MSE of PID, APPC, ASMC and ERL-ASMC for 6.8 and 17.7 cm reference inputs

	Tank1	Tank2
PID	**0.1926**	**0.1483**
APPC	0.3501	0.2099
ASMC	0.2721	1.7255
ERL	0.2774	1.3075

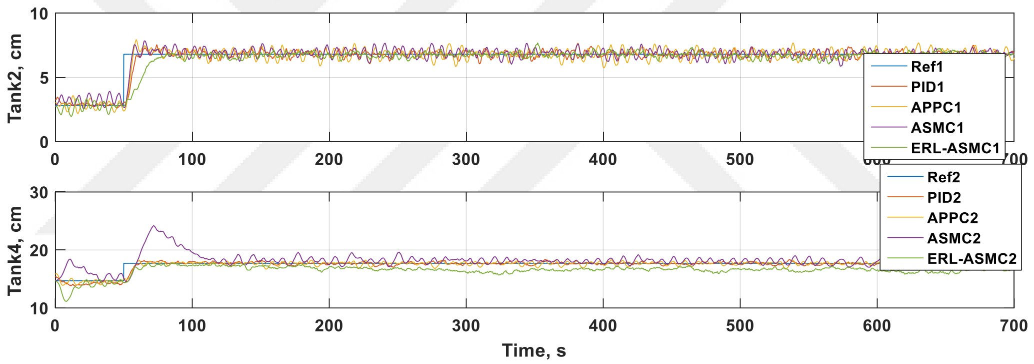

Figure 6.7 Level of Tanks of PID (red), APPC (yellow) , ASMC (purple) and ERL-ASMC (green) of QTP in Minimum Phase with 6.8 and 17.7 cm reference inputs (blue).

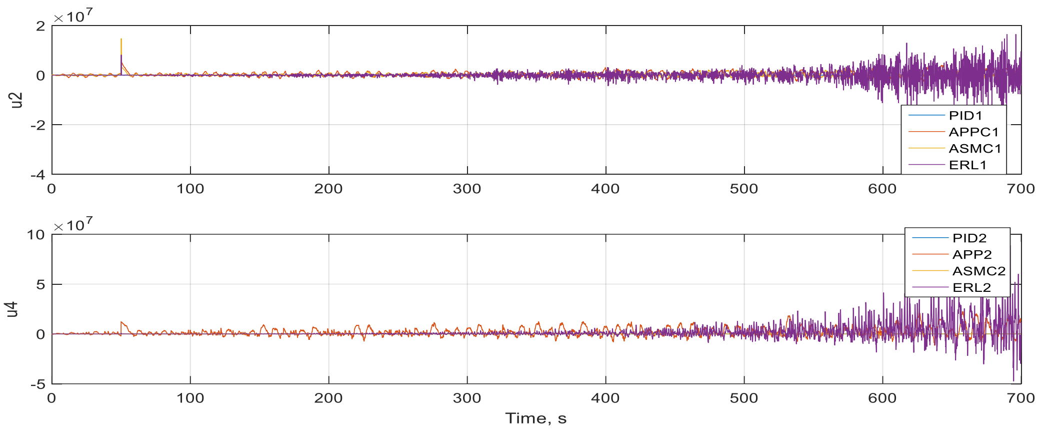

Figure 6.8 Control signal of PID (blue), APPC (red) , ASMC (yellow) and ERL-ASMC (purple) of QTP in Minimum Phase with 6.8 and 17.7 cm reference inputs.

The output responses of Tank2 at 6.8 cm position and Tank4 at 17.7 cm are illustrated in Figure 6.7. It is clearly visible that in the figure, the output response of ASMC has higher overshoots especially in Tank4. The proposed ERL-ASMC also has the biggest settling time in Tank2. The control signal of ERL-ASMC is the largest in both Tanks in Figure 6.3.

6.2 Disturbance Rejection

The robustness of the controllers to disturbances inputs are being by fully opening v_{a2} and v_{b2} at 300 s as the QTP is still in operation in Figure to allow more water to enter Tank2 and Tank4. The results of the experiment are illustrated in Figure 6.9 and 6.10 with the MSE values being depicted in Table 6.4.

Table 6.4 Mean Square Error, MSE of PID, APPC, ASMC and ERL-ASMC for 10.5 and 18 cm reference inputs with disturbances

	Tank1	Tank2
PID	0.1038	0.0708
APPC	0.0969	**0.0620**
ASMC	**0.0834**	0.0948
ERL	0.0857	0.3538

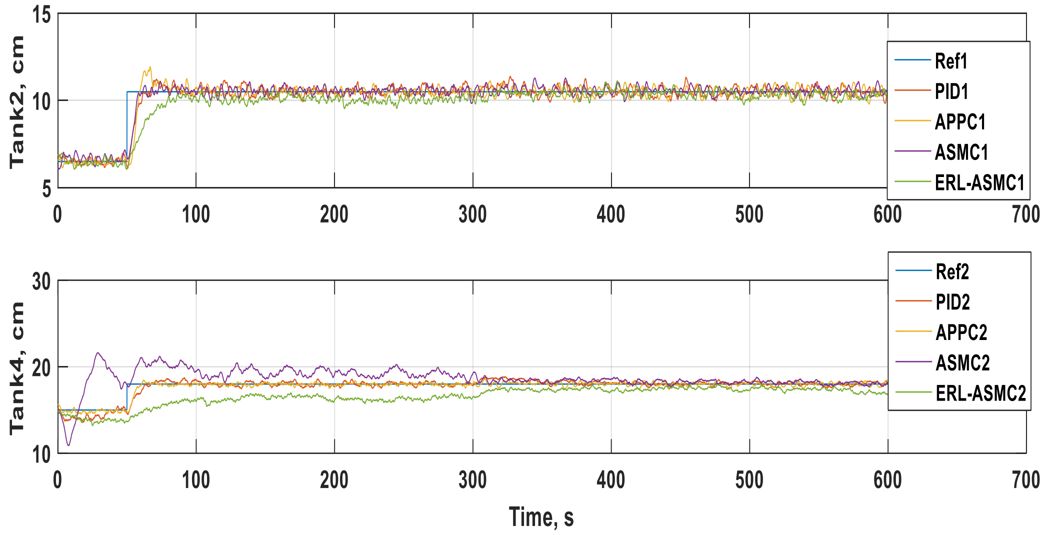

Figure 6.9 Level of Tanks of PID (red), APPC (yellow) , ASMC (purple) and ERL-ASMC (green) of QTP in Minimum Phase with 10.5 and 18 cm reference inputs (blue) with disturbances

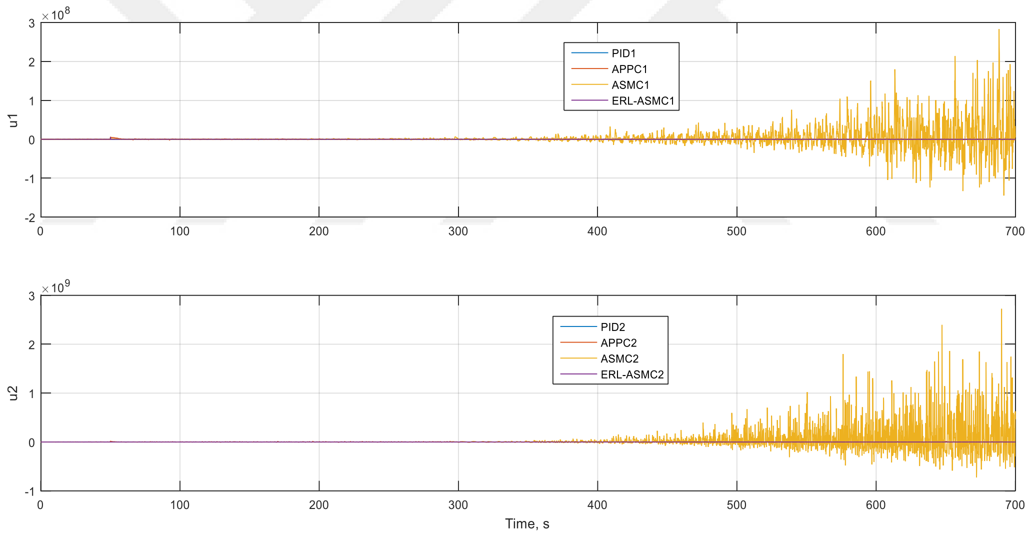

Figure 6.10 Control signal of PID (blue), APPC (red) , ASMC (yellow) and ERL-ASMC (purple) of QTP in Minimum Phase with 10.5 and 18 cm reference inputs with Disturbances

The level responses of Tank2 with set point of 10.5 cm and Tsnk4 with set point of 18 cm are shown in Figure 6.9. As it can be seen in Figure, APPC and PID have the fastest response time. The MSEs are calculated after 300 s as indicated in Table 6.4. ASMC and ERL-ASMC started slowly with huge errors especially in Tank4. As more water are added at 300 s, their performances began to improve. This made ASMC to get the smallest MSE value for Tank2 in Table 6.4, followed by ERL-

ASMC while APPC has the smallest MSE value for Tank4 but with huge control inputs as depicted in Figure 6.10, followed by PID.

6.3 Parametric Uncertainty

The parametric uncertainty is tested by varying v_{b2} to high or low position from its original position. This has been accomplished by allowing the system to run until 200 s. At 200 s, the valve is closed to prevent watering reaching Tank1 and then through to Tank2. The valve is opened at half of it initial position at 300 s to allow little amount of water to pass through. At 400 s, $v_{b2}$is opened further to its original position. The valve is then opened a little above its usual position to allow more water to the tanks at 500 s. lastly, at 600 s it is closed back to its initial positon for the rest of the experiment duration. The results are represented in Figure 6.11 and 6.12. The MSE figures are given in Table 6.5.

Table 6.5 MSE of PID, APPC, ASMC and ERL-ASMC for 10.5 cm reference input with parametric uncertainty

	Tank1
PID	6.8754
APPC	7.1056
ASMC	7.3169
ERL	**5.2651**

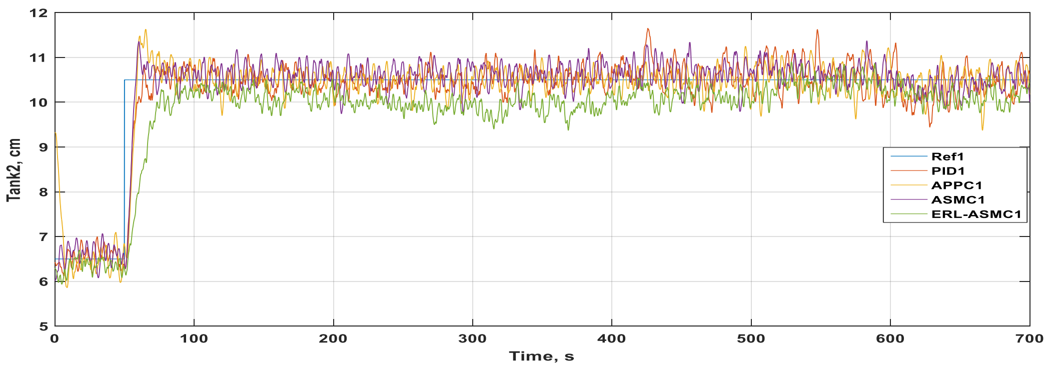

Figure 6.11 Level of Tanks of PID (red), APPC (yellow) , ERL-ASMC (purple) and ERL-ASMC (green) of QTP in Minimum Phase with 10.5 cm reference input (blue) with parametric uncertainty

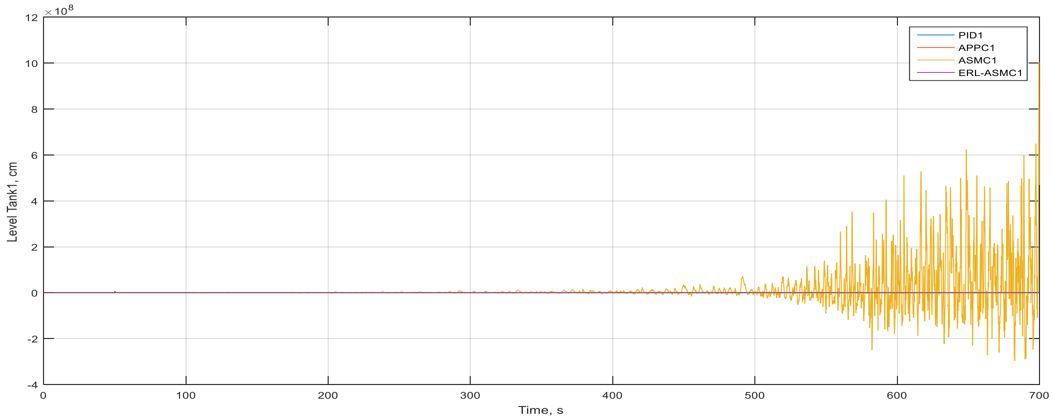

Figure 6.12 Control signal of PID (blue), APPC (red) , ERL-ASMC (yellow) and ERL-ASMC (purple) of QTP in Minimum Phase with 10.5 cm reference inputs with parametric uncertainty

The output responses of Tank2 at 10.5 cm level are represented in Figure 6.11. The settling time of all the controllers are almost equal. On the contrary. ERL-ASMC has the lowest MSE in Table 6.5. This is followed by PID. ASMC has the worst MSE value as well as the largest control signal that is being produced as shown in Figure 6.12.

6.4 Nonlinear Test

The physical QTP is considered to be in non-minimum phase when a lot of water is allowed to enter the lower tanks. Therefore, v_{a2}, v_{b2}, v_{a3} and v_{b3} are fully opened throughout the experiment. The results of this experiment for an input are shown in Figure 6.13 and 6.14 while the error values are depicted in Table 6.6.

Table 6.6 MSE of PID, APPC, ASMC and ERL-ASMC for 12.9 and 9.2 cm reference inputs

	Tank1	Tank2
PID	**0.2287**	**0.2370**
APPC	1.3484	0.7832
ASMC	1.0182	0.2096
ERL	0.9181	0.2380

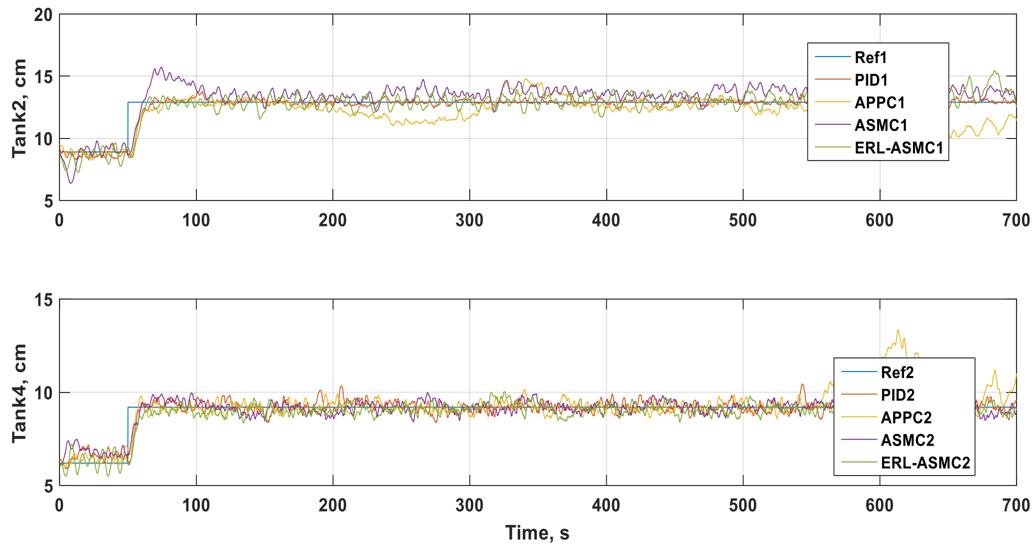

Figure 6.13 Level of Tanks of PID (red), APPC (yellow) , ASMC (purple) and ERL-ASMC (green) of QTP in Non-minimum Phase with 12.9 and 9.2 cm reference inputs (blue).

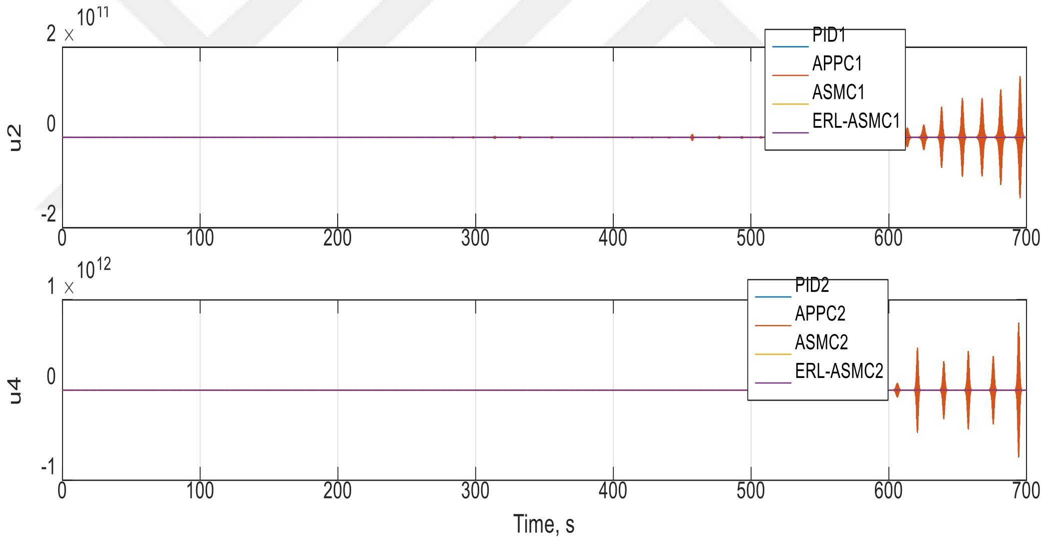

Figure 6.14 Control signal of PID (red), APPC (yellow) , ASMC (purple) and ERL-ASMC (green) of QTP in Non-minimum Phase with 12.9 and 6.2 cm reference inputs (blue).

The level responses of Tank2 with 12.9 cm and Tank4 with 9.2 cm are represented in Figure 6.13. In the Figure, all the controllers have almost the same settling time except the ASMC in Tank1. MSE of PID has the smallest Table 6.6. This is followed by the Proposed ERL-ASMC.

CHAPTER VII

DISCUSSION

Based on the simulations that have been carried out for the different input values applied to the modeled QTP, the settling times of the controllers as indicated in Table 5.3, 5.5, and 5.7 which have been obtained from Figure 5.4, 5.9 and 5.14 respectively has shown that, the proposed ERL-ASMC has outperformed ASMC, PID and APPC. This is because it is able to adapt to the variation of the switching function of the discontinuous control. The adjustment ability allows it to reach the sliding surface in a very short time. As a result, the controller takes a less amount of time to arrive at the desired input value. Close to the performance of the proposed ERL-ASMC is the ASMC, which uses a fixed gain in relation with a switching function to ensure a very rapid output response. It can be noted that the SMC controllers had very small response times which are due to the fact that in sliding mode the sliding surfaces dynamics are independent of the parameter changes in the system. APPC also has a faster settling because it makes use of parameter estimation in order to get the actual dynamic of the process. PID has the worst outcome due to the inability of the controller to adjust to parameter changes that are occurring within the system.

As the performance indices have been calculated in Table 5.2, 5.4 and 5.6 as well as in Figure 5.7, 5.8, 5.12, 5.3, 5.11, 5.12, 5.17, 5.18 and 5.28, the proposed ERL-ASMC performed relative the same as the ASMC when the level is either high or low. Even at a normal level, both controllers have been able to track the reference inputs much better especially in tank2. The proposed ERL-ASMC has nearly zero overshoots which makes it much preferable choice as compared to ASMC. However, in tank1, the persistent error caused by the discontinuous switching control enhance the performance indices to be very large. APPC has performed poorly in tank2 as a result of large overshoots which are being increased by the initial delay. PID had the worst performance of its bigger overshoots.

In terms of disturbances rejection which has been tested by using a low frequency square input as depicted in Figure 5.20, the proposed ERL-ASMC has been effective in handling the effects on the systems output responses. This is because the proposed ERL-ASMC had the smallest performance indices as tabulated in Table 5.8. Second in line is the ASMC which also uses the same mechanism to keep the effects low. The mechanism in this case is the invariant nature of both controllers in sliding mode which results in making the controller more robust. In this table, APPC has less error values than the PID. This is as a result of the ability of the APPC to estimate the parameters of the plant in addition to the disturbances.

With regard to parametric uncertainty, this has been implemented by using a random signal which varies within a certain range as illustrated in Figure 5.25. Just like the disturbances, the proposed ERL is the best in withstanding parameter variations taking place within the QTP model. The next in command are ASMC, APPC and PID respectively.

The experimental results for different level responses of Tank2 and Tank4 are presented in Figure 6.3, 6.5 and 6.7. In the figures, the proposed ERL had performed badly as this was not expected based on the simulation results. ASMC has performed a little bit better than the proposed ERL with regards to lower MSE value even though it is more likely to produce huge control signals. This may because of the high sensitive nature of the sliding mode controllers. The commonly used PID had the overall best performance and it also generates small control input as well. APPC has performed satisfactorily well in tracking the desired level with minimum control input.

Disturbances are being added in the experiment by opening the upper closed valves at full range while the system is in operation to allow a lot of water to enter the Tanks. The output levels are shown in Figure 6.9. In the figure, as more water is allowed into the Tanks, the effectiveness of the proposed ERL and ASMC began to improve. As the MSE values were being calculated at the moment the water was injected, the ASMC had the smallest MSE value as indicated in Table 6.4. But higher control inputs are need to obtain that highly effective performance. The proposed ERL did relative the same with regard to rejecting the disturbances with lesser control signal input.

Similar to adding water by opening the upper valves so as to test for disturbance, water is being injected by varying the initial position of the valve, v_{b3} depicted in Figure 6.1 above or below so as to allow water to pass through to Tank2. The level responses are illustrated in Figure 6.11. In the figure, the response time of the proposed ERL-ASMC appeared to be little slower while in Table 6.5, it has the smallest MSE. This shows that the proposed ERL-ASMC is very effective in reducing parameter changes in the system. Next to this controller is PID, APPC and ASMC.

The designed controllers are robust against disturbances and uncertainties. The proposed ERL-ASMC has satisfactory performance in handling disturbances and varying changes within the valves.

As more water are being added as depicted in Figure 6.13, the performance of the proposed ERL-ASMC began to improve. Its MSE is slightly higher than PID as illustrated in Table 6.6. Even though the PID has outperformed the proposed ERL-ASMC in this case, it has much higher control signal.

CHAPTER VIII

CONCLUSION

8.1 Concluding Remarks

The goal of this thesis is to design a controller that can track different inputs, reject disturbances and uncertainties. APPC, ASMC and ERL-ASMC which uses parameter estimation mechanism to determine the parameters of the QTP have designed, simulated and implemented on the real system. The proposed ERL has outperformed all the other controllers based on the settling time and performance indices especially in the simulation and satisfactory performance in regards to the experiment.

It is evident that all the designed controllers can track the reference inputs of different signals whether it is simulation or experiment. The output responses have also been smooth and there is no chattering.

In the simulation, it has been clear that the Adaptive controllers have better performances in terms of settling time, disturbance rejection and dealing with parametric uncertainties than PID. This is because of the fact that the adaptive controllers use parameter estimation in order to get the correct parameters of the system. The sliding control controllers have faster response time and small overshoots than APPC. In comparing the two different sliding mode controllers, the proposed ERL-ASMC has smaller settling times, better rejection of disturbances and uncertainties and lesser overshoots. This is due to the exponential variation of the discontinuous switching gain, which creates smaller switching time than ASMC. This mechanism has made the proposed ERL-ASMC the most effective controller.

In the experiments, the proposed ERL-ASMC has underperformed with different levels of inputs. This may be because of the sensitive nature of the controller. However, with regards to disturbances and parameter uncertainty, it has shown tremendous improvements. The same is true of ASMC except that it tends to generate larger control signal which may cause some problems to certain electrical equipment. The proposed ERL-ASMC has the position to handle nonlinearity very effectively thanks to its ability to reject disturbances and parameter changes. Additionally, it always produces low overshoots even though it can be sluggish at some instances. However, there is the problem of selecting the right control gain of the sliding mode controllers.

8.2 Future Work

The proposed ERL-ASMC controller could be deploy in the food and beverage industries where optimal levels of efficiency are required during the production process.

It can also be applied to robot manipulator due to the high degree of flexibility of the joints and uncertainties.

Moreover, it can be combine with neural networks to provide a better effective performance. The neural works in this case are used to estimate the model uncertainties and disturbances of the system.

REFERENCES

[1] K. J. Astrom, M. Lundh (1992). Lund control program combines theory with hands-on experience. *IEEE Control Systems Magazine*, **12(3**),22-30.

[2] R. C. Amara (1959). Application of matrix methods to the linear least squares synthesis of multivariable control systems, *Journal of Franklin Institute*, **268 (1)**, 1–16.

[3] H. Seraji, M. Tarokh (1977). Design of PID controllers for multivariable systems, *International Journal of Control*, **26 (1)**, 75–83.

[4] P. N. Paraskevopoulos (1980). On the design of PID output feedback controllers for linear multivariable systems, *IEEE Transactions on Industrial Electronics and Control Instrumentation*, **27 (1)**, 16–18.

[5] Z. Wang, P. Wei, (2020). Analytical multiloop control for multivariable systems with time delays, *Complexity*, 1–9.

[6] X. Li, Z. Zhao, F. Liu (2020). Latent variable iterative learning model predictive control for multivariable control of batch processes, *Journal of Process Control*, **94**, 1–11.

[7] B.M. Al-Hadithi, J. M. Adánez, A. Jiménez (2020). Control of multivariable delayed systems with colored noise using incremental state formulation, *European Journal of Control*, **53**, 78–87.

[8] H. Victor, B. Xavier, M. H. Juan, R.-M. Gilberto (2020). A loop pairing method for non-linear multivariable control systems under a multi-objective optimization approach, *IEEE. Access*, **8**, 41262–8.

[9] J. G. Balchen, M. Handlykken, A. Tysso (1981). The need for better laboratory experiments in control engineering education, *Eighth Triennial World IFAC Control Science Technology World Congress*, **7**, 3363–8.

[10] M. Mansour, W. Schaufelberger (1981). Digital computer control experiments in the control group of eth-zuerich, *Eighth Triennial World IFAC Control Science and Technology World Congre*ss.

[11] J. Biston, J. Dufour, G. Gilles (1981). An example of computer control systems practical teaching, *Eighth Triennial World IFAC Control Science and Technology World congress*.

[12] S. Pranav, H. Sandeep (2020). Modelling and simulation of Quadruple Tank system using SBL-PI controller, *2020 International Conference on Industry 4.0 Technology (I4Tech) Vishwakarma Institute of Technology*.

[13] Pavel, P. Libor, M. Radek (2019). Control of a multivariable system using optimal control pairs: A Quadruple Tank Process, *IEEE. Access*, **8**, 2537–63.

[14] Johansson K.H (2000). The Quadruple-Tank Process: A Multivariable Laboratory Process with an Adjustable Zero, *IEEE Transactions on Control Systems Technology*, **8 (3)**, 456- 465.

[15] K.J.Astrom, K.H.Johansson, Q. G.Wang (2002). Design of decoupled PI controllers for two-by-two systems, IEE Proceeding, Control Theory Application. Vol. 149, No. 1

[16] Utkin VI. Variable structure systems with sliding modes (1977). IEEE Transactions on Automatic Control, **22 (2)**, 212 – 222.

[17] Decarlo RA, Zak SH, Mathews GP (1988). Variable structure control of nonlinear Systems, *A Tutorial IEEE Proceeding*, **76 (3)**.

[18] J.Y.Hung,W. Gao, and J. C.Hung (1993). Variable structure control: A survey, *IEEE Transactions on Industrial Electronics*, **40 (1)**, 2–21.

[19] Lino P, Maione B, Rizzo A (2007). Nonlinear modeling and control of a common rail injection system for diesel engines, *Elsevier, Applied Mathematical Modeling*, **31**, 1770–84.

[20] M. Vidyasagar (1993). Nonlinear systems analysis. Second edition. Englewood Cliffs, New Jersey: Prentice-Hall.

[21] H. K.Khalil (2002). Nonlinear systems. 3rd ed. Upper Saddle River, NJ: Prentice Hall.

[22] C. Vinita, T. Bhagyashri, K. Shailaja (2020). Robust liquid level control of quadruple tank system– second order sliding mode approach, *IFAC Papers Online*, **53 (1)**, 7–12.

[23] L. Xiaodi, Y. Xueyan, (2020). Lyapunov stability analysis for nonlinear systems with state-dependent state delay, *Automatica. (Oxf)*, **112**, 1–6.

[24] F. Liu, B. Zhang, Z. Yang (2019). Lyapunov stability and numerical analysis of excursive instability for forced two phase boiling flow in a horizontal channel, *Applied Thermal Engineering*, **159**, 1–12.

[25] T. Kara, A. H. Mary (2018). Robust trajectory tracking control of robotic manipulators based on model-free PIDSMC approach, *Journal of Engineering Research*, **6 (3)**, 170–88.

[26] S. Yang, G. Tao, B. Jiang (2020). Robust adaptive control of nonlinearly parametrized multivariable systems with unmatched disturbances, *International Journal of Robust Nonlinear Control*, **30 (9)**, 3582–3606.

[27] D. Asadi, K. Ahmadi (2020). Nonlinear robust adaptive control of an airplane with structural damage, *J. Aerospace*, 1–13.

[28] Iglesias E, García Y, Sanjuan M, Camacho O, Smith C (2007). Fuzzy surface-based sliding mode control, *ISA Transaction*, **46**, 73–83.

[29] Chen CT, Peng ST (2006). A sliding mode control scheme for non-minimum phase non-linear uncertain input-delay chemical processes, *Elsevier, Journal of Process Control*, **16**, 37 – 51.

[30] Yound KD, Utkin VI, Ozguner U (1999). A control engineer’s guide to sliding mode Control, *IEEE Transaction on Control System Technology*, **7 (3)**, 328 – 42.

[31] G. Bartolini, A. Ferrara, E. Usai (1998). Chattering avoidance by second order sliding mode control, *IEEE Transactions Automatic Control*, **43**, 241–246.

[32] G. Bartolini, A. Ferrara, E. Usai, V.I. Utkin (2000). On multi-input chattering-free second-order sliding mode control, *IEEE Transactions on Automatic Control*, **45**, 1711–1717.

[33] G. Bartolini, A. Pisano, E. Usai (2001). Digital second-order sliding mode control for uncertain nonlinear systems, *Automatica*, **37**, 1371–1377.

[34] G. Bartolini, A. Pisano, E. Punta, E. Usai (2003). A survey of applications of second-order sliding mode control to mechanical systems, *International Journal of Control*, **76**, 875–892.

[35] I. Boiko, L. Fridman, A. Pisano, E. Usai (2007). Analysis of chattering in systems with second-order sliding modes, *IEEE Transactions on Automatic Control*, **52**, 2085–2102.

[36] Xinghuo Yu, Okyay Kaynak (2009). Sliding-Mode Control with Soft Computing: A Survey, *IEEE Transaction on Industrial Electronics*, **56 (9)**, 3275-3284.

[37] Alessandro Pisano, Elio Usai (2011). Sliding mode control: A survey with applications in math, Mathematics and Computers in Simulation, **81**, 954–979.

[38] Vadim Utkin (2015). Discussion Aspects of High Order Sliding Mode Control, *IEEE Transactions on Automatic Control*, 1-6.

[39] Saleh Mobayen (2015). An adaptive chattering-free PID sliding mode control based on dynamic sliding manifolds for a class of uncertain nonlinear systems, *Springer Science*, **82**, 53-60.

[40] Chiew Tsung Heng, Zamberi Jamaludin, Ahmad Yusairi Bani Hashim, Lokman Abdullah, and Nur Aidawaty Rafan (2017). Design of Super Twisting Algorithm for Chattering Suppression in Machine Tools, *International Journal of Control, Automation and Systems,* **15 (3)**, 1259-1266.

[41] Pinak P. B, Rishi S, Subhabrata R, Amar Nath S (2009). Sliding mode control of quadruple tank process, *Elsevier*, *Mechatronics*, **9**, 548 – 561.

[42] J. Jayaprakash, D. Davidson, H. J. P. Subha (2013). Comparison of controller performance for MIMO process, *International Journal of Emerging Technology and Advanced Engineering,* **3**, 52–59.

[43] D. H. Shah, D. M. Patel (2019). Design of sliding mode control for quadruple-tank MIMO process with time delay compensation, *Journal of Process Control*, **76**, 46–61.

[44] Robert L. Carroll D. P. Lindorff (1972). An Adaptive Scheme for Observing the State of an Unknown Linear System, *Technical Report.*

[45] Robert l. C, David P. L (1973). An Adaptive Observer for Single-Input Single-Output Linear Systems, IEEE Transactions on automatic control, **18 (5)**, 428 – 435.

[46] Gerd. L, K. S. Narendra (1973). An Adaptive Observer and Identifier for a Linear System, *IEEE Transactions on automatic control*, 495 – 499.

[47] K S. Narendra, L.S. Valavani (1978). Stable Adaptive Controller Design - Direct Control, *IEEE Transactions on Automatic Control*, **23 (4)**, 570-583.

[48] K. S. Narendra, P. Kudva (1974). Stable Adaptive Schemes for System Identification and Control---Part I, *IEEE Transactions on Systems, Man, and Cybernetics*, **4 (6)**, 542 – 551.

[49] K S. Narendra, L.S. Valavani (1976). Stable Adaptive Observers and Controllers, *Proceedings of the IEEE*, **64 (8)**, 1198-1208

[50] Richard V. Monopoli (1974). Model Reference Adaptive Control with an Augmented Error Signal, *IEEE Transactions on automatic control*, **19 (5)**, 474 - 484

[51] K. S. Narendra, R. P. Singh (1981). A Globally Stable Adaptive Controller for Multivariable Systems, *IEEE*.

[52] David G. Luenberger (1964). Observing the State of a Linear System, *IEEE Transactions on Military Electronics*.

[53] Bernard Goldstein (1972). Control of Linear Uncertain Systems Utilizing Mismatched State Observers, *Ph. D Thesis, The University of Connecticut, School of Engineering*.

[54] Gerd. L, K. S. Narendra (1974). A new canonical form for an adaptive observer, *IEEE Transactions on Automatic Contr*ol, **9**, 117-119.

[55] K. S. Narendra, P. Kudva (1974). Stable Adaptive Schemes for System Identification and Control---Part II, *IEEE Transactions on Systems, Man, and Cybernetics*, **4 (6)**, 552 – 560.

[56] D. A. Vijula, and D. N. Devvarajan (2014). Design of decentralized pi controller using model reference adaptive control for quadruple tank process,” *International Journal of Engineering and Technology*, **5 (6)**, 5057–66.

[57] L. Hongjing, L. Guangliang, H. Zhang, H. Tingwen, (2020). Neural-network-based event- triggered adaptive control of nonaffine nonlinear multiagent systems with dynamic uncertainties, *IEEE Transactions on Neural Networks Learning Systems*, 1–12.

[58] W. Yuanqing, Y. Chang, A. F. Alkhateeb, N. D. Alotaibi, (2019). Adaptive fuzzy output-feedback tracking control for switched nonstrict-feedback Nonlinear Systems with prescribed performance, *Circuits System Signal Processes*, **40**, 88–113.

[59] P. V. Osburn, H. P (1961). Whitaker, 4. Keezer. New developments in the design of adaptive contro1 system, *Institute of Aeronautical Sciences*, 61-39.

[60] D. D. Donalson, C. T. Leondes (1963). A model reference parameter tracking technique for adaptive control systems-The principal of adaptation, IEEE Transactions on Applications and Industry, **82**, 241-262.

[61] P. C. Parks (1966). Lyapunov redesign of model reference adaptive control systems, *IEEE Transactions on Automatic Control*, **11 (3)**, 363-367.

[62] Chang-Chieh Hang, Patrick C. Parks (1973). Comparative Studies of Model Reference Adaptive Control Systems, IEEE Transaction on Automatic Control, **18 (5)**, 419-428.

[63] Kalman R. E. (1958). Design of a self-optimizing control system. *Transactions on ASME*, **80**, 468-478.

[64] Astrom, K. J, B. Wittenmark (1973). On self-tuning regulators, *Automatica*, **9**, 185.

[65] Peterka, V. (1970). Adaptive digital regulation of noisy systems. *Proceedings of 2nd IFAC Symposium on Identification and Process Parameter Estimation*.

[66] Astrom, K. J, B. Wittenmark (1980). Self-tuning controllers based on pole-zero placement, *lEE Proc.*, **127**, 120.

[67] Graham C. Goodwin, Peter J. Ramadge, E. Caines (1979). Discrete Time Multivariable Adaptive Control, *IEEE.*

[68] I.D. LANDAU, R. Lozano (1981*).* Unification of discrete time explicit model reference adaptive control design, *Automatica*, **17** (**4),** 593-611.

[69] J.M. Dion, L. Dwaw (1982). Direct Adaptive Control of Discrete Time Multivariable Systems.

[70] R. V. Monopoli, C. C. Hsing (1975). Parameter adaptive control of multivariable systems, *Int. J. Control*, **22 (3)**, 313-327.

[71] D. L. Prager, P. E. Wellstead (1980). Multivariable Pole Assignment Self-Tuning Regulators, *IEEE Proceedings*, **128 (1)**, 9-18.

[72] H. Elliott, W. A. Wolovich, M. Das (1980). Arbitrary Adaptive Pole Placement for Linear- Multivariable Systems. *IEEE*.

[73] V. Borrison (1979). Self-turning Regulatorsf or a Class of Multivariable Systems," Automatic, **15**, 209-215.

[74] H. N. Koivo (1980). A Multivariable Self-Tuning Controller, Automatica, **16**, 351-366.

[75] Elliott, H, W. A. Wolovich (1984). Parameterization issues in multivariable adaptive control, **32 (6)**, 833-848.

[76] Tao, G, P. A. Ioannou (1988). Robust model reference adaptive control for multivariable plants, *International Journal Adaptive Control and Signal Processes*, **2**, 217-248.

[77] Chien, C. J, L. C. Fu (1992). A new robust model reference control with improved performance for a class of multivariable unknown plants. *International Journal of Adaptive Control and Signal Processes*, **6**, 69-93.

[78] Hsu, L., A. D. Araújo, and R. R. Costa (1994). Analysis and Design of I/O Based Variable Structure Adaptive Control, *IEEE Transactions on Automatic Control*, **39 (1)**, 4-21.

[79] Chien, C.-J., K.-C. Sun, A.-C. Wu, L.-C. Fu (1996). A Robust MRAC Using Variable Structure Design for Multivariable Plants, *Automatica*, **32 (6)**, 833-848.

[80] Liu Hsu, Ramon R. Costa, José Paulo Vilela Soares da Cunha (2003). Model-Reference Output-Feedback Sliding Mode Controller for A Class of Multivariable Nonlinear Systems, *Asian Journal of Control*, **5 (4)**, 543-556.

[81] Walcott, B. L, S. Żak (1988). Combined Observer-Controller Synthesis for Uncertain Dynamical Systems with Applications, IEEE Transactions on Systems, Man Cybernetics, **18 (1)**, 88-104.

[82] Edwards, C, S. K. Spurgeon (1996). Robust Output Tracking Using a Sliding-Mode Controller/Observer Scheme, *International Journal of Contr*ol, **64 (5)**, 967-983.

[83] Hsu, L., R. R. Costa (1989). Variable structure model reference adaptive control using only input and output measurement: Part 1, *International Journal of Control*, **49**, 339-416.

[84] Miller. D. E, E. J. Davison (1991). An adaptive controller that provides an arbitrarily good transient and steady-state response, *IEEE Transactions on Automatic* Control, **36**, 68-81.

[85] Fu, L. C. (1991). A robust model reference adaptive control using variable structure adaptation for a class of plants, *International Journal of Control*, 1359-1375.

[86] D. Bestle, M. Zeitz (1983). Canonical form observer design for nonlinear time-variable systems, *Int. J. Contr.*, **38 (2)**, 419-431.

[87] G. Meyer, R. Su, L. R. Hunt (1984). Application of nonlinear transformations to automatic flight control, Automatica, **20 (1)**, 103-107.

[88] W. Baumann, W. Rugh (1986). Feedback control of nonlinear systems, *IEEE Transactions on Automatic Control*, **31 (1)**, 40-47.

[89] David Cartes, Lei Wu (2015). Experimental evaluation of adaptive three-tank level control, *ISA Transactions*, **44**, 283–293.

[90] M. Makoudi, L. Radouane (2000). A Robust Model Reference Adaptive Control for Non-Minimum Phase Systems with Unknown or Time-Varying Delay, *Automatica*, **36**, 1057-1065.

[91] X. Y. Gu, C. Shao (1993). Robust adaptive control of time-varying linear plants using polynomial approximation, *IEE Proceedings-D*, **140**, 111-118.

[92] Nabiha Touijer, Samira Kamoun (2014). Development of Robust Self-Tuning Control for MIMO Linear Systems with dead-zone approach, *International Journal of Circuits, Systems and Signal Processing*, **8**, 101-108.

[93] M. S. Mahmoud (1994). Stabilizing control for a class of uncertain interconnected systems, *IEEE Transactions on Automatic Control*, **39**, 2484-2488.

[94] J. Lavaei, A.G. Aghdam (2007). High-performances decentralized control design for general interconnected systems with applications in cooperative control, *International Journal of Control*, **80**, 935-951.

[95] N. N. Son (2020). Level control of quadruple tank system based on adaptive inverse evolutionary neural controller, *International Journal of Control, Automation and Systems.*, **18**, 1–12.

[96] P. Roy and, B. Roy (2016). Dual mode adaptive fractional order PI controller with feedforward controller based on variable parameter model for quadruple tank process, *ISA Transactions*, **63**, 365–376.

[97] N. Arjin, T. Thanit, T. Vittaya (2018). Adaptive fractional order PIλDμ control for multi-configuration tank process (MCTP) toolbox, *International Journal of Intelligent Engineering and Systems*, **11 (5)**, 21–34.

[98] G. Tao, "Multivariable adaptive control (2014)," *Automatica. (Oxf)*, **50**, 2737–64.

[99] K. J. Astrom, B. Wittenmark, (1973). On self-tuning regulators, *Automatica. (Oxf)*, **9 (2)**, 185–99.

[100] D. Angeline Vijula, Dr.N. Devarajan (2014). Design of Decentralised PI Controller using Model Reference Adaptive Control for Quadruple Tank Process, *International Journal of Engineering and Technology (IJET)*, **5 (6)**, 5057-5066.

[101] Narendra, K. S., Balakrishnan, J. (1997). Adaptive control using multiple models, *IEEE Transactions on Automatic Control*, **42(2)**, 171–187.

[102] Hespanha, J., Liberzon, D., Morse, A. S., Anderson, B. D. O., Brinsmead, T. S., & Bruyne, F. D. (2001). Multiple model adaptive control part 2:

switching, *International Journal of Robust and Nonlinear Control*, **11(5)**, 479–496.

[103] Chang Tan, Gang Tao, Ruiyun Qi, Hui Yang (2017). A direct MRAC based multivariable multiple-model switching control Scheme, *Automatica*, **84**, 190–198.

[104] D. T. Magill (1965). Optimal adaptive estimation of sampled stochastic processes, *IEEE Transactions on Automat.Control*, **10**, 434–439.

[105] D. G. Lainiotis (1976). Partitioning: A unifying framework for adaptive systems—I: Estimation; II: Control, *Proceedings of IEEE*, **64**, 1126–1143 and 1182–1197.

[106] Elliott, H., Wolovich, W. (1984). Parameterization issues in multivariable adaptive control, *Automatica*, **20 (5)**, 533–545.

[107] Wang, C., Lin, Y. (2010). Adaptive dynamic surface control for linear multivariable Systems, *Automatica*, **46 (10)**, 1703–1711.

[108] Ci Chen, Changyun Wen, Zhi Liu, Kan Xie, Yun Zhanga, C.L. Philip Chen (2017). Adaptive asymptotic control of multivariable systems based on a one-parameter estimation approach, *Automatica*, **83**, 124–132.

[109] Devika K. B, Susy Thomas (2017). Power Rate Exponential Reaching Law for Enhanced Performance of Sliding Mode Control, *International Journal of Control, Automation and* System, **15 (6)**, 2636-2645.

[110] Charles J. Fallaha, Maarouf Saad (2011). Sliding-Mode Robot Control With Exponential Reaching Law, *IEEE Transactions on Industrial Electronics*, **58 (2)**, 600-610.

[111] M. Arıcı, T. Kara (2018). Model reference adaptive control of a quadruple tank process with actuator faults, *Industrial and Engineering Chemistry Research*, Vol. 57, no. 29, pp. 9537–53.

[112] M. Arıcı, T. Kara (2020). Robust adaptive fault tolerant control for a process with actuator faults, *Journal of Process Control*, **92**, 169–84.

[113] Petros Ioannou, B. Fidan. Adaptive Control Tutorial, Society for Industrial and Applied Mathematics, Philadalephia, USA.

[114] P. Ioannou, J. Sun (1996). Robust Adaptive control. Upper Saddle River, NJ: Prentice-Hall.

[115] F. C. Silva, Jr., A. D. Araújo (2005). Variable structure adaptive pole placement control," in *Proceedings of the 44th IEEE Conference on Decision and Control, and the European Control Conference*, 2859-2864.

[116] Jinkun Liu, Xinhua Wang. Advanced Sliding Mode Control for Mechanical Systems, Tsinghua University Press, Beijing.

[117] Y. Shtessel, C. Edwards, L. Fridman, A. Levant (2014). Sliding mode control and observation, control engineering series. Heidelberg, New York: Springer.

[118] W. Gao, J. C. Hung (1993). Variable structure control of nonlinear systems: A new approach," *IEEE Transaction on Industrial Electronics*, **40 (1)**, 45–55.

[120] Zhijun Li, Changbing Zheng (2014). H-Infinity Loop Shaping Control for Quadruple Tank System, *Sixth International Conference on Intelligent Human-Machine Systems and Cybernetics*, 117-120.

[121] S. V. Emel'yanov (2007). Theory of variable-structure control systems: inception and initial development, *Computational Mathematics and Modeling*, **18 (4)**, 321-331.

[122] K. K. D. Young (1977). Asymptotic stability of model reference systems with variable structure control, *IEEE Transaction on Automatic Control*, **22 (4)**, 279-281, 1977.

[123] Borojevic, H. Naitoh, F. C. Lee (1986). Soft variable-structure based adaptive PI control for dc motor position control, *in Proceeding of IEEE Industry Applications Society Annual Meeting*, 283-288.

[124] K. Furuta, K. Kosug, H. Kobayashi (1988). Self-tuning, sliding mode and adaptive control for direct drive motor, *in Proceedings of IEEE Industrial Electronic Conference*, 459-465.

[125] M. Kaynak, F. Harashima, and H. Hashimoto (1984). Variable structure systems theory applied to sub-time optimal position control with an invariant trajectory, *Transactions on IEE*, **104**, 47-52.

[126] A. Sabanovic and D. G. Izosimov (1981). Application of sliding modes to induction motor control, *IEEE Transactions on Industry Applications*, **17 (1)**, 41-49.

[127] A. Savanovic, D. B. Izosimov, F. Bilalovic, 0. Music (1983). Sliding modes in controlled motor drives, in Proc. IFAC Conf. on Control in Power Electronics and Electrical Drives, Lausanne, Switzerland, 133-138.

[128] J. C. Kantor (1989). Nonlinear sliding-mode controller and objective function for surge tanks, *International Journal of Contr*ol, **50 (5)**, 2025-2047.

[129] S. Kawata, A. Yamamoto, M. Masubuchi, N. Okabe, and K. Sakata (1990). Modeling and sliding mode temperature control of a semi-batch polymerization rector implemented at the mixer, *in Proceedings of 11th IFAC World Congr*, **6**, 112-117.

[130] G. E. Young, S. Rao (1987). Robust sliding-mode control of a nonlinear process with uncertainty and delay, *Journal of Dynamic System Measure Control*, **109**, 203-208.

[131] Y. Itkis (1976). Control Syst*ems* of Variable Structure. New York: Wiley.

[132] Katsuhiko Ogata (2010). Modern Control Engineering. Fifth Edition. Upper Saddle River, New Jersey: Prentice Hall.

[133] Stuart Bennet (1993). Development of the PID Controller, *IEEE Control Systems*, 58-65.

[134] J.G. Ziegler, N.B. Nichols (1942). Optimum settings for automatic controllers. *Transaction ASME*, **64**, 759-768.

[135] J.G. Ziegler, N.B. Nichols (1943). Process lags in automatic control circuits, *Transaction ASME*, **65**, 433-444.

[136] G.H. Cohen, G.A. Coon (1953). Theoretical consideration of retarded control, *Transaction ASME*, **75**, 827-834.

[137] W.R. Evans (1950). Control Systems Synthesis by Root Locus, *AIEE Transactions*, **69**, 66-69.

[138] S. Sastry (1999). Nonlinear systems, analysis, stability and control. New York: Springer Verlag

APPENDIX

M-File: Min (Minimum Phase)

data = iddata(y1,u1,0.001);

data1=iddata(y2,u2,0.01);

M-File: Nonmin (Non-minimum Phase)

datan = iddata(y1,u1,0.001);

datan1=iddata(y2,u2,0.01);

Simulation

M-File: error_squares.m

```
IAE1=0;
ITAE1=0;
ITAE2=0;
ISE1=0;
IAE2=0;
ISE2=0;
for i=1:250001

    IAE1=IAE1+abs(e1(i));
    ITAE1=ITAE1+abs(e1(i))*i;
    ISE1=ISE1+(e1(i))^2;
    IAE2=IAE2+abs(e2(i));
    ISE2=ISE2+(e2(i))^2;
    ITAE2=ITAE2+abs(e2(i))*i;
end
MSE1=ISE1/250001;
MSE2=ISE2/250001;
```

```
M-File: real_error_squares.m
IAE1=0;
ITAE1=0;
ISE1=0;

for i=1:7001
    e1(i)=u1(i)-y1(i);
    IAE1=IAE1+abs(e1(i));
    ITAE1=ITAE1+abs(e1(i))*i;
    ISE1=ISE1+(e1(i))^2;
```

```
end
MSE1=ISE1/7001;
```

```
M-File:steady.m
stepinfo(y,t,yd)
```

CURRICULUM VITAE

Alhassan OSMAN, Ph. D.

EDUCATION

Ph. D in Electrical and Electronic Engineering, Gaziantep University, Gaziantep, Turkey 2021

M. Sc. in Electrical and Electronic Engineering, University of Boumerdes, Boumerdes, Algeria 2014

B. Sc. in Electrical and Electronic Engineering, Univerity of Boumerdes, Boumerdes, Algeria 2012

Certificate in Turkish Language, Gaziantep University, Gaziantep, Turkey 2016

Certificate in French Language, University of Boumerdes, Boumerdes, Algeria 2009

RESEARCH EXPERIENCE

Graduate Student, lab of Dr. Tolgay Kara 2016 - 2021

Control Engineering, Gaziantep University, Sehit Kamil, Gaziantep, Turkey

- designed, stimulated and implemented adaptive control strategies on the real Quadruple Tank Processes (QTP)
- discovered that in the simulation, Exponential Reaching Law based Adaptive Sliding Mode Control has faster response time, lower overshoot and smaller errors of the performance indices.
- realized that in the experiment, Exponential Reaching Law based Adaptive Sliding Mode Control has satisfactory results.

TEACHING EXPERIENCE

English Speaking Teacher, English Language, American Culture College 2021

- communicate, interact and make activities with the pupils
- look after the pupils during break time and making sure they play peacefully

SCHOLARSHIPS

Turkish Government Scholarship 2015-2021

- tuition, stipend, accommodation and health insurance for 6 years

Ghana Government Scholarship and Algeria Government Scholarship 2008-2014

- tuition, stipend, books allowance, accommodation and health allowance for 6 years

LANGUAGES

Computer Languages

- Matlab, Phyton

Foreign Languages

- English (advanced level)
- French (Intermediate)
- Turkish (Advanced level

PUBLICATIONS

Peered review

- Alhassan Osman, Tolgay Kara & Mehmet Arıcı, Robust Adaptive Control of a Quadruple Tank Process with Sliding Mode and Pole Placement Control Strategies, IETE Journal of Research 2021

In Preparation

- Alhassan Osman, Tolgay Kara, Robust Adaptive Control of Physical Quadruple Tank Processes (under review by supervisor)